2001 Hurricane Field Program Plan

HURRICANE RESEARCH DIVISION
NOAA/Atlantic Oceanographic and Meteorological Laboratory
Miami, Florida

2001 Hurricane Field Program Plan

National Oceanic and Atmospheric Administration
Atlantic Oceanographic and Meteorological Laboratory
4301 Rickenbacker Causeway
Miami , FL 33149

Prepared By:
Frank D. Marks, Jr., Michael L. Black, and Howard Friedman
Hurricane Research Division

Hugh E. Willoughby
Director, Hurricane Research Division

Date: 14MAY01

Cover: (left) NOAA-14 Advanced Very-High Resolution Radiometer (AVHRR) multispectral false-color image of Hurricane Floyd at 2041 UTC, 13 September 1999. At the time of the image Floyd had a minimum central pressure of 923 hPa and peak surface winds of 135 kt. Photo courtesy of NOAA Operationally Significant Event Imagery website: http://www.osei.noaa.gov/. Images of NOAA WP-3D and G-IVSP, and NASA DC-8 and ER-2 aircraft.

CONTENTS

2001 HURRICANE FIELD PROGRAM PLAN

National Oceanic and Atmospheric Administration
Atlantic Oceanographic and Meteorological Laboratory
Hurricane Research Division

INTRODUCTION

The objective of the National Oceanic and Atmospheric Administration (NOAA) hurricane research field program is the collection of descriptive data that are required to support analytical and theoretical hurricane studies. These studies are designed to improve the understanding of the structure and behavior of hurricanes. The ultimate purpose is to develop improved methods for hurricane prediction.

Seven major experiments have been planned, by principal investigators at the Hurricane Research Division (HRD)/Atlantic Oceanographic and Meteorological Laboratory (AOML) of NOAA, and those for the NASA Fourth Convection and Moisture Experiment (CAMEX-4) for the 2001 Hurricane Field Program. These experiments will be conducted with the NOAA/Aircraft Operations Center (AOC) WP-3D, Gulfstream IV-SP (G-IV), the NASA DC-8 and ER-2, and the Canadian Atmospheric and Environment Service (AES) Convair 580 aircraft. The experiments also comprise the U. S. Weather Research Program's (USWRP) Hurricane Landfall Experiment 2001 (HL 2001). The main objectives of HL 2001 in order of priority are:

1) to capture two complete snapshots of a given tropical cyclone (TC), mapping the storm structure out to 1000 km from the center, from the top of the troposphere to 200 m into the ocean, for use in observational and modeling studies of the processes related to rapid intensification (or weakening);
2) to collect observations of the storm structure (particularly microphysics) and dynamics, especially near landfall;
3) to collect observations useful in studies of storm motion; and
4) to collect observations useful in studies of extra-tropical transition.

The only experiments that do not address the HL 2001 main objectives are the Tropical Cyclogenesis and Clouds and Climate experiments. The Clouds and Climate experiment is included to allow for potential missions into Florida convective systems in conjunction with other NASA supported projects such as TRMM. The Tropical Cyclogenesis experiment, a priority for HRD, is included to allow for the contingency of genesis occurring within the target area.

(1) Coordinated Observations of Vortex Evolution and Structure (COVES) Experiment: This experiment is designed to produce a "snapshot" of a mature hurricane from the top of the troposphere to 200 m deep in the ocean and from the center to a radius of 1000 km. It will also document the interaction of the hurricane with the ocean. This *multi-option, multi-aircraft* experiment will employ coordinated, simultaneous observations from the two NOAA WP-3D's, the NASA ER-2 and DC-8. Included are measurements from several remote sensing instruments *(e.g.*, coordinated airborne Doppler observations) as well as many GPS-sondes dropped out to a radius of 400 km, and airborne expendable ocean probes. A pre-storm and two in-storm missions will be flown on successive days. Data beyond 400 km will be augmented by GPS-sondes launched from the G-IV.

(2) Extended Cyclone Dynamics Experiment: This is a *multi-option, single-aircraft* experiment which uses in–situ and radar data from the WP-3Ds flying at 500 hPa, the G-IV at 200 hPa, to monitor the structure and evolution of a TC on a spatial scales ranging from the convective and mesoscale in the vortex core (10-100 nmi [18-185 km] radius) to the synoptic-scale (1,000 nmi [1,850 km] radius) in the surrounding large-scale environment over a nominal period of 48 h. The WP-3D and G-IV data will be augmented by flight–level data from Air Force WC-130s flying reconnaissance at 700 hPa within 110 nmi (200 km) of the center, and the NASA DC-8 and ER-2 flying at 37,000 ft and 65,000 ft, respectively. The experiment goal is a better understanding of how lateral interactions between the vortex and the synoptic–scale environment control TC intensity and motion.

(3) Tropical Cyclone Wind Fields Near Landfall: This experiment is a *multi-option*, *single-aircraft* experiment designed to study the changes in TC near surface wind structure near and after landfall. An accurate description of the TC surface wind field near and after landfall in real-time is important for warning, preparedness, and recovery efforts. HRD is developing a real-time surface wind analysis system to aid the TPC/NHC in the preparation of warnings and advisories in TCs. The analyses could reduce uncertainties in the size of hurricane warning areas. Flight-level and Doppler wind data collected by a NOAA WP-3D will be transmitted to TPC/NHC where they could result in improved real-time and post-storm analyses. Doppler data collected near a WSR-88D would yield a time series of three-dimensional wind analyses showing the evolution of the inner core of TCs near and after landfall.

(4) Hurricane Synoptic-Flow Experiment: With the arrival of the new NOAA G-IV high-altitude jet, the Hurricane Synoptic Flow Experiment makes the transition from a research program to operations. Beginning in 1997, the G-IV started conducting routine "hurricane surveillance" missions that are essentially HRD Synoptic Flow experiments. When coordinated with these operational G-IV flights, the HRD Synoptic Flow experiment now becomes a *single-option, multi-aircraft* experiment. As in previous years, the experiment seeks to obtain accurate, high-density wind and thermodynamic data sets from the environment and vortex regions of TC that are within 72 h of potential landfall. The availability of the G-IV, however, greatly increases the amount of environment sampled. GPS-based dropwindsondes (GPS-sondes) deployed from the G-IV and the two NOAA/AOC WP-3D aircraft provide these data over the normally data-void oceanic regions at distances up to 810 nmi (1500 km) from the TC center. Mandatory and significant level GPS-sonde data, transmitted in real time, are used to prepare official forecasts at the Tropical Prediction Center/National Hurricane Center (TPC/NHC). These data are also incorporated into objective statistical and dynamical TC prediction models at TPC/NHC and the National Centers for Environmental Prediction (NCEP). In a research mode, these data help improve short and medium term (24-72 h) TC track predictions, study the influence of synoptic-scale fields on vortex track and intensity, and assess methods for obtaining satellite soundings.

(5) Extratropical Transition Experiment: This *multi-option, multi-aircraft* experiment is designed to study the interactions between a TC and midlatitude baroclinic environment. Specific objectives are to identify the physical mechanisms associated with the asymmetric expansion of wind, cloud, precipitation, and ocean surface wave fields during the initial stage of extratropical transition. To examine the relative roles of the TC and midlatitude circulation, aircraft will be used to monitor the changes in TC structure and the interface between the TC and midlatitude circulation into which it is moving.

(6) Tropical Cyclogenesis Experiment: This *multi-option, multi-aircraft* experiment is designed to study one of the most important unanswered questions in tropical meteorology is: How does a tropical disturbance become a tropical depression with a closed surface circulation? This experiment seeks to answer the question through multilevel aircraft penetrations using dropsondes, flight-level data, and radar observations on the synoptic, meso, and convective spatial scales. It will focus particularly on both thermodynamic transformations in the mid-troposphere and lateral interactions between the disturbance and its synoptic-scale environment. The possible addition of the DC-8 this season will allow sampling of the upper tropospheric structure using flight-level and GPS-sondes in these developing disturbances.

(7) Clouds and Climate: This experiment uses the airborne Doppler radar and microphysics instrumentation to accumulate a database of cloud precipitation properties over a wide range of environments. With the addition of the DC-8 and ER-2 this becomes a *single-option*, *multi-aircraft* experiment. This study emphasizes the exploitation of airborne in-situ microphysics and remote sensing (radar), together with satellite observations of clouds. It will provide a data base for studies of clouds and precipitation mechanisms, their effect on climate, and provide ground truth for satellite techniques, particularly the NASA Tropical Rain Measurement Mission (TRMM). This experiment will be coordinated with other TRMM validation experiments under the auspices of CAMEX-4.

CONCEPT OF OPERATIONS

1. Location

The primary base of operations for the NOAA aircraft will be Tampa, Florida, with provision for deployments to Bermuda, Barbados, Puerto Rico, and St. Croix for storms in the Atlantic basin (including the Atlantic Ocean and the Caribbean Sea). The primary base of operations for the NASA aircraft will be Jacksonville NAS, Florida with no planned deployments.

Deployments of the NOAA aircraft may be implemented to U.S. coastal locations in the western Gulf of Mexico for suitable Gulf storms and to western Mexico for eastern Pacific storms. Occasionally, post mission recovery may be accomplished elsewhere. In case of a NOAA aircraft deployment to Mexico after 15 September 2001, the NASA aircraft will deploy to NASA Dryden Flight Research Center for joint flights in the eastern Pacific.

2. Field Program Duration

The hurricane field research program will be conducted from 6 August through 31 October 2001. The CAMEX-4 will be conducted from 16 August through 24 September 2001.

3. Research Mission Operations

The decision and notification process used for hurricane research missions is illustrated, in flow chart form, by Fig. A-1 (Appendix A). The names of those persons who are to receive primary notification at each decision/notification point shown in Fig. A-1 are in Tables A-1 and A-2 (Appendix A). In addition, contacts are maintained each weekday among the directors of HRD/AOML, TPC/NHC, AOC, and NASA CAMEX-4 to discuss the "storm outlook."

Research operations must consider that the research aircraft are required to be placed in the National Hurricane Operations "Plan of the Day" (POD) 24 h before a mission. If operational "fix" requirements are accepted, the research aircraft must follow the operational constraints described in section 7.

4. Task Force Configuration

One NOAA/AOC WP-3D aircraft (N42RF), equipped as shown in Table B (Appendix B), will be available for research operations throughout the 2001 Hurricane Field Program (on or about 6 August through 31 October). When possible, the G-IV jet aircraft will be used with the WP-3D during the Synoptic-Flow Experiment. The NASA DC-8 (NA817), equipped as shown in Table B-2 (Appendix B), will be available for research operations from 16 August through 24 September. The NASA ER-2 (NA809), equipped as shown in Table B-3 (Appendix B), will be available for research operations from 16 August through 24 September. The Canadian Atmospheric and Environment Service (AES) Convair 580 aircraft will participate in flights into a TC undergoing extratropical transition. The instrumentation onboard the Convair 580 is listed in Table B-4 (Appendix B).

5. Field Operations

5.1 Scientific Leadership Responsibilities

The implementation of HRD's 2001 Hurricane Field Program Plan is the responsibility of the field program director, who is, in turn, responsible to the HRD director. The field program director will be assisted by the field program ground team manager. In the event of deployment, the field program ground team manager shall be prepared to assume overall responsibility for essential ground support logistics, site communications, and HRD site personnel who are not actively engaged in flight. Designated lead project scientists are responsible to the field program director or designated assistants. While in flight, lead project scientists are in charge of the scientific aspects of the mission being flown.

During CAMEX-4 the field program director will coordinate any joint research missions with the NASA CAMEX-4 Mission Planning Committee, who are responsible for the NASA mission objectives. While in flight the designated NASA CAMEX-4 lead scientists and flight coordinators are in charge of the scientific missions being flown.

5.2 Aircraft Scientific Crews

Tables C-2.1 through C-2.7 (Appendix C) list the NOAA scientific crew members needed to conduct the 2001 hurricane field experiments. Actual named assignments may be adjusted on a case-by-case basis. Operations in 2001 will include completion of detailed records by each scientific member while on the aircraft. General checklists of NOAA science-related functions are included in E.2 through E.6 (Appendix E).

5.3 Principal Duties of the Scientific Personnel

A list of primary duties for each NOAA scientific personnel position is given in D.1 through D.12 (Appendix-D).

5.4 HRD Communications

The HRD/Miami Ground Operations Center (MGOC) will operate from offices at AOML on Virginia Key (4301 Rickenbacker Causeway, Miami, Florida) or from TPC/NHC (11691 S.W. 17th Street, Miami, Florida).

During actual operations, the senior team leader of the MGOC, or his designee, can be reached by commercial telephone at (305) 221-4381 (HRD/TPC/NHC) or at (305) 361-4400 (HRD/AOML). At other times, an updated, automated telephone answering machine [(305) 221-3679] will be available at the MGOC. Also, MGOC team leaders and the field program director can be contacted by calling their respective telepager phone number (available later).

MGOC, operating from AOML or TPC/NHC, will serve as "communications central" for information and will provide interface with AOC, CAMEX-4, TPC/NHC, and CARCAH (Chief, Aerial Reconnaissance Coordinator, All Hurricanes). In the event of a deployment of aircraft and personnel for operations outside Miami, HRD's field program ground team manager will provide up-to-date crew and storm status and schedules through the field program director or the named experiment lead project scientist. HRD and CAMEX-4 personnel who have completed a flight will provide information to MGOC, as required.

6. Data Management

All requests for NOAA data gathered during the 2001 Hurricane Field Program should be forwarded to: Director, Hurricane Research Division/AOML, 4301 Rickenbacker Causeway, Miami, Florida 33149.

7. Operational Constraints

Hurricane research missions are routinely coordinated with hurricane reconnaissance operations. As each research mission is entered into the planned operation, a block of time is reserved for that mission and operational reconnaissance requirements are assigned. A mission, once assigned, *must be flown in the time period allotted and the tasked operational fixes met.* Flight departure times are critical. Scientific equipment or personnel not properly prepared for flight at the designated pre-take-off or "show" time will remain inoperative or be left behind to insure meeting scheduled operational fix requirements.

8. Calibration of Aircraft Systems

Calibration of aircraft systems is described in Appendix C (en-route calibration). True airspeed (TAS) calibrations are required for each NOAA flight, both to and from station and should be performed as early and as late into each flight as possible (Fig. C-1).

EXPERIMENTS

9. Coordinated Observations of Vortex Evolution and Structure (COVES) Experiment

Program Significance: Research in the last two decades suggests that several environmental controls influence the change in TC intensity and structure, including wind shear, sea-surface temperature distribution, and upper-tropospheric interactions. Also important are the internal physics of the vortex, including dynamic, thermodynamic, and microphysical characteristics.

The COVES experiment is designed to collect data from a single TC using several different observing platforms and diagnose the qualities mentioned above. It also addresses a significant element of the USWRP HL initiative. This involves capturing complete snapshots of a TC's structure, horizontally within 540 nmi (1000 km) of the center and vertically from the top of the troposphere to at least 200 m below the ocean surface, for use in intensification studies. By combining NOAA's aircraft resources (two WP-3D and a supplemental G-IV) from the Hurricane Field Program with NASA's (a DC-8 and an ER-2) from CAMEX-4, COVES provides a unique opportunity to obtain a thorough depiction of the storm and its environment through a coordinated interagency effort that employs a greater variety of instruments than is usually available during the Hurricane Field Program.

One of the primary atmospheric instruments utilized is the GPS-sonde. In this experiment, GPS-sondes are capable of being deployed from all the COVES aircraft. They measure pressure, temperature, relative humidity, and winds every 0.5 s as they descend (~5 m vertical resolution near the surface). Since their introduction in 1996, reliability has proven to be outstanding and observational accuracy is quite high; the average error is less than 0.5° C for temperature, within 10% for humidity, and 1-2 m s^{-1} for winds. Most notably, the probes have helped to document extremely fine thermodynamic and kinematic variations in vertical structure, particularly in the boundary layer, and have permitted highly accurate point measurements near the surface in turbulent conditions.

The COVES experiment will add new contexts to the airborne Doppler observations often made in TCs. Recent studies using Doppler radar data collected by two WP-3D aircraft flying simultaneous orthogonal tracks have found that the wind structure in a TC can change drastically in as little as three hours. For example, in Hurricane Olivia (1994) increasing environmental shear eventually affected the eyewall circulation and caused as much as a 15-20 m s^{-1} decrease of the mean swirling wind in the mid-to-upper troposphere in less than 3 h. Unfortunately, since little was measured outside the 54 nmi (100 km) radius, it was difficult to gauge the strength of the environmental shear and how that shear was modified as it interacted with the vortex.

COVES combines many dropsonde observations in the TC inner core and rainband regions out to 216 nmi (400 km) from the center with Doppler radar observations within ~22 nmi (40 km). The drops will be particularly dense immediately outside the Doppler coverage area but will be spaced farther apart at larger radial distances. This data distribution will help us to verify our present theories concerning both the interaction of the vortex with environmental shear and the modification of the vortex by upper-tropospheric interactions. The data may also be supplemented with other environmental observations within 540 nmi (1000 km) of the center, including sondes dropped by the G-IV. It is hoped that data gathered at larger scales away from the center than those available when observing Hurricane Olivia will allow for accurate intercomparisons with nested models. The combination of *in situ* GPS-sonde and Doppler radar data will also permit small-scale dynamic features to be studied more extensively, such as vortex Rossby waves; results from Hurricane Olivia suggest that Rossby waves may be important features in the inner core circulation of developed TCs.

Modifications of the TC wind and pressure fields by oceanic thermodynamic influences are accomplished in two general fashions. First, pre-existing ocean temperature and circulation features modify the fluxes at the air-sea boundary as the storm passes over them. Such features include permanent currents, such as the Gulf Stream and Gulf Loop current; semi-permanent circulations, such as the Gulf of Mexico Warm Eddies; and transitory features, such as cold wakes from previous storms.

Second, immediate modifications of SST and ocean mixed layer depth under the storm itself will affect the surface fluxes. Thus in this experiment we propose to use a mobile observing strategy that allows SSTs and mixed-layer depth structures to be mapped before, during, and after TC passage using Airborne Expendable Bathythermographs (AXBTs). Upper ocean current, temperature, and salinity during TC passage will also be mapped using Airborne Expendable Current Probes (AXCPs) and Airborne Expendable Conductivity, Temperature, and Depth (AXCTDs) probes. It is important to separate other environmental influences from those of the ocean. Surface and tropospheric wind field measurements from instruments including the GPS-sondes, Doppler radar, Ku/C-band Scatterometer (Ku/CSCAT), and Stepped Frequency Microwave Radiometer (SFMR) out to several hundred km from the center will help achieve this. Finally, surface-wave observations will be made by a Scanning Radar Altimeter (SRA).

Rainbands and outer eyewalls are internal components of the TC that modify the thermodynamic characteristics of the boundary layer air flowing into the storm. Their circulations tend to suppress convection and the secondary circulation in the inner eyewall. They may also protect the inner eyewall from the full effect of environmental wind shear. The large number of GPS-sondes dropped both in the inner core and rainband regions should help to monitor the effects of rainbands and the degree to which surface fluxes are able to restore the warm moist properties of the inflow air. Additionally, the near-surface inflow will be determined from SFMR and Ku/CSCAT data collected along the flight tracks.

Convection in the eyewall is usually quite asymmetric and tilted outward. Because there is a large shear of the swirling flow, convection should theoretically also be tilted azimuthally. This has been difficult to document from Doppler three-dimensional composites, since updrafts evolve quite rapidly and consequently undergo significant change during the time required to collect the data needed to create a composite wind field. One method to avoid problems resulting from evolution is to observe vertical incidence observations with two aircraft flying in the same direction, one somewhat downwind of the other. This type of pattern has been flown successfully in Hurricane Edouard (1996). COVES presents an opportunity to perform this between the NASA aircraft and a WP-3D. The lower WP-3D may also fly an optional module, which will map the three-dimensional structure of eyewall convection.

Microphysical measurements contribute to a complete depiction of the TC. Cloud particle imagery and statistics permit more reliable estimates of the rainfall and rain content from land-based, airborne, and satellite-born radars, including TRMM. Ice imagery and measurements of cloud water, particle charge, and electric field help to document the roles of electric charge separation and ice multiplication. Accurate microphysics can improve dynamic models by permitting better estimates of the distribution and strength of precipitation drag and evaporation and the release or absorption of latent heats of condensation and fusion. Thus measurements of particle types and size distributions are essential for a full understanding of TCs. Furthermore, increased charge separation and resultant electrification and lightning imply the existence of cloud liquid water at temperatures well below freezing. In the naturally well-seeded TC environment, this suggests rapid vertical motion, which often accompanies intensification. Thus increases in lightning signal potential strengthening. Microphysical measurements at the -10°C level by the upper WP-3D may be possible in the latter part of the COVES flight pattern. Furthermore, microphysical observations near the -40°C level will be made by the NASA DC-8.

COVES will provide an opportunity to acquire the broadest set of observations ever collected in the TC eyewall and rainband regions. Hopefully, the myriad of mechanisms and factors mentioned here will be documented, leading to a better understanding of their relative roles in intensity and structural changes.

Objectives: The primary goal of this experiment is to fully document the three-dimensional kinematic structure and temporal evolution of a mature TC and its environment from the top of the troposphere to 200 m into the ocean. This will be accomplished using a variety of airborne instruments, deployed expendable probes, remote sensing devices, and microphysics instruments. A TC undergoing a period of rapid intensification or weakening will be a prime candidate. Combined with GPS-sonde observations from a simultaneous G-IV synoptic surveillance mission, rawinsonde observations of opportunity, and supplementary satellite data, a comprehensive snapshot of convective, mesoscale, and synoptic features shall be obtained within ~540 nmi (1000 km) of the center.

Other scientific goals are:

- To examine the relationship of environmental wind shear with TC structure, evolution, intensity change, and rainfall distribution.
- To study the role that convective asymmetries play in TC evolution and motion.
- To validate and refine numerical models of TC eyewall vertical structure and evolution.
- To determine kinematic and thermodynamic attributes of rainbands and adjacent regions.
- To evaluate real-time empirical and satellite estimates of surface wind in TCs using *in situ* data.
- To compare airborne and satellite remote measurements with those from buoys and expendable probes.
- To study three-dimensional sensible and latent heat fluxes, energy and moisture fluxes in the atmospheric boundary layer.
- To measure changes in SST, mixed layer depth, currents, and waves caused by TCs.
- To study the role ocean processes play in modifying the TC boundary layer through air-sea interactions. and determine statistical relations.
- To improve estimates of upper ocean heat content before and during TC passage.
- To quantify the roles mixing and horizontal advection of SST and salinity gradients have on the ocean mixed layer and the effect TC precipitation has on mixed layer response.
- To improve TC forecast model initialization and parameterization of air-sea processes, upper oceanic features, and boundary layer conditions
- To study the distribution, structure, and temporal evolution of electrical charging mechanisms in TCs.
- To record the types and concentrations of all hydrometeors observed in TCs, particularly in electrically active areas.

Mission Description: In COVES, four to five aircraft provide simultaneous, coordinated observations of the TC. The aircraft involved are the two NOAA WP-3D as well as the NASA ER-2 and DC-8. Missions should be planned to correspond with a NOAA G-IV synoptic surveillance flight, which will provide most of the observations between 270 and 540 nmi (500 and 1000 km) from the storm center. The experiment consists of the pre-storm ocean survey and coordinated in-storm modules. Other optional modules are also presented here.

These are the following requirements to commit:

- A hurricane or strong tropical storm within 540 nmi (1000 km) of land, which is a threat to the U.S. coast, but is not expected to make landfall for 48-72 h.
- Both WP-3D aircraft must have operational tail and lower-fuselage radars, and be fully equipped to launch and monitor GPS-sondes and AXBTs.
- Upper WP-3D must have working Ku/C-SCAT, SFMR, and microphysical instrumentation.
- Lower WP-3D (which will also be the pre-storm ocean survey aircraft) must have working SFMR, SRA, radome-mounted gust probe, and AXCP and AXCTD probes and receiver equipment.
- NASA ER-2 and DC-8 must have operational GPS-sonde equipment.
- ER-2 Doppler radar (EDOP) and DC-8 microphysics instrumentation should also be operational.

- If AFRES operational reconnaissance missions are carried out concurrently, coordination will be required.
- If available, three drifting buoy platforms should be deployed by AFRES WC-130 aircraft prior to the pre-storm ocean survey.

Pre-Storm Survey Module: This module should be executed approximately 24-72 h prior to a forecasted landfall. The patterns shown in Fig. 1a and 1b correspond to full mission options designed to accurately measure the undisturbed structure of a (predetermined) asymmetric or a symmetric ocean feature, respectively, just prior to encountering the storm. A single WP-3D aircraft with AXBT/AXCP/AXCTD launching capability maps the ocean boundary and mixed layer structure of the ocean feature at least one day before TC/ocean feature interaction occurs. These patterns should be flown with the initial leg parallel to a TOPEX/POSEIDON satellite altimeter ground track (±32° inclination from true north) if possible. A constant altitude of 5,000 to 6,000 ft should be maintained throughout the mission. Doppler radar should be set to F/AST mode on all legs if there are any scatterers. Another single aircraft experiment, such as the XCDX, should ideally be conducted simultaneously or immediately following either of these options to measure internal storm structure prior to interaction. A third pattern shown in Fig. 1c corresponds to an option that may be flown by either WP-3D aircraft following a primary storm survey module. During this pattern, the upper ocean mixed layer thermal structure is sampled directly ahead of the storm track. For all options of this module oceanic coverage should include an area over which the TC will potentially traverse for at least a 24-36 h period.

A) **Asymmetric Ocean Feature Option:** This is best suited for an elongated or irregularly-shaped ocean feature, such as the Gulf Stream in the Atlantic or the Loop Current in the Gulf of Mexico. The "lawn mower" pattern (Fig. 1a) consists of flying four 135 nmi (250 km) transects, bisected by the feature's major orientation axis and spaced apart by 54 nmi (100 km) intervals. These are followed by a return leg approximately 216 nmi (400 km) aligned with the feature's major axis. 9 GPS-sondes, 18 AXBTs, 12 AXCTDs, and 17 AXCPs should be launched at regular intervals, as shown in Fig. 1a. The AXCTDs in the spine of the feature should be deployed during the initial set of perpendicular legs. In the event the feature is the Gulf Loop Current, the positions of the other AXCTDs and the adjacent AXCPs on these legs should be reversed. The time on station needed to complete this option is about 5 h.

B) **Symmetric Ocean Feature Option:** If the ocean feature is circular in shape, such as a Gulf of Mexico Warm Eddy (GOMWE) ring, the pattern in Fig. 1b should be executed. This pattern has six radial legs (three inbound and three outbound), and two downwind legs (**2-3** and **4-5** in Fig. 1b); all have nominal length of 108 nmi (200 km) and are spaced 60° apart azimuthally. During each radial leg one or two probes will be launched at every 25 km interval beyond the feature center. A GPS-sonde and an AXBT will be dropped concurrently at 54 nmi (100 km) and 108 nmi (200 km) from the center. Another set of simultaneous GPS-sonde and AXBT probes will be launched at the midpoint of the two downwind legs. An additional solo AXBT will be launched at 13.5 nmi (25 km) from the center on each radial leg, and a GPS-sonde will be dropped in the center during the second pass. An AXCP will be deployed at 40.5 nmi (75 km), 67.5 nmi (125 km), and 94.5 nmi (175 km) from the center during each radial leg; and an AXCTD will be released at 27 nmi (50 km) and 81 nmi (150 km) from the center. The time on station needed to complete this option is about 4.5 h.

C) **Ahead of Storm Track Option:** Following the conclusion of a primary storm survey module, a 60° 90° wedge pattern is flown (Fig. 1c). Two lines of AXBTs are deployed at positions roughly 12 h **(2-3)** and 24 h **(4-5)** ahead of and normal to the storm track. The actual pattern is highly dependent on the storm motion, as well as the time available. For example, if the storm is moving 10 kts, then the first line of AXBTs would be 120 nmi (222 km) ahead of the current storm position; and the second line would be 240 nmi (444 km) ahead. Whereas, if the motion is 8 kts, then the first line of AXBTs would be ~100 nmi (185 km) ahead of the storm; and the second line ~200 nmi (370 km) ahead. If the region 12 h ahead of the TC has already been well-sampled during the storm survey module, then only the second line of AXBTs needs to be dropped. For a slow moving storm (3-6 kts) it may be possible to drop AXBTs up to 36 h ahead of the storm, depending on time constraints and other factors. A maximum of 12 AXBTs will be launched during the pattern; the number may be decreased due to aircraft payload restrictions. The time on station needed to complete this option should be 2 h or less.

(**Note:** This option can be flown in conjunction with a single-aircraft XCDX mission.)

Primary Storm Survey Modules: One of the two primary storm modules should be executed on at least two successive days before the forecasted landfall. These are called the "Main" and "Coordinated-Leg" modules. The Main module is designed to maximize the radial coverage of the two NOAA WP-3D aircraft, permitting close coordination with the NASA aircraft only during the first center penetration. The Coordinated-Leg module shortens the WP-3D flight legs to permit coordination of all aircraft for all three center penetrations. A separate "Inner-Core" module may be substituted for the lower aircraft to fly in place of its standard pattern in the "Main" module. All other aircraft still fly the Main-module flight plans. Finally, a module called the "WP-3D-only" module is included in the event the NASA aircraft are unable to fly. For brevity, the flight plans for the upper WP-3D, the ER-2 and DC-8 are all described according to reference points, which are numbered the same for all modules.

1) *NASA DC-8 and ER-2 Aircraft*. The NASA aircraft are not scheduled to fly in the WP-3D-only or inner core modules. The DC-8 will fly at a constant altitude throughout the pattern between 33,000 (FL310) and 37,000 (FL370) ft. The altitude selected should be optimized for the collection of microphysical data. Ideally, this should be at the level of the TC warm-core maximum, where the peak tangential wind decays most rapidly with height. The ER-2 aircraft will initially fly between 65,000 (FL650) and 68,000 (FL680) ft., and climb to 70,000 ft (FL700) by the end of the module. The pattern has six radial legs (three inbound and three outbound), and two downwind legs (**B-C** and **D-E** in Figs. 2a and 3a); all have nominal length of 216 nm (400 km) except for the first leg in the Main module, which begins 324 nm (600 km) from the center (Fig. 2a). Coordination will take place 108 nmi (200 km) from the center along the first inbound leg **(A-§** in Fig. 2a) in the Main module, and at **A, C** and **E** on the three inbound legs in Fig. 3a for the Coordinated-Leg module. The ER-2 and DC-8 are scheduled to drop a total of 12 and 18 GPS-sondes, respectively. The ER-2 will drop sondes on both inbound and outbound legs at radii of 54 nmi (100 km) and 216 nmi (400 km) from the storm center. The DC-8 will drop sondes on both inbound and outbound legs at radii of 81 nmi (150 km), 108 nmi (200 km), and 162 nmi (300 km) from storm center. Either the DC-8 or ER-2 may drop discretionary sondes in the inner core; however, to avoid hazards, coordination with the WP-3D's and any tasked AFRES WC-130 aircraft should be exercised before dropping extra sondes. The DC-8 and the ER-2 will be on station for 4 to 4.25 h in this module.

2) Upper WP-3D Aircraft. The upper WP-3D aircraft will fly initially at 18,000 ft (FL180) and climb to the maximum sustainable altitude by the end of the module. The altitudes should be chosen to avoid icing and electrical discharge. The pattern is essentially the same for all modules. In the Main and Coordinated-Leg modules, it will enter 90° to the left (upwind) of the NASA aircraft track. The pattern has six radial legs (three inbound and three outbound) that are orthogonal to those of the NASA aircraft and the lower WP-3D and two downwind legs. All radial legs extend to a radius of 189 nmi (350 km) in the Main and WP-3D-only modules and 135 nmi (250 km) in the Coordinated-Leg module. Coordination with the lower WP-3D along all inbound legs (**1-§, 3-§, and 5-§** in Figs. 2a and 3a) will take place 62 nmi (115 km) from the center; however the responsibility for altering track for coordination will lie with the lower WP-3D. The upper WP-3D will release a total of 9 GPS-sondes on each radial leg in the Main, Inner-Core or WP-3D-only modules or 8 sondes in the Coordinated-Leg module, for a total of 54 or 48 sondes, respectively. The inner most radii for GPS-sonde release in the Main, Coordinated-Leg, and Inner Core modules are 13.5 nmi (25 km), 27 nmi (50 km), 40.5 nmi (75 km), 54 nmi (100 km), 67.5 nmi (125 km), 81 nmi (150 km), and 108 nmi (200 km). Outer sondes will be dropped at 148 nmi (275 km) and 189 nmi (350 km) in the Main and Inner-Core modules, and 135 nmi (250 km) in the Coordinated-Leg module. The distances for the 9 sondes per leg in the WP-3D-only module are at 13.5 nmi (25 km), 27 nmi (50km), 40.5 nmi (75 km), 54 nmi (100 km), 81 nmi (150 km), 108 nmi (200 km), 135 nmi (250 km), 162 nmi (300 km), and 189 nmi (350 km). Twenty AXBTs should be launched concurrently with selected GPS-sondes as shown in Figs. 2a for the Main and Inner-Core modules, eighteen AXBTs for the Coordinated-Leg module (Fig. 3a). Fourteen AXBTs should be launched concurrently with the sondes in the WP-3D-only module as shown in Fig. 4; in addition, two more AXBTs along downwind leg **2-3**. It may be desirable to launch additional GPS-sondes in the eye during the first and/or last penetration. The Main, Inner-Core, and WP-3D-only modules will last approximately 6 h, while the Coordinated-leg module will last 4 h.

3) Lower WP-3D Aircraft (Main, Coordinated-Leg and WP-3D-only modules). In all modules, the lower WP 3D has the responsibility for coordinating with the upper WP-3D and with NASA, and it will alter its track as necessary to remain coordinated with the other aircraft. The lower WP-3D should fly between 5,000 and 12,000 ft in the Main and Coordinated-Leg modules, depending upon the storm intensity, flight level of potential AFRES missions, and observational focus. The altitude in the WP-3D-only module should be 2,000-4,000 ft below the upper WP-3D, to increase the depth of the soundings. All three modules have six radial legs (three inbound and three outbound) that are orthogonal and downwind of the corresponding upper WP-3D legs. The nominal leg lengths of the Main, Coordinated-Leg and WP-3D-only modules are 162 nmi (300 km), 108 nmi (200 km), and 176 nmi (325 km), respectively. Coordination with the upper WP-3D and NASA aircraft along all inbound legs **(1-§, 3-§, 5-§** in Figs. 2b, 3b, and 4) will occur at 54 nm (100 km) from the center in the Main and WP-3D-only modules (Figs. 2b and 4), and at points ***1***, ***3***, and ***5*** in the Coordinated Leg module (Fig. 3b). The Main and WP-3D-only modules will last approximately 6 h, while the Coordinated-leg module will last about 4 h.

In the Main and Coordinated-Leg modules an AXCTD will be deployed at a radius of 27 nmi (50 km) along each inbound and outbound radial leg for a total of 6. AXCPs will be deployed along each radial leg in the eyewall and at radii of 40.5 (75 km), 67.5 (125 km) and 94.5 nmi (175 km), for a total of 24.

AXBTs and GPS-sondes will be dropped differently in each module to coordinate with the upper WP-3D drops. In the Main module (Fig. 2b) AXBTs and GPS-sondes will be dropped concurrently at inbound and outbound radii of the eyewall, 54 nmi (100 km) and 108 nmi (200 km) along ***1-2*** and ***3-4***, and at inbound and outbound radii of the eyewall and 54 nmi (100 km) along ***5-6***. Four more AXBTs and GPS-sondes will be dropped together at ***2, 3***, and at two equally spaced points between ***2*** and ***3***. Other GPS-sondes may be dropped in the eyewall at the discretion of the lead scientist

In the Coordinated-Leg module (Fig. 3b), AXBTs and GPS-sondes will be dropped concurrently at the eyewall and at radii of 54 nmi (100 km) and 108 nmi (200 km) along all inbound and outbound radial legs. Two others will be dropped at equally spaced intervals between ***2*** and ***3***. Additional GPS-sondes may be dropped in the eyewall at the discretion of the lead scientist.

In the WP-3D-only module (Fig. 4) the lower plane releases 54 GPS-sondes. There will be 9 sondes per radial leg dropped at radii 13.5 nmi (25 km), 27 nmi (50 km), 40.5 nmi (75 km), 54 nmi (100 km), 67.5 nmi (125 km), 94.5 nmi (175 km), 121.5 nmi (225 km), 148.5 nmi (275 km), and 175.5 nmi (325 km). Concurrent AXBTs will be dropped at radii of 27 nmi (50 km), 94.5 nmi (175 km), and 148.5 nmi (275 km) along ***1*-§** and ***3*-§**; at radii of 27 nmi (50 km) and 94.5 nmi (175 km) along **§-*2*, §-*4*, and *5*-§**; and at radii of 27 nmi (50 km), 54 nmi (100 km), 94.5 nmi (175 km), and 148.5 nmi (275 km) along **§-*6***. No AXCPs or AXCTDs are launched in this module.

4) Lower WP-3D Aircraft (Inner-Core module). This is the only module where the tail radar will be operated in continuous mode. F/AST should be used on downwind legs, while continuous mode normal to the aircraft track should be used on all radial legs. The lower WP-3D will fly a wedge pattern between 5,000 to 12,000, depending on the storm intensity and the altitude of the AFRES WC-130. This pattern includes 7 inbound and 7 outbound radial legs that are 54 nmi (100 km) long (Fig. 2c). The legs from **2,13-§** and **§-12,16** will be flown twice. There are just two coordination points with the upper WP-3D at **2** and **15.** AXBTs and GPS-sondes will be dropped concurrently at **10-15**. On the radial legs from **4-§, §-5, 6-§, §-7, 8-§**, and **§-9** an AXBT will be dropped in the eyewall with a GPS-sonde. Other GPS-sondes will be dropped at the discretion of the lead scientist along each radial leg with the goal of obtaining a representative distribution of eyewall soundings. No AXCPs or AXCTDs are launched in this module. Optionally, the lower WP-3D may begin the module at **2** one half hour after the upper WP-3D reaches its

IP and/or end the module at **16** one half hour after the upper WP-3D reaches its FP. The module should take 5-6 h to complete.

Auxiliary Storm Survey Modules: These are stand-alone "plug-in" modules that are two hours or less in duration and can be executed after the selected primary storm module. Execution is dependent on storm attributes, storm track, aircraft instrumentation, aircraft fuel and weight restrictions, and proximity to operations base.

(1) Electrification of TC Convection Module: This module, described in the Tropical Cyclone Landfall Experiment, documents the microphysical characteristics of electrically active convection using a single WP-3D aircraft. The PMS 2-D grayscale probes, the new PMS FSSP-100, five DRI field mills, the tail Doppler radar, the NASA HVPS, and the Johnson-Williams cloud liquid water probe are essential. It is desirable to have 4-6 GPS-sondes deployed to obtain soundings outside the convection in the inflow near the areas of interest.

In the event that the NASA DC-8 aircraft is available to survey the high-altitude areas of the storm in cooperation with the WP-3D aircraft, it should attempt to fly downwind (as shown in Fig. 13a) through the same electrically active area being investigated by the WP-3D aircraft, taking care to penetrate the active convective cores. The DC-8 should make its initial pass at or near cloud top, or maximum altitude, whichever is lower. Each subsequent pass should occur 6,500 ft lower in altitude from the previous pass until the DC-8 is not less than 6,500 ft higher than the WP 3D maximum altitude or 28,000 ft, whichever is higher; is as low as the NASA crew deems practical; or the WP-3D aircraft leaves the area. At such time, the DC-8 should climb back to cloud top level and seek a new area along with the WP-3D.

(2) C-BLAST Module: This module is designed to test the logistics of flying a stair-step pattern and the feasibility of estimating the momentum and sensible heat flux near the top and bottom of the well-mixed layer. A single WP-3D flies a series of stair-step descents from 5,000 ft to the lowest altitude deemed 'safe.' This pattern is executed in crosswind and upwind/downwind directions within both a rain-free, gale-force wind region and a storm-force to hurricane-force wind region. Typically, the former will be located radially outward from the outer principle rainband, while the latter will be located between the eyewall and an outer convective rainband. Fig. 5 shows a typical upwind/downwind flight pattern. The legs are approximately parallel to the low-level inflow. Companion legs normal to the flow are also desired to resolve secondary circulation features in the well-mixed layer. The capability of measuring latent heat flux will be added as instrumentation becomes available.

The stair-step descent (SSD) consists of a series of 37-50 nmi (60-80 km) long legs, each lasting 1-2 minutes and executed at a successively lower altitude than the previous leg. Typical altitudes will be 5,000, 3,000, 2,000, 1,500, 1,000, 500, and 300 ft; these levels may be adjusted depending on the altitude of the top of the well-mixed layer. It is desirable to have two legs positioned above the well-mixed layer. The lower levels are flown only if the turbulence and visibility are assessed as safe. At no time does the aircraft need to fly into rainbands, the eyewall, or any strong cells in between these two features. The aircraft should launch three GPS-sondes, one at the beginning, midpoint, and end of the pattern, to assess changes in the bulk mixed-layer and surface layer thermodynamic and kinematic structure along the flight path. Concurrent AXBTs should be deployed with the two GPS-sondes at the beginning and end of the pattern. Also, 2-3 other AXBTs should be deployed at 20-km intervals along the flight path. The total time for this module is about 2 h.

(3) Rainband Thermodynamic Structure Module: This module is described in the TC Landfall Experiment (and shown in Fig. 12).

COVES EXPERIMENT

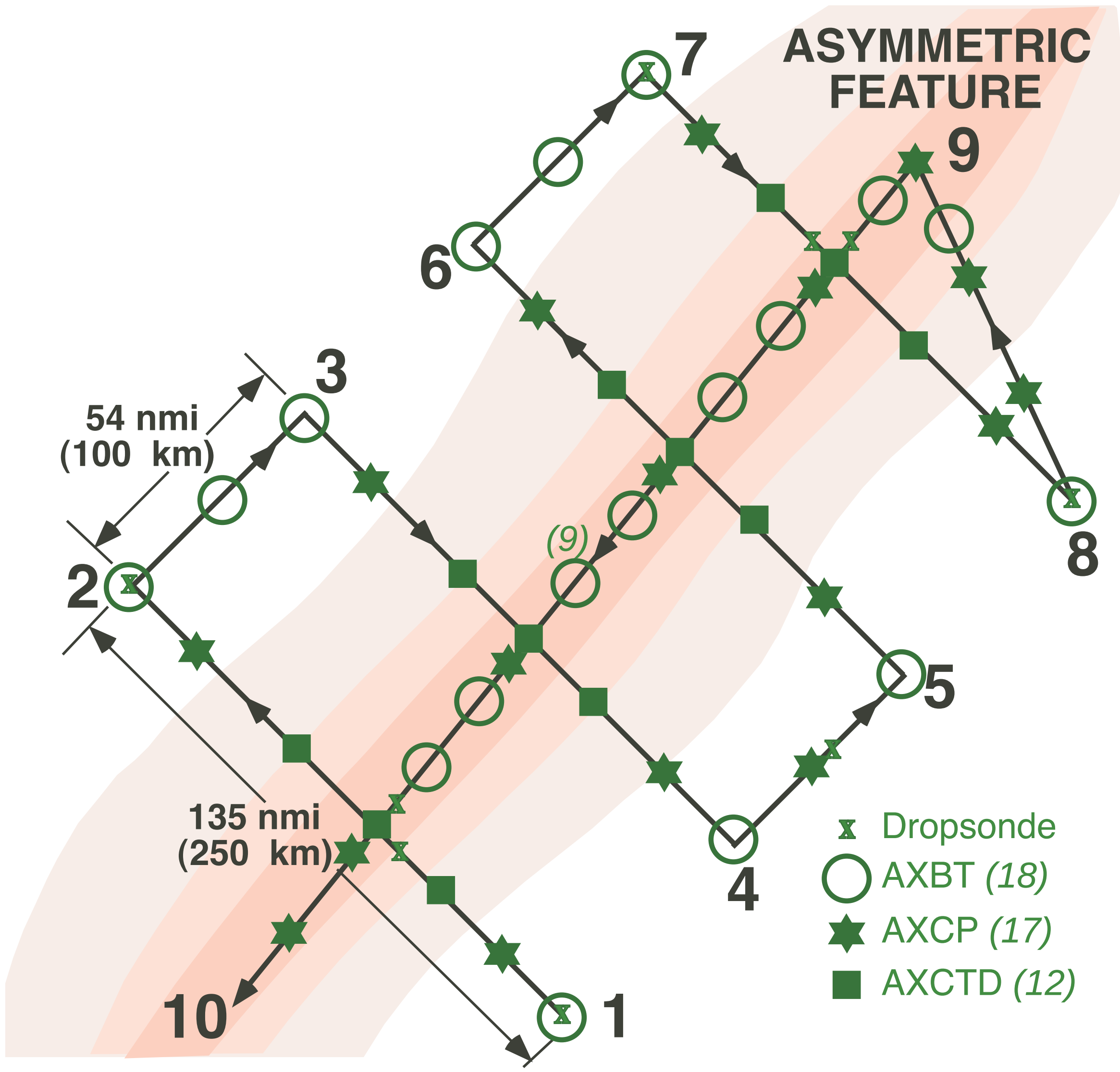

Fig. 1. (a) Pre-storm Ocean Survey Pattern

• Note 1.	Flight altitude should be 5,000 ft RA
• Note 2.	IAS should be decreased to 190 kt when launching AXCPs

COVES EXPERIMENT

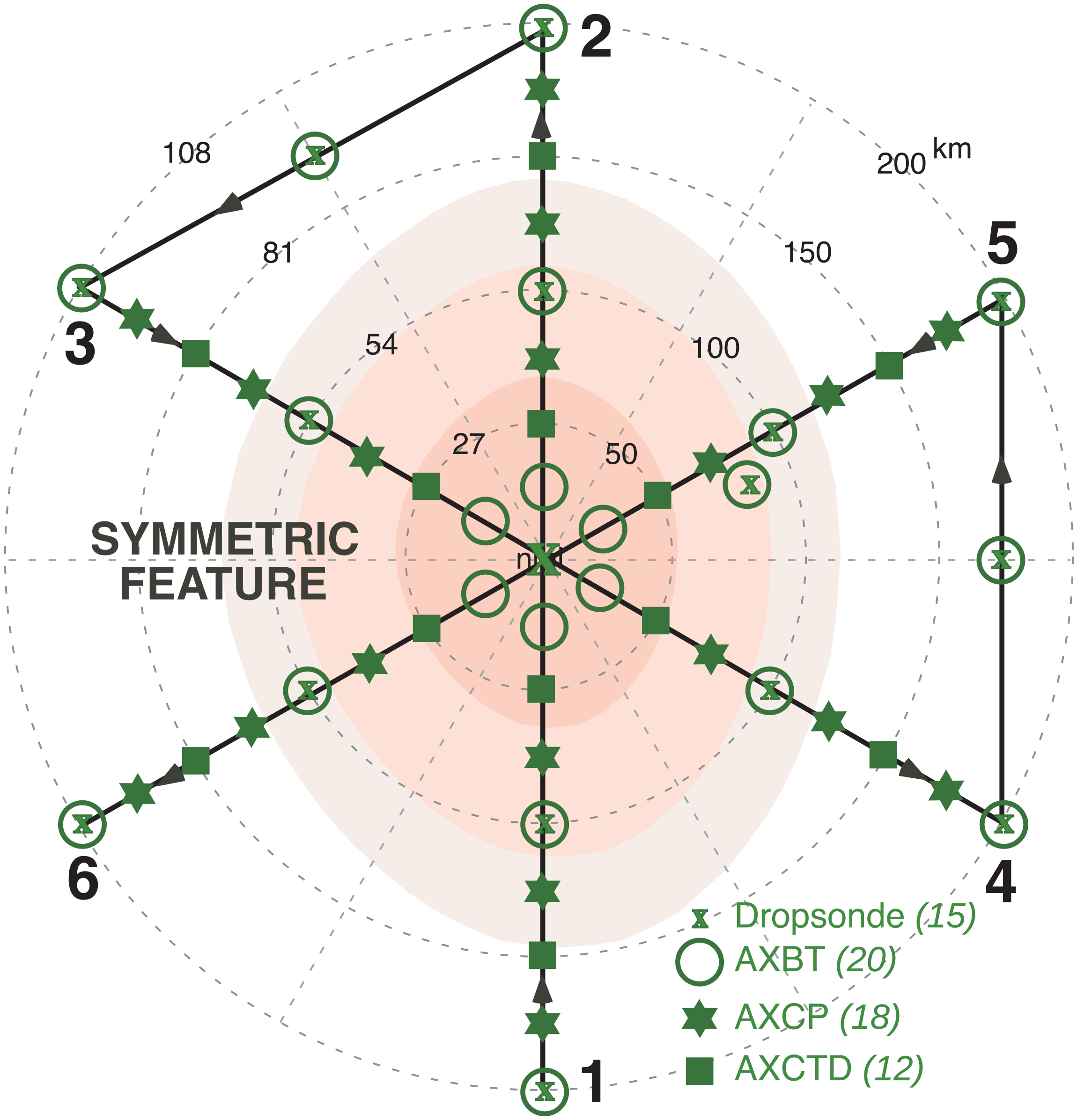

Fig. 1. (b) Pre-storm Ocean Survey Pattern

• Note 1.	Flight altitude should be 5,000 ft RA
• Note 2.	IAS should be decreased to 190 kt when launching AXCPs

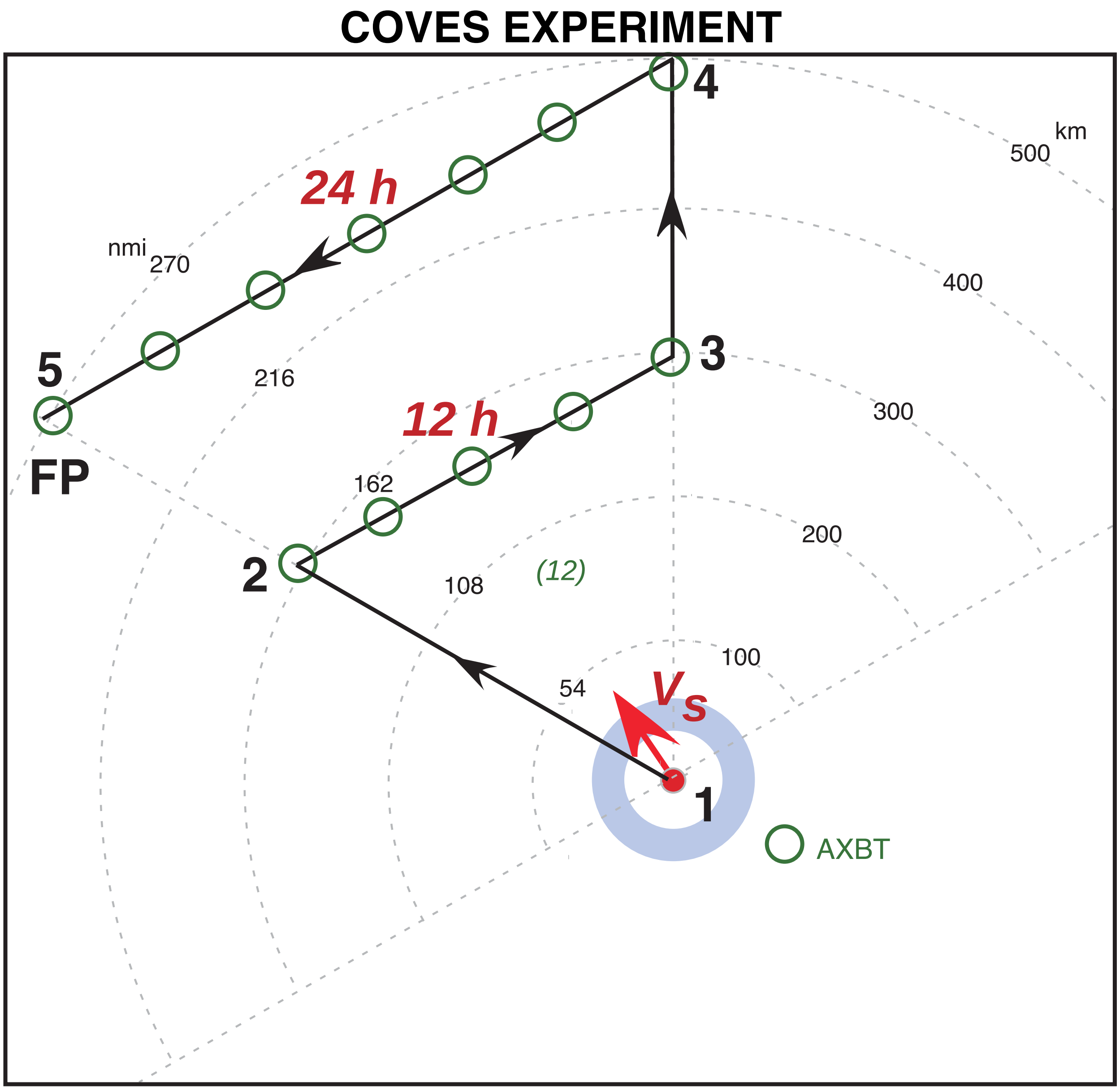

Fig. 1. (c) Pre-storm Ocean Survey Module

• Note 1.	Aircraft should begin pattern at the end of the COVES mission if there is enough time to complete it during the ferry home.
• Note 2.	The pattern may be entered at any compass heading, and entry azimuth should be at least 30° downwind of the current storm motion (V_s) with cross track legs at estimated 12-h and 24-h storm displacements based on current storm track.
• Note 3.	The first cross-track leg (**2-3**) may be omitted if this portion of the storm was already well-sampled during the primary mission.
• Note 4.	If there are any scatterers the airborne Doppler radar should be operated in F/AST mode, with a single PRF of 2400 or greater, and a tilt of 20°.

COVES EXPERIMENT

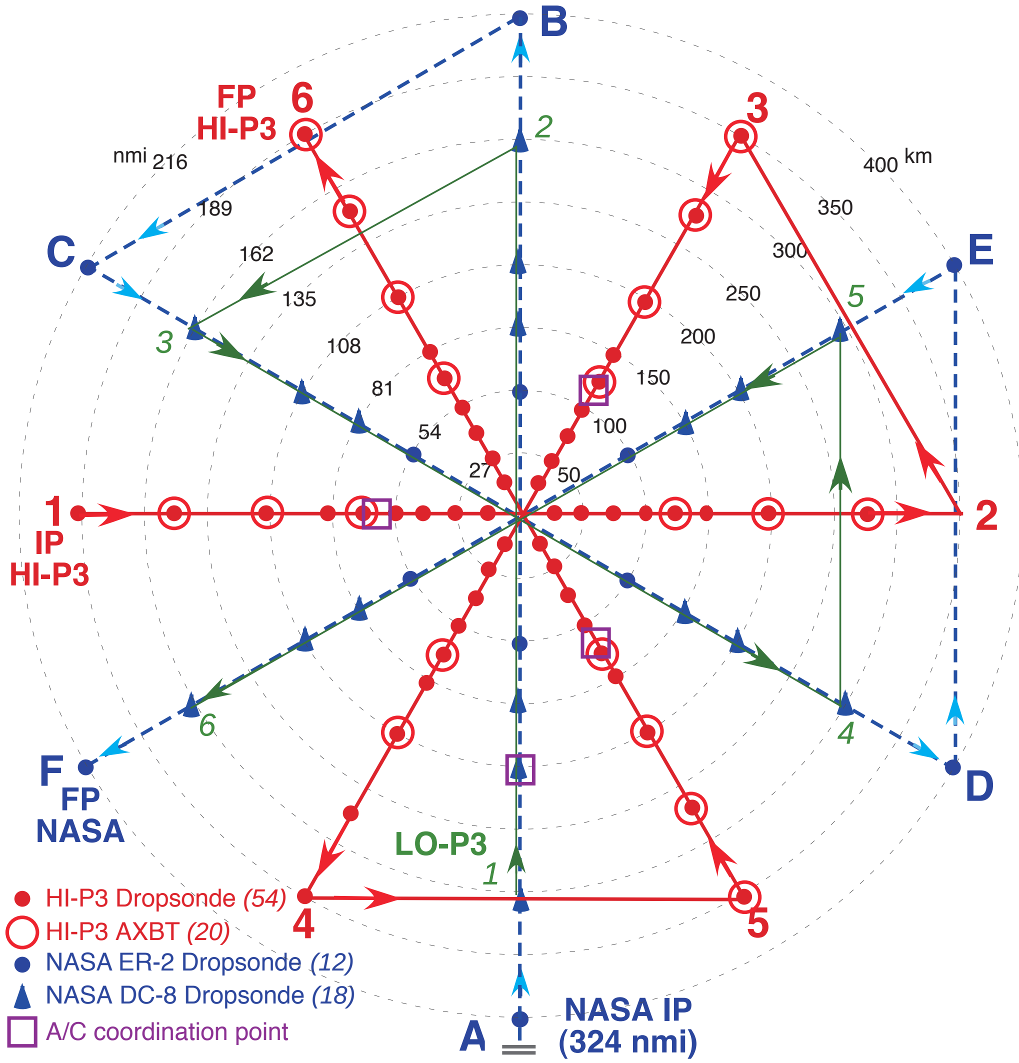

Fig. 2. Coordinated Pattern: (a) Upper WP-3D, DC-8, and ER-2

• Note 1.	All aircraft should reach their respective IP's as simultaneously as possible, and the upper WP-3D is responsible to ensure that all aircraft depart the coordination points together.
• Note 2.	Aircraft should not deviate from pattern to find the center in the eye.
• Note 3.	The pattern may be entered at any compass heading and the DC-8 and ER-2 entries should be along the same heading as the lower WP-3D, 90° downwind from the upper WP-3D.
Note 4.	The DC-8 should attain the 250-hPa level (about 37,000 ft or FL370) as early in the mission as possible and then maintain this altitude for the duration of the pattern. Upper WP-3D should begin pattern at 18,000 ft, then climb to maintain maximum safe altitude.
• Note 5.	WP-3D Doppler radar should be operated in F/AST mode at a single PRF ≥2400 and 20° tilt.
• Note 6.	GPS-sondes and the downward-pointing laser on the NASA aircraft may pose a hazard to the WP-3D or WC-130. Communication with these aircraft is the responsibility of the NASA aircraft and must be obtained before sondes are released.

COVES EXPERIMENT

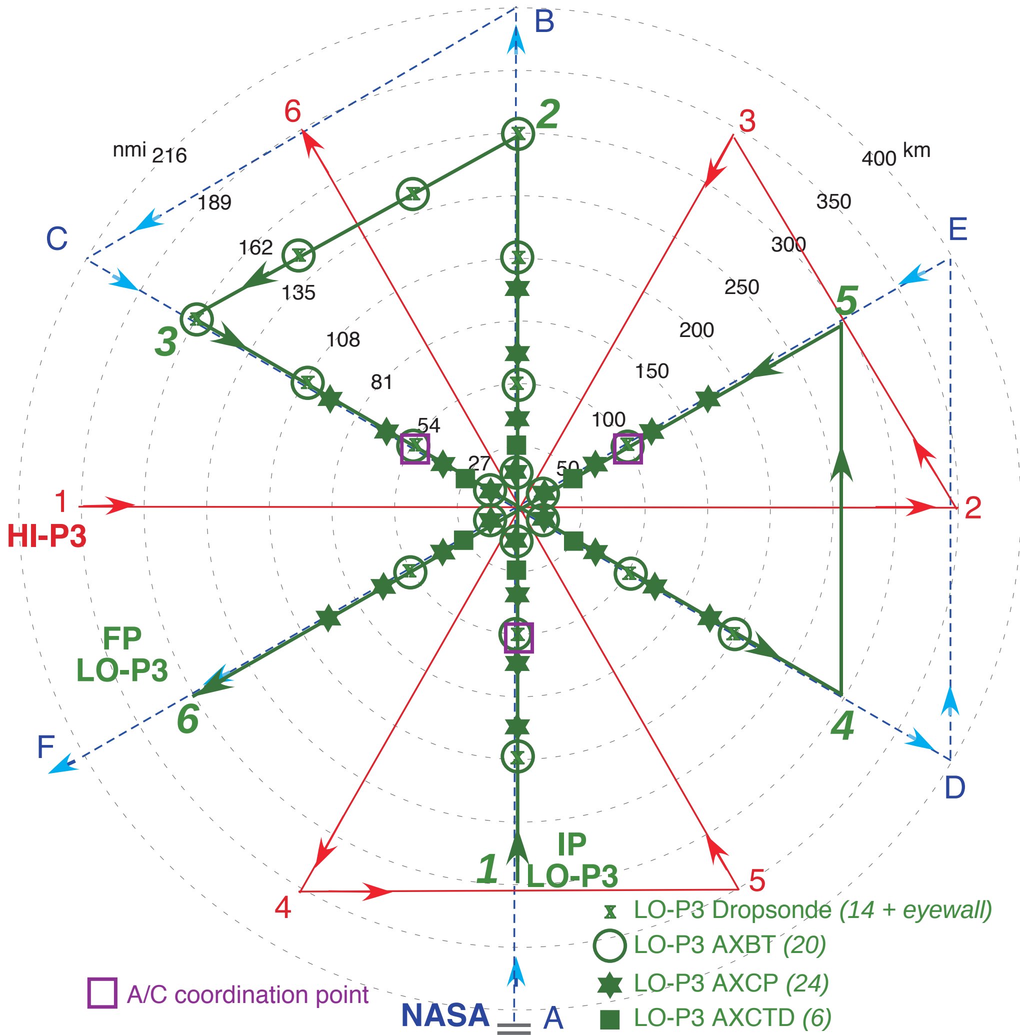

Fig. 2. Coordinated Pattern: (b) Lower WP-3D

• Note 1.	All aircraft should reach their respective IP's as simultaneously as possible.
• Note 2.	Aircraft should not deviate from pattern to find the center in the eye.
• Note 3.	The pattern may be entered at any compass heading and the DC-8 and ER-2 entries should be along the same heading as the lower WP-3D.
• Note 4.	The lower WP-3D aircraft should fly at 5,000-12,000 ft.
• Note 5.	WP-3D Doppler radar should be operated in F/AST mode at a single PRF ≥2400 and 20° tilt.
• Note 6.	Lower WP-3D sondes and AXBTs within the eyewall are launched at the discretion of the lead scientist.

COVES EXPERIMENT

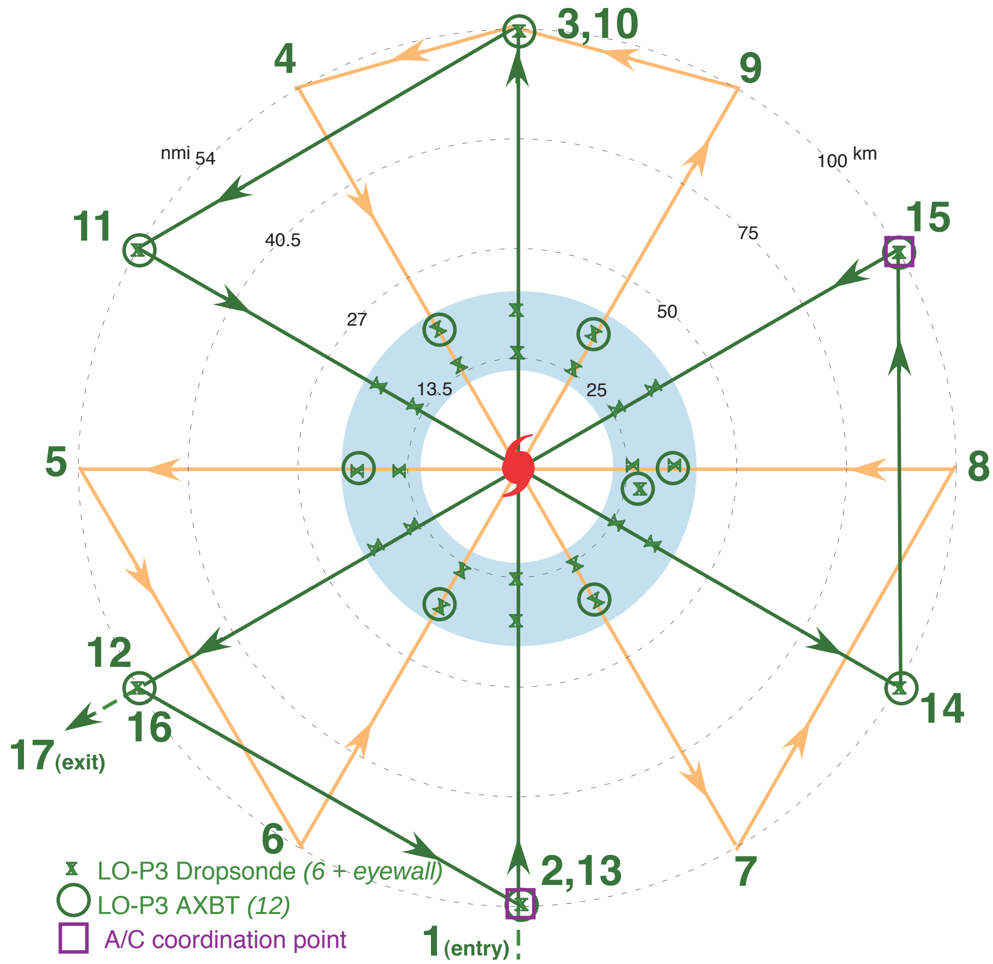

Fig. 2. Inner Core Pattern: (c) Lower WP-3D only

• Note 1.	All aircraft should reach their respective IP's as simultaneously as possible.
• Note 2.	No AXCPs or AXCTDs are launched during this module.
• Note 3.	Lower WP-3D aircraft should fly at 5,000-12,000 ft (1,500-3,500 m).
• Note 4.	Lower WP-3D aircraft will modify pattern to coordinate with upper WP-3D at **2** and **15**.
• Note 5.	Lower WP-3D sondes and AXBTs dropped in the eyewall are launched at the discretion of the lead scientist.
• Note 6.	WP-3D Doppler radar should be operated in continuous modes on all radial penetrations and F/AST mode on all downwind legs.

COVES EXPERIMENT

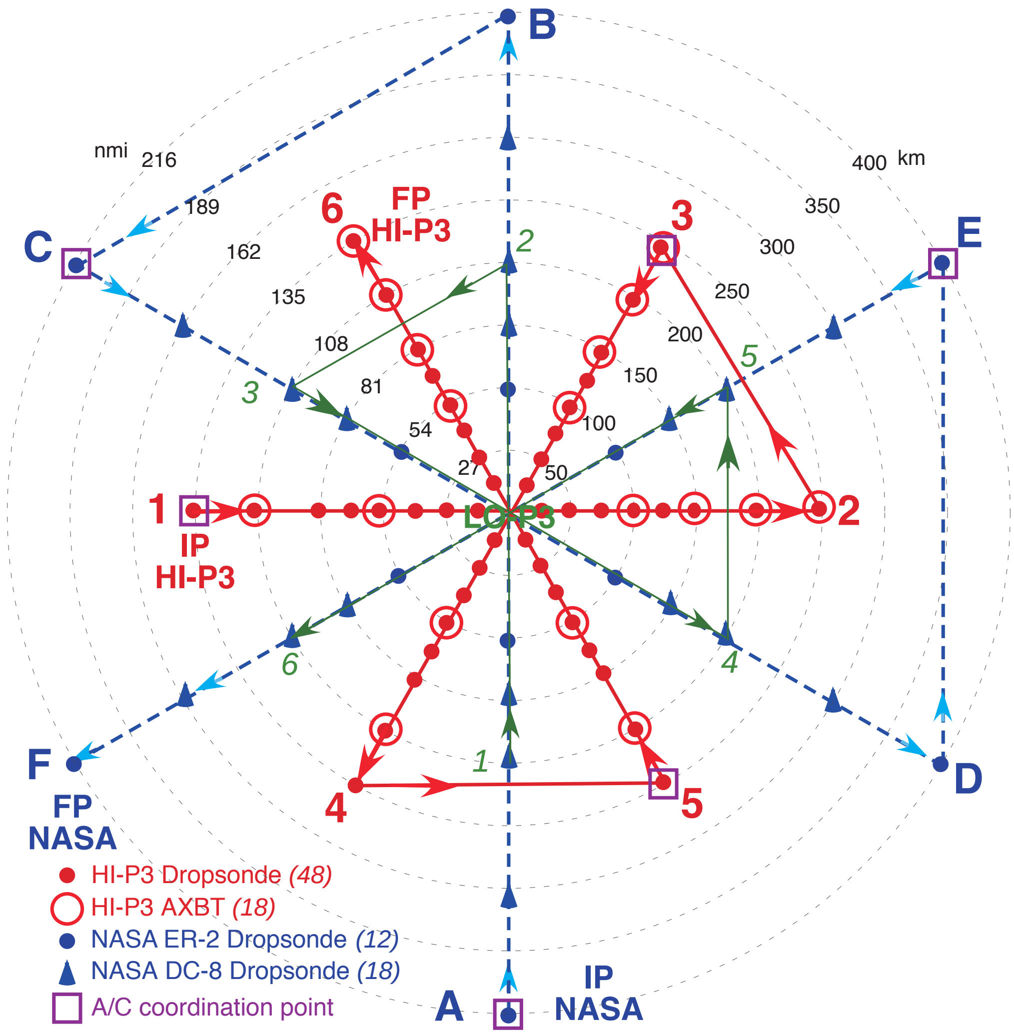

Fig. 3. Coordinated Short Pattern: (a) Upper WP-3D, DC-8, and ER-2

- Note 1. All aircraft should reach their respective IP's as simultaneously as possible, and the upper WP-3D is responsible to ensure that all aircraft depart the coordination points together.
- Note 2. Aircraft should not deviate from pattern to find the center in the eye.
- Note 3. The pattern may be entered at any compass heading and the DC-8 and ER-2 entries should be along the same heading as the lower WP-3D, 90° downwind from the upper WP-3D.

Note 4. The DC-8 should attain the 250-hPa level (about 37,000 ft or FL370) as early in the mission as possible and then maintain this altitude for the duration of the pattern. Upper WP-3D should begin the pattern at 18,000 ft, then climb to maintain maximum safe altitude.

- Note 5. WP-3D Doppler radar should be operated in F/AST mode at a single PRF $\geq$2400 and 20° tilt.
- Note 6. GPS-sondes and the downward-pointing laser on the NASA aircraft may pose a hazard to the WP-3D or WC-130. Communication with these aircraft is the responsibility of the NASA aircraft and must be obtained before sondes are released.

COVES EXPERIMENT

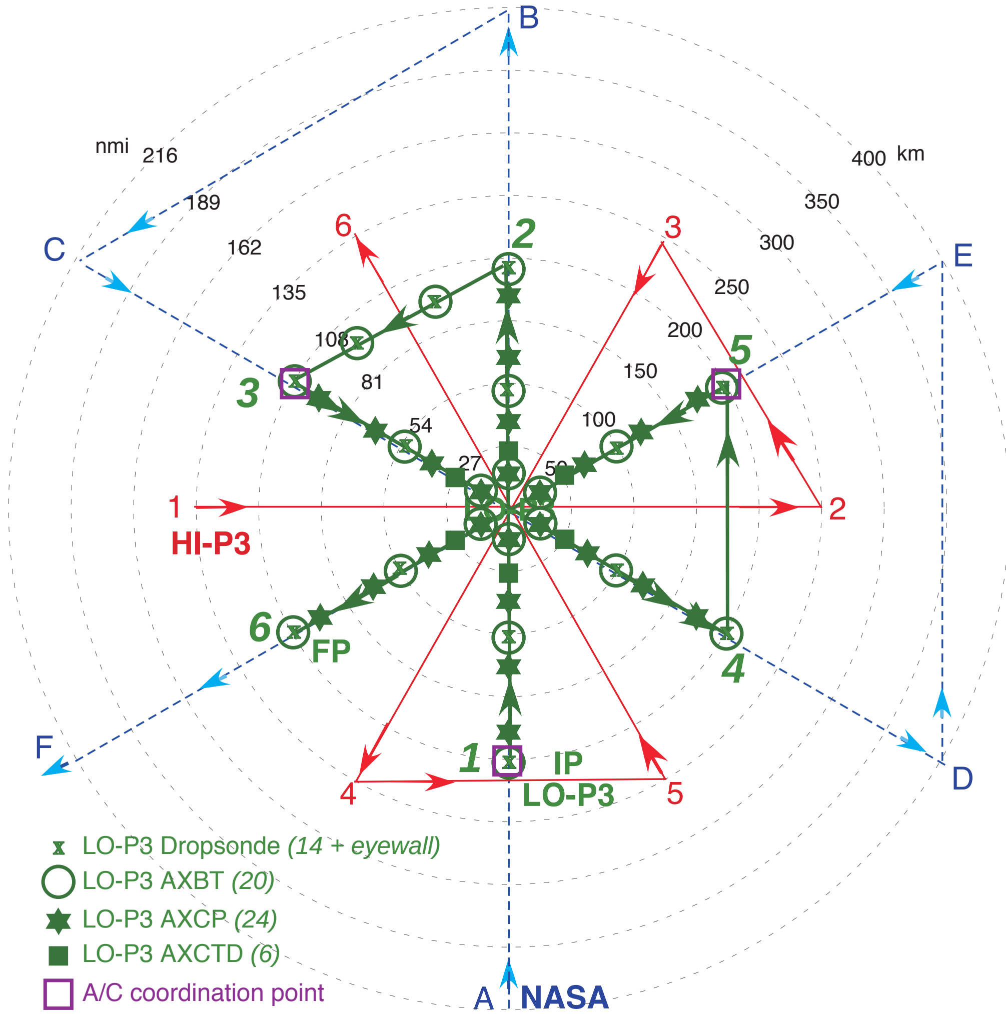

Fig. 3. Coordinated Short Pattern: (b) Lower WP-3D

• Note 1.	All aircraft should reach their respective IP's as simultaneously as possible.
• Note 2.	Aircraft should not deviate from pattern to find the center in the eye.
• Note 3.	The pattern may be entered at any compass heading and the DC-8 and ER-2 entries should be along the same heading as the lower WP-3D.
• Note 4.	The lower WP-3D aircraft should fly at 5,000-12,000 ft.
• Note 5.	WP-3D Doppler radar should be operated in F/AST mode at a single PRF ≥2400 and 20° tilt.
• Note 6.	Lower WP-3D sondes and AXBTs within the eyewall are launched at the discretion of the lead scientist.
• Note 7.	Lower WP-3D is responsible for remaining coordinated with DC-8 and ER-2 during legs 2-3.

COVES EXPERIMENT

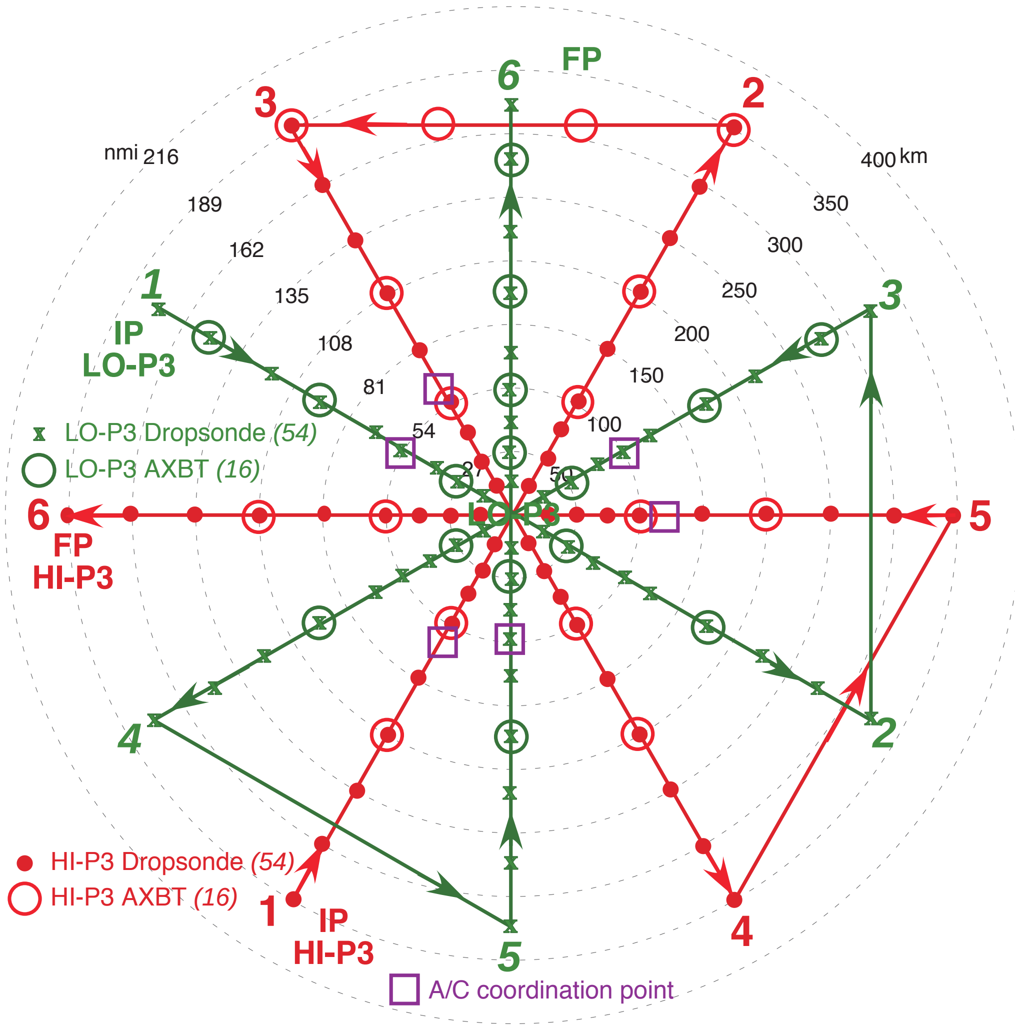

Fig. 4. Coordinated WP-3D Only Pattern

• Note 1.	Aircraft should not deviate from pattern to find the center in the eye.
• Note 2.	The pattern may be entered at any compass heading, with higher WP-3D entering 90° downwind of lower WP-3D.
• Note 3.	Aircraft should reach their respective IP's as simultaneously as possible, and the upper WP-3D is responsible to ensure that all aircraft depart the coordination points together.
• Note 4.	Upper WP-3D should begin the pattern at 18,000 ft, then climb to maintain maximum safe altitude. Lower WP-3D aircraft should fly ≥2,000 ft below the upper WP-3D.
• Note 5.	WP-3D Doppler radar should be operated in F/AST mode at a single PRF ≥2400 and 20° tilt.
• Note 6.	Lower WP-3D sondes and AXBTs within the eyewall are launched at the discretion of the lead scientist.

COVES EXPERIMENT

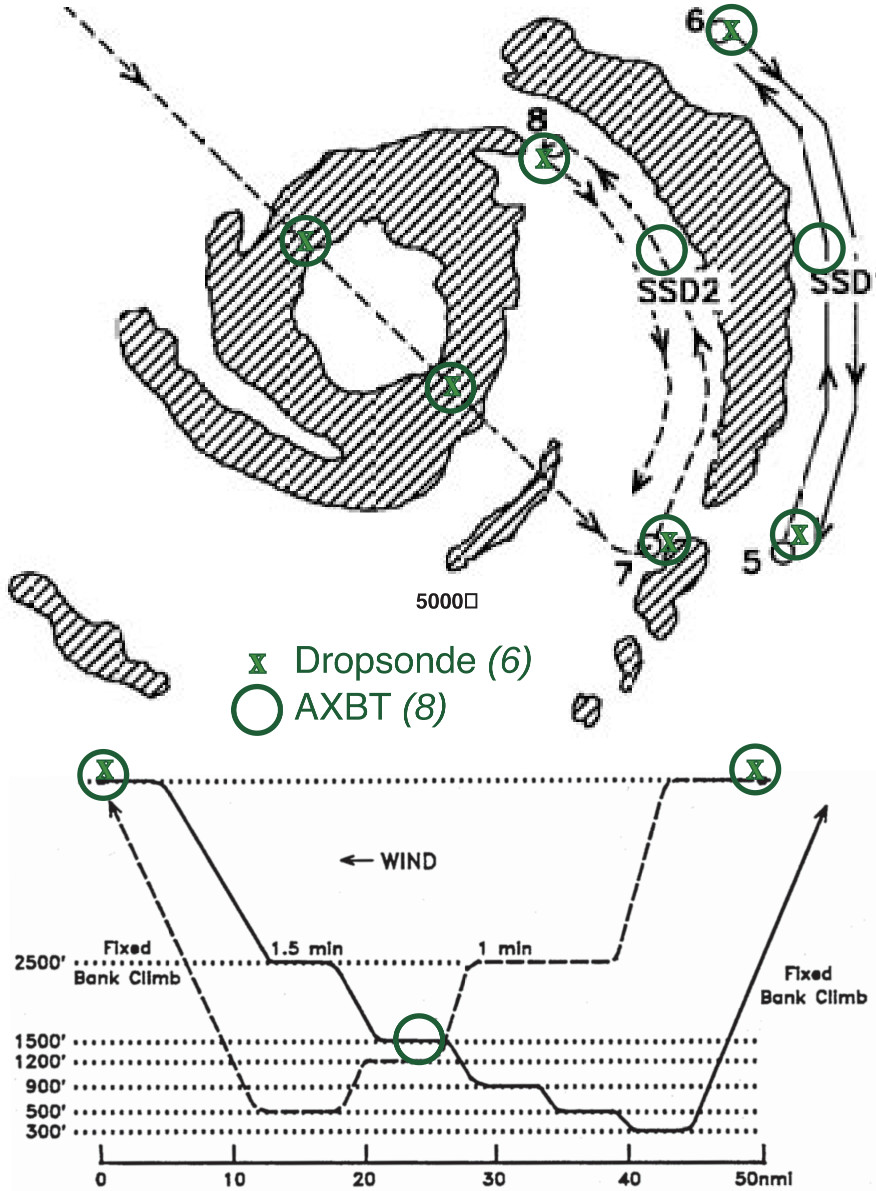

Fig. 5. CBLAST Option Pattern

• Note 1.	Aircraft commences stair-step descent (SSD) patterns in clear between **5–6**, **7–8**, maintaining ~5 nmi (10 km) separation from edge of band.
• Note 2.	Descent/ascent rate of 1,000 ft min^{-1}.
• Note 3.	WP-3D Doppler radar should be operated in F/AST mode at a single PRF ≥2400 and 20° tilt

10. Extended Cyclone Dynamics Experiment (XCDX)

Program significance: The original Vortex Dynamics Experiment has produced several hundred statistically independent samples of Atlantic or Eastern Pacific TCs since the late 1970s. HRD currently extends this data base by augmenting its own observations with flight–level observations from reconnaissance flights by the IWRS–equipped WC–I30Hs of the Air Force Reserves' (AFRES) 53rd Weather Squadron. The value of the otherwise excellent AFRES observations is compromised by a lack of accompanying oceanographic, vertical velocity, cloud microphysics, or radar reflectivity data. The AFRES aircraft typically remain on station for 4–6 h, flying figure–4 (ALFA) patterns at 850 or 700 hPa [5,000 or 10,000 ft (1.5 or 3.0 km) altitude] with 150 nmi (278 km) legs oriented along the cardinal directions. Between sorties, there is usually a gap of 6–7 h, during which no aircraft is in the TC, except near landfall when the interval between fixes decreases to 3 h. Experience with AFRES observations shows that they document the evolution of the TC core well, but that they are even more valuable when augmented by occasional sorties of the NOAA WP–3Ds. Flight patterns designed to achieve this purpose also provide a general characterization of the storm for a moderate expenditure of flight hours and air–dropped probes. For this reason, successive sorties with the same patterns are a proven strategy for documentation of the storm's life cycles. The flight patterns are also well suited to operation with NASA aircraft during CAMEX-4.

A warm ocean with a mixed layer deep enough to inhibit storm–induced cooling provides the necessary energy for TC intensification. The conventional reason offered for shears negative effect on intensification has been that it ventilates the vortex by blowing warm air out of the core aloft. Recent work suggests that the asymmetric distribution of convection and shear–induced tilt of the vortex may be more significant. Eddy momentum import may play a role as well—not through direct spin up of the swirling wind, but rather through induced outflow near the tropopause, which destabilizes the tropospheric column and strengthens the convection. Rapid intensification, apparently triggered by some combination of a warm ocean, low shear, and possibly favorable eddy momentum fluxes, is a one of the most challenging problems that forecasters face.

Objective: This experiment is designed to provide a general characterization of the TC out to a radius of ~500 km in order to study the mechanisms by which environmental shear and eddy fluxes control TC intensity changes. A secondary objective is to obtain a time series of eye soundings to study the thermodynamics of intensity change.

Mission Description: The Vortex Option combines flight–level data, AXBTs, GPS sondes, and Radar data from the WP-3Ds with continuous coverage AFRES flight-level data in the lower troposphere and perhaps periodic observations from NASA's DC8 and ER2 in the upper troposphere or lower stratosphere to document the TCs life cycle and interactions with the environment. The WP-3Ds fly successive star, ALFA, or rotating ALFA patterns out to 200–300 km at 600–500 hPa {15,000–18,000 ft), dispensing AXBTs from the external chutes and GPS sondes. Thus, combined flights with the NASA aircraft can observe both the near–field environmental forcing and the vortex response. The ideal target is a northward moving TC that has a fairly small Central Dense Overcast (CDO) and is expected to interact with vertical shear, an approaching mid-latitude trough, or a upper-level low.

The WP-3Ds will fly at 500–600 hPa isobaric level (15,000–18,000 ft). Nominal flight tracks appear in Figs. 6-8. In order to avoid too much aircraft icing and electrical charging, altitude will be either the highest attainable or well below the 0°C isotherm. It is crucial to the analysis that a fixed pressure altitude be maintained throughout. The nominal leg length will be 250-300 nmi (460-550 km), but the size of the pattern will be adjusted to make the legs as long as possible given the available aircraft range. The WP-3D will deploy GPS sondes in a symmetrical pattern with increased density near the center to map the vertical kinematic and thermodynamic structure below flight level. On the first and last pass through the center it will deploy a sonde as close to the axis of vortex rotation as possible to study the thermodynamic transformations of the eye. It will also deploy AXBTs ahead of the storm and on the right hand side of the track to map the preexistent oceanic structure and storm–induced response.

The full–blown XCDX is three maximum-endurance sorties in 42 h or four in 56 h, with alternating aircraft and crews. Nominal flight duration will be 10 h with 4-h gaps between flights. The second aircraft will takeoff 14 h after the first. The third sortie, the second flight by the first aircraft, will depart 14 h after the second sortie or 18 h after the first sortie landed. Thus, take-off times by the same aircraft and crew will shift 4 h later in the next day on subsequent flights. The aircraft may, depending upon altitude, spend a third or a quarter of its time in icing conditions under the CDO, which may compromise range. A variation of the XCDX is one or more sorties at the same altitude with shorter legs and more frequent drops in the eye to focus on eye thermodynamics or cooperation with aircraft from other agencies.

A CAMEX-4 objective is to obtain wind and precipitation measurements in the inner core of the storm using the remote sensors on the DC-8 and ER-2 (Appendix B). This mission is best when coordinated with another multi-plane experiment, to provide ground truth for the remote sensing instruments. A sample inner core mission is shown in Fig. 9a. The DC-8 aircraft and the ER-2 will take off a half to one hour after the two WP-3D aircraft in order to coordinate the in-storm patterns. Subject to safety and operational constraints, the DC-8 will fly as high as possible between 20,000 ft (FL200) and 40,000 ft (FL400) and at an altitude low enough to minimize cloud interference with nadir lidar (LASE) water vapor measurements. The WP-3D lead scientist will pass storm position, storm motion, and a recommended IP to the DC-8 lead scientist. The nominal leg length will be 200-300 nmi (370-550 km), but the size of the pattern will be adjusted to make the legs as long as possible given the available aircraft range. A sample inner core pattern (Fig. 9b), designed to provide detailed observations of the eye and eyewall structure, is executed at the discretion of the DC-8 lead scientist in coordination with the WP-3D lead scientist.

XCDX EXPERIMENT

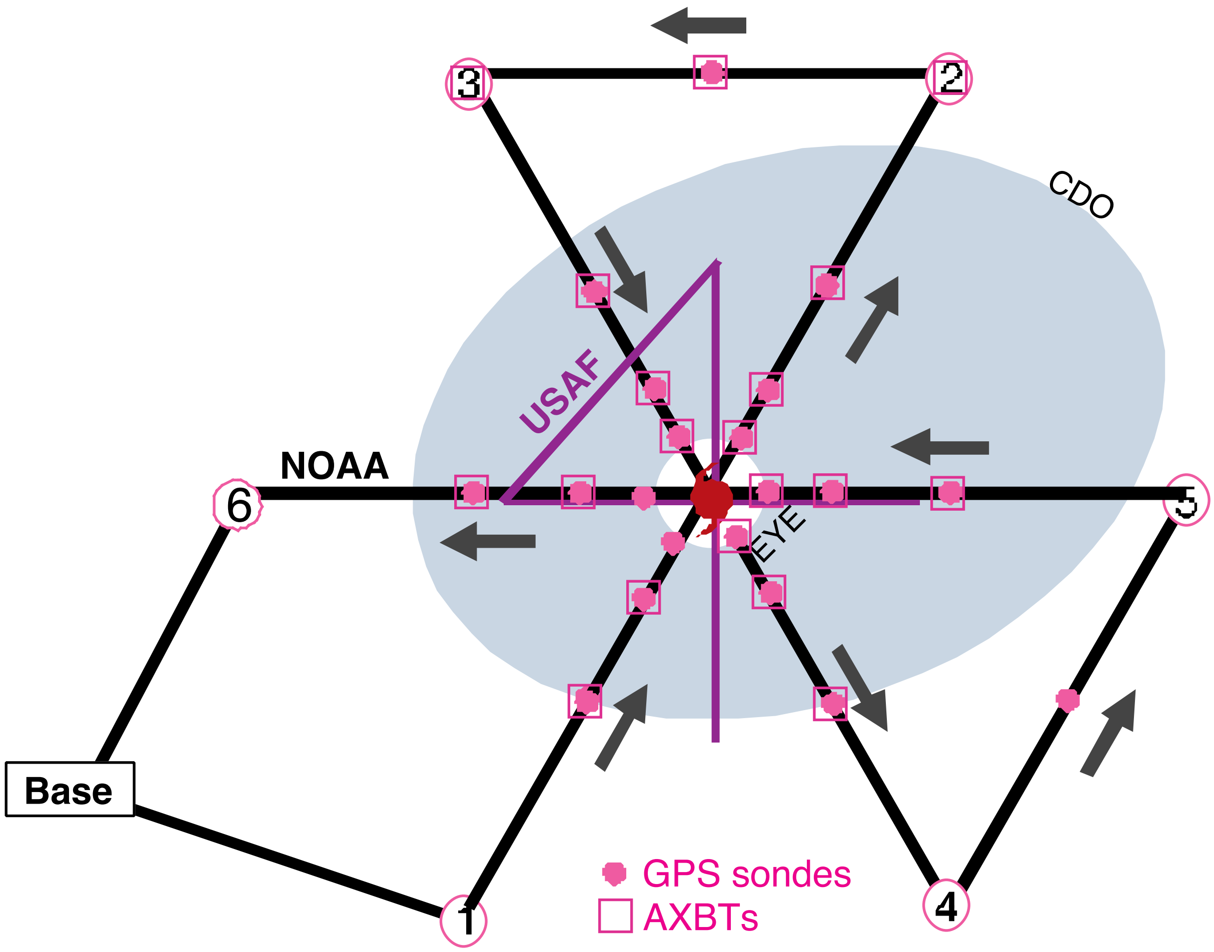

Fig. 6. **Basic (STAR) Flight Pattern**

• Note 1.	WP-3Ds fly **1–§–2–3–§–4–5–§–6** at 500 hPa pressure altitude if the CDO is small, or at 15,000 ft (4.5 km) radar altitude to avoid icing if it is large. The leg length is the longest possible given aircraft range and ferry distance to the storm.
• Note 2.	Dropwindsonde (and AXBTs as indicated) observations occur after numbered turns, at the midpoints of the legs, at the 3/4 point half way between the midpoint and the center, and in the center on the first and last passage through the eye.
• Note 3.	When successive WP-3D sorties are flown, each WP-3D sortie will take off is 19 h after the previous one.
• Note 4.	Airborne Doppler radar scans perpendicular to the aircraft track within 50 nmi (95 km) of the center on penetration and exit, and on F/AST elsewhere.

XCDX EXPERIMENT

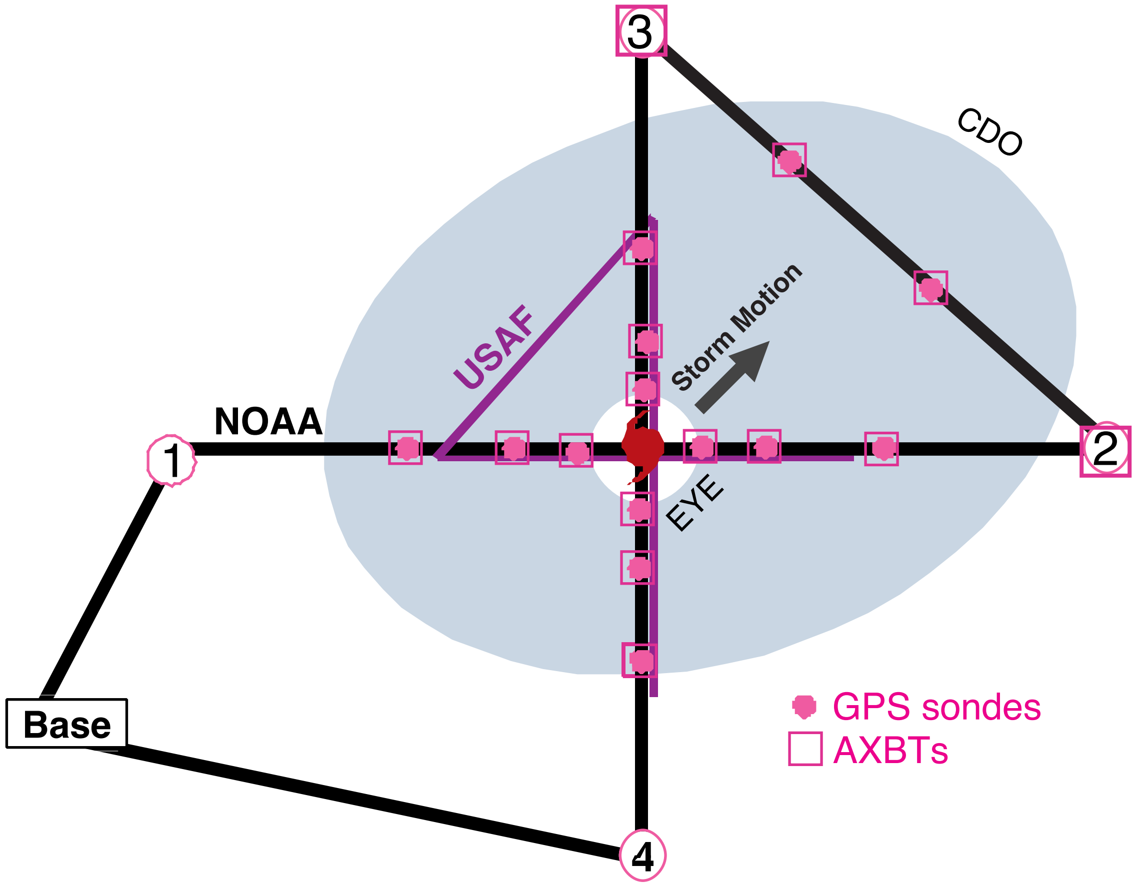

Fig. 7. **Figure–4 (ALFA) Flight Pattern**

• Note 1.	WP-3Ds fly **1—§—2—3—§—4** at 500 hPa pressure altitude if the CDO is small, or at 15,000 ft (4.5 km) radar altitude to avoid icing if it is large. The leg length is the longest possible given aircraft range and ferry distance to the storm.
• Note 2.	Dropwindsonde (and AXBTs as indicated) observations occur after numbered turns, at the midpoints of the legs, at the 3/4 point half way between the midpoint and the center, and in the center on the first and last passage through the eye.
• Note 3.	When successive WP-3D sorties are flown, each will take off 19 h after the previous one.
• Note 4.	Airborne Doppler radar scans perpendicular to the aircraft track within 50 nmi (95 km) of the center on penetration and exit, and on F/AST elsewhere.

XCDX EXPERIMENT

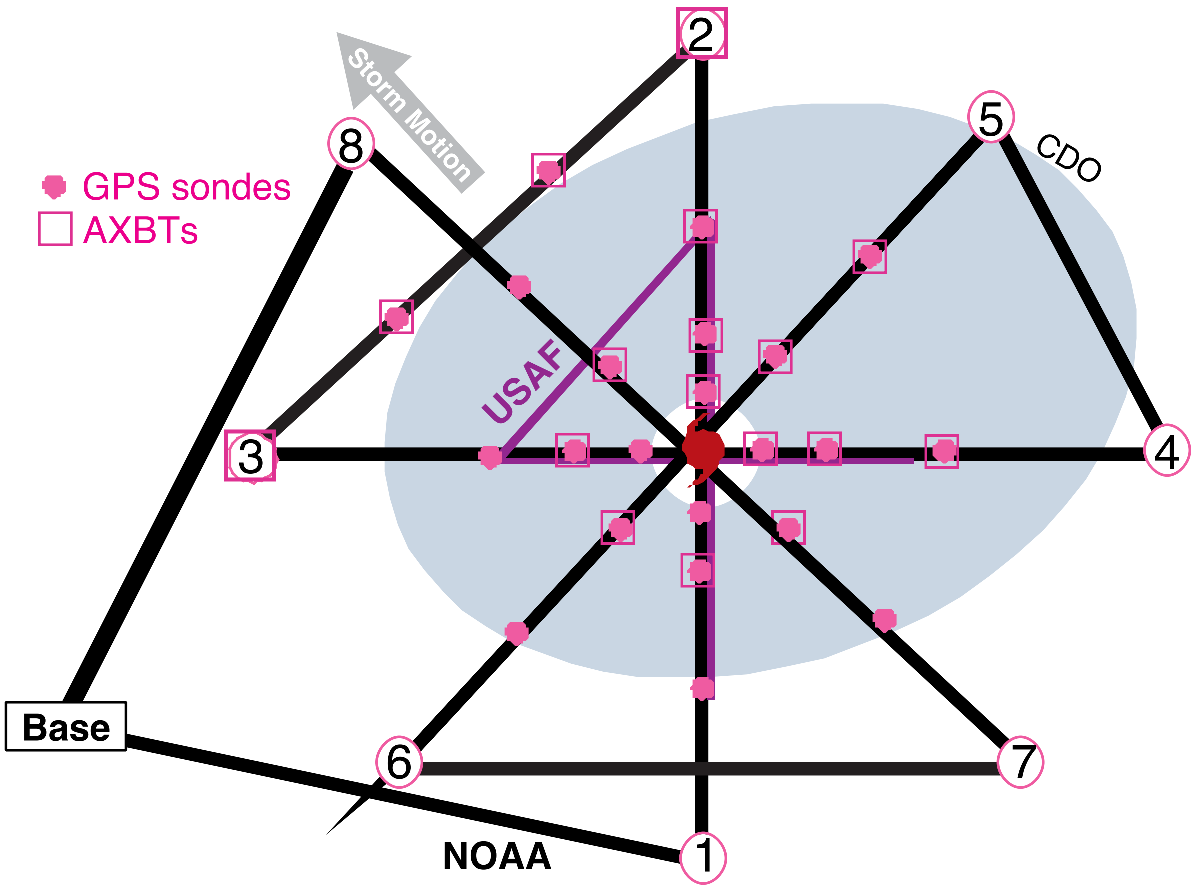

Fig. 8. **Rotating Figure–4 (ALFA) Flight Pattern**

• Note 1.	WP-3Ds fly **1—§—2—3—§—4—5—§—6—7—§—8** at 500 hPa pressure altitude if the CDO is small, or at 15,000 ft (4.5 km) radar altitude to avoid icing if it is large. The leg length is the longest possible given aircraft range and ferry distance to the storm.
• Note 2.	Dropwindsonde (and AXBTs as indicated) observations occur after numbered turns, at the midpoints of the legs, at the 3/4 point half way between the midpoint and the center, and in the center on the first and last passage through the eye.
• Note 3.	When successive WP-3D sorties are flown, each will take off 19 h after the previous one.
• Note 4.	Airborne Doppler radar scans perpendicular to the aircraft track within 50 nmi (95 km) of the center on penetration and exit, and on F/AST elsewhere.

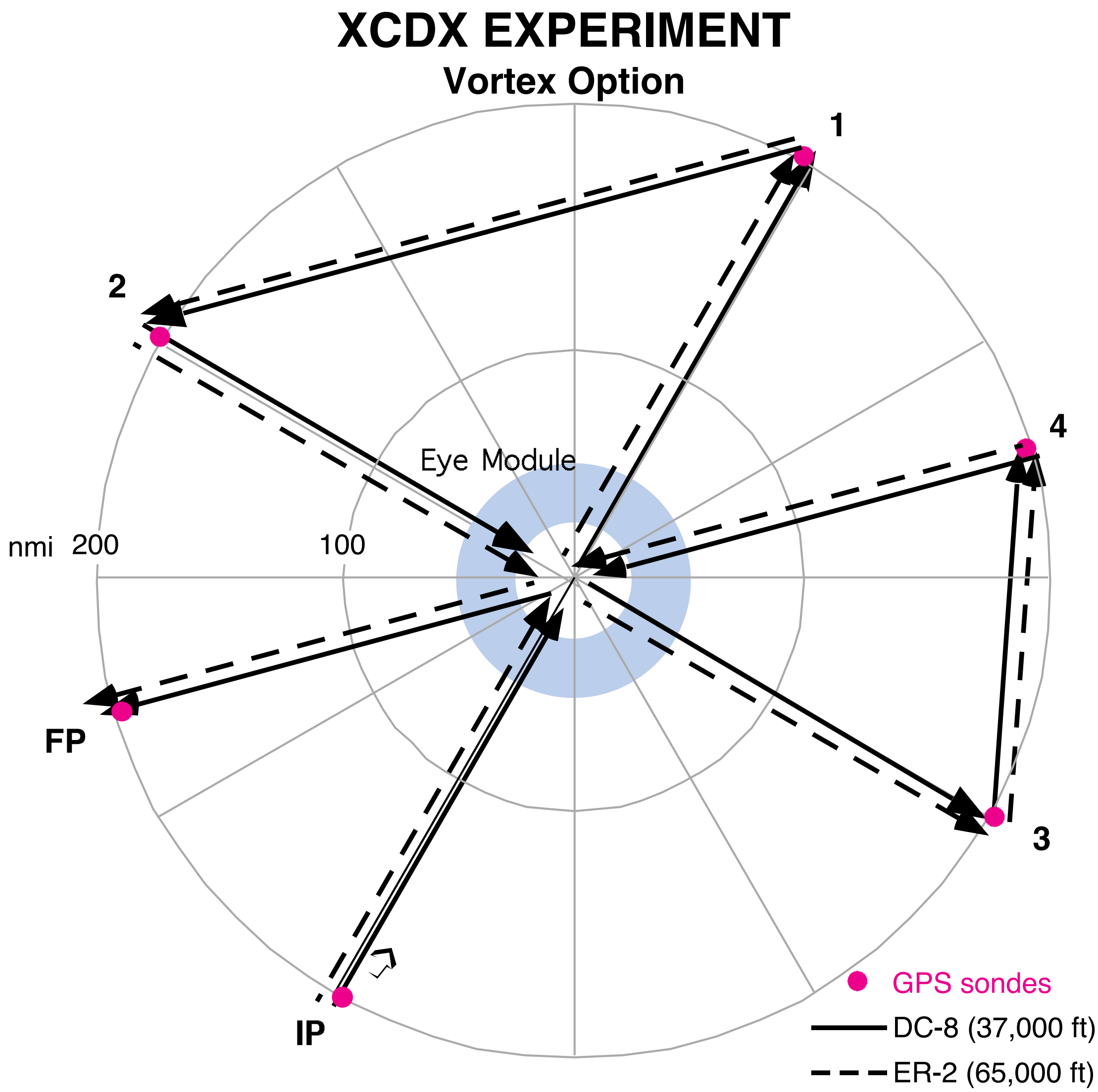

Fig. 9. (a) DC-8 and ER-2 Sample Pattern

- Note 1. Aircraft should begin pattern at approximately the same time as the WP-3D's, but precise coordination is not required.
- Note 2. Aircraft should not deviate from pattern to find the wind center in the eye.
- Note 3. The pattern may be entered at any compass heading, and entry azimuth should be at least 30° downwind of the entry azimuth of the WP-3D or WC-130 aircraft.
- Note 4. The DC-8 should attain the 250-hPa level (about 37,000 ft [FL 370) as early in the mission as possible and then maintain this altitude for the duration of the pattern.
- Note 5. If desired GPS sondes should be released at IP and turn points.
- Note 6. GPS sondes and the downward-pointing lasers may pose a hazard to the WP-3D or WC-130 aircraft. Therefore positive communication with these aircraft must be obtained before these sondes are released.
- Note 7. Total pattern length is approximately 1800 nmi (3330 km).

XCDX EXPERIMENT

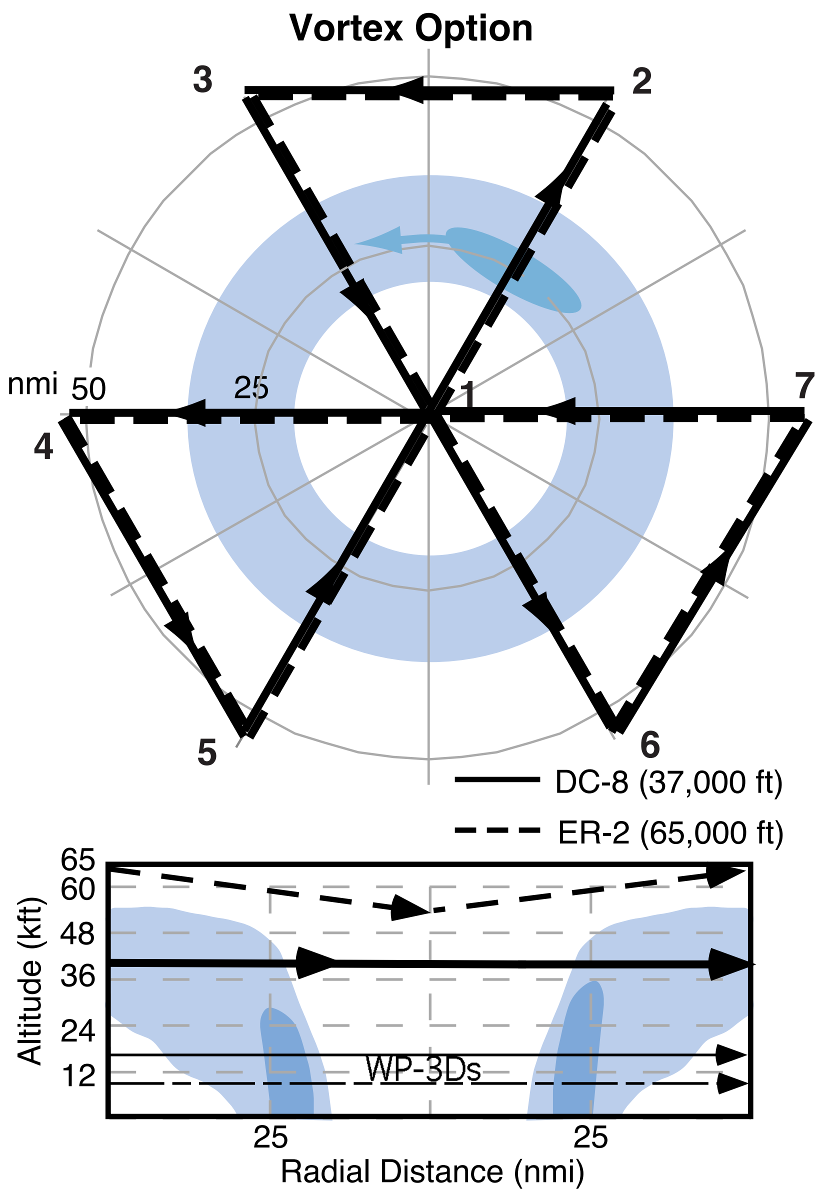

Fig. 9. (b) DC-8 and ER-2 Sample Eyewall Module

- Note 1. Aircraft should begin pattern at approximately the same time as one of the WP-3D's crosses the eyewall, but does not have to be precisely coordinated.
- Note 2. The radial legs should be rotated counterclockwise to insure that they cross the region of interest as it rotates around the eyewall.
- Note 3. The DC-8 flies at 37,000 ft and the ER-2 at 65,000 ft except when it performs a slight dip in the eye to 58,000 ft for an ozone and moisture profile.
- Note 4. Pattern should take no more than 1 h.

11. Tropical Cyclone Wind Fields Near Landfall Experiment

Program Significance: An accurate real-time description of the TC surface wind field near and after landfall is important for warning, preparedness, and recovery efforts. During a hurricane threat, an average of 300 nmi (550 km) of coastline is placed under a hurricane warning, which costs about $50 million in preparation per event. The size of the warned area depends on the extent of hurricane and tropical storm force winds at the surface, evacuation lead-times, and the forecast of the storm's track. Research has helped reduce uncertainties in the track and landfall forecasts, but now there is an opportunity to improve the accuracy of the surface wind fields in TCs, especially near landfall.

HRD is developing a real-time surface wind analysis system to aid the TPC/NHC in the preparation of warnings and advisories in TCs. The real-time system was first tested in Hurricane Emily of 1993. It reduces uncertainties in the size of hurricane warning areas and is used for post-storm damage assessment by emergency management officials. The surface wind analyses can also be useful for validation and calibration of an operational inland wind forecast model that HRD has developed under Federal Emergency Management Agency (FEMA) sponsorship. The operational storm surge model (SLOSH) could also be run in real-time with initial data from the surface wind analysis.

As a TC approaches the coast, surface marine wind observations are normally only available in real-time from National Data Buoy Center (NDBC) moored buoys, C-MAN platforms, and a few ships. Surface wind estimates must therefore be based primarily on aircraft measurements. Low-level (<5,000 ft (1.5 km] altitude) NOAA and Air Force Reserve aircraft flight-level winds are adjusted to estimate surface winds. These adjusted winds, along with C-SCAT, SFMR, and GPS-sonde wind estimates, are combined with actual surface observations to produce surface wind analyses. These surface wind analyses were initially completed after Hurricane Hugo's landfall in South Carolina and Hurricane Andrew's landfall in South Florida in support of post-landfall damage surveys conducted by FEMA. In recent years, these analyses have been produced in real-time for operational use by the NHC for many of the TCs that have affected the Western Atlantic basin, including such notable landfalling storms as Opal (1995), Fran (1996), Georges (1998), Bret (1999), and Floyd (1999).

The surface wind analyses may be improved by incorporating airborne Doppler radar-derived winds for the lowest level available (~3,000 ft [1.0 km]). To analyze the Doppler data in real-time, it is necessary to use a Fourier estimation technique. The Velocity-Track Display (VTD) was developed to estimate the mean tangential and radial circulation in a vortex from a single pass through the eye. The technique was applied to Doppler data collected in Hurricane Gloria (1985) and found that the mean winds corresponded well with winds derived by pseudo-dual Doppler (PDD) analysis. The extended VTD (EVTD) was subsequently developed to combine data from several passes through the storm, resolving the vortex circulation up through the wave # 1 component. EVTD was used on data collected during six passes into Hurricane Hugo (1989) to show the development of mean tangential winds >100 kt (50 m s-1) over 7 h. EVTD analyses are computed quickly on the airborne HRD workstation and could be sent to TPC/NHC shortly after their computation. The wind estimates could then be incorporated into the real-time surface wind analyses.

Dual-Doppler analysis provides a more complete description of the wind field in the inner core. While these techniques are still too computationally intensive for real-time wind analysis, the data are quite useful for post-storm analysis. An observational study of Hurricane Norbert (1984), using a PDD analysis of airborne radar data to estimate the kinematic wind field, found radial inflow at the front of the storm at low levels that switched to outflow at higher levels, indicative of the strong shear in the storm's environment. Another study used PDD data collected in Hurricane Hugo near landfall to compare the vertical variation of winds over water and land. The profiles showed that the strongest winds are often not measured directly by reconnaissance aircraft.

By 1989, both NOAA WP-3D aircraft were equipped with Doppler radars. A study of Eastern Pacific Hurricane Jimena (1991) utilizing several three-dimensional wind fields from true dual-Doppler data collected by two WP-3D's showed that a pulse of radial wind developed in the eyewall with a corresponding decrease in the tangential winds. By the fourth pass, however, the radial pulse was gone and the tangential winds had returned to their previous value. These results suggested that the maintenance of a mature storm might not be a steady-state process. Further study is necessary to understand the role of such oscillations in eyewall maintenance and evolution.

While collection of dual-Doppler radar data by aircraft alone requires two WP-3D aircraft flying in well-coordinated patterns, a time series of dual-Doppler data sets could be collected by flying a single WP-3D toward or away from a ground-based Doppler radar. In that pattern, the aircraft Doppler radar rays are approximately orthogonal to the ground-based Doppler radar rays (Fig. 10), yielding true Dual-Doppler coverage. Starting in 1997, the Atlantic and Gulf coasts were covered by a network of Doppler radars (WSR-88D) deployed by the National Weather Service (NWS), Department of Defense, and Federal Aviation Administration (Fig C-5 in Appendix C). Each radar has a digital recorder to store the base data (Archive Level II). In precipitation or severe weather mode, the radars will collect volume scans every 5-6 min.

If a hurricane or strong tropical storm (i.e., one with sufficient radar scatterers to define the vortex) moves within 125 nmi (230 km) of the coast of the Eastern or Southern United States, then a WP-3D will obtain Doppler radar data to be combined with data from the closest WSR-88D radars in dual-Doppler analyses. The tail radar is tilted to point 20° forward and aft from the track during successive sweeps (the fore-aft scanning mode F/AST). These analyses could resolve phenomena with time scales <10 min, the time spanned by two WSR-88D volume scans. This time series of dual-Doppler analyses will be used to describe the storm's inner core wind field and its evolution. The flight pattern for this experiment is designed to obtain dual-Doppler analyses at intervals of 10-20 min in the inner core. Unfortunately, these WSR-88D /aircraft dual-Doppler analyses will not be available in real-time, but the Doppler wind fields could be incorporated into post-storm surface wind analyses. The data set will also be useful for development and testing of TC algorithms for the WSR-88D. The Doppler data will be augmented by dropping GPS-sondes near the coast, where knowledge of the boundary-layer structure is crucial for determining what happens to the wind field as a strong storm moves inland. If conditions permit, GPS-sondes will also be dropped in the eyewall in different quadrants of the TC, to add to the climatology of vertical wind profiles. To augment the inner core analyses, dual-Doppler data can also be collected in the outer portions of the storm, beyond the range of the WSR-88D, because the alternating forward and aft scans in F/AST mode intersect at 40°, sufficient for dual-Doppler synthesis of winds.

There are outstanding questions on TC rainbands and electrification that can be studied during a landfall mission. Spiral-shaped patterns of precipitation characterize radar and satellite images of TCs. The earliest radar observations of TCs detected these bands, which are typically 3-36 nmi (5-50 km) wide and 55-160 nmi (100-300 km) long. Nevertheless, many aspects of their formation, dynamics, and interaction with the symmetric vortex are still unresolved. The precipitation-free lanes between bands tend to be somewhat wider than the bands. The trailing-spiral shape of bands and lanes arises because the angular velocity of the vortex increases inward and distorts them into equiangular spirals. As the TC becomes more intense, the inward ends of the bands approach the center less steeply approximating arcs of circles. A dynamical distinction exists between convective bands that spiral outward from the center and convective rings that encircle the center.

The lack of rainband observations leaves us to infer and assume critical elements of rainband structure that may be of fundamental importance to our understanding of the TC. It seems clear that concentric eyewalls can affect TC intensity, and available evidence suggests that convectively active non-concentric rainbands may play a role in the intensity changes in the TC core. It is extremely important that we understand the structure of rainbands and secondary eyewalls and how they may impact the TC environment. The rainband module is designed to address these issues by gathering kinematic data in and around TC rainbands. In addition, with the new GPS-sondes, it is possible to sample some of the thermodynamic aspects of the TC boundary layer. The fluxes at the top of either the mixed layer or the thicker inflow layer are not well understood. There are no reliable measurements of the flux at the top of the inflow layer, nor are there reliable estimates of the depth of the inflow. This is despite the conclusions from budget studies and simple numerical models that identify the mixing at the top of these layers as a vital part of the TC circulation.

Recent analyses of an intense rainband in Hurricane Gilbert (1988) support the hypothesis that the fluxes at the top of the inflow layer are large and downward into the inflow layer. This is counter to the typical situation where the flux of energy is out of the layer and into the middle troposphere. These fluxes can rival the fluxes at the air-sea interface. There appeared to be regions in Gilbert where the inflow layer rapidly increased in θ_e, and other regions where the flux divergence of θ_e resulted in very slowly changing conditions. Rainband circulations have been implicated in this highly asymmetric input of energy into the storm's inflow layer. Strong rainbands like the one sampled in Gilbert are similar in circulation to an eyewall. We hypothesize that the eyewall circulation itself will have a profound affect on its own inflow, and may lead to a recycling of high θ_e, into the top of the inflow layer.

Neither the microphysical nor the electrical structure of TC clouds that exhibit lightning is known. Laboratory experiments have shown that more charge is separated when ice crystals collide with a rimed target in the presence of supercooled water than is separated without supercooled water. They also showed that the sign of the charge transferred reversed at about -20 C. Other laboratory experiments showed that the growing conditions encountered by the ice particles determined the sign of the charge that was transferred between them during collisions. Observations in continental thunderstorms support this hypothesis and suggest that charge separation occurs most rapidly on the boundary between the main updraft and the downdraft near -15 C. More recent observations showed that sublimating graupel acquire negative charge and graupel undergoing deposition acquire positive charge. As these processes depend critically upon the graupel temperature and cloud liquid water content, it is highly desirable to obtain suitable measurements in natural clouds.

In mature TCs, updraft velocities are usually low. In addition, graupel and ice particles are plentiful, but supercooled cloud water is rare in TCs at temperatures as warm as -5 C. Studies of two mature Atlantic TCs have shown that the little supercooled water present in the strongest eyewall updrafts was immediately adjacent to areas that contained high concentrations of small ice particles. When one considers the lack of supercooled water in mature TCs, it is not surprising that mature TCs are not always electrified. However, the National Lightning Detection Network (NLDN) detected lightning in several hurricanes and tropical storms as they approached land.

A recent investigation noted that there appeared to be a relationship between the occurrence of CG lightning in the eyewall and a subsequent intensification. A similar relationship was proposed by studies of lightning observations in two developing TCs. In each case, lightning was qualitatively associated with exceptionally strong convection, which occurred when the storms were rapidly intensifying. In addition, recent observational studies of CG lightning in TCs using data from the NLDN showed that CG lightning is most prevalent in the outer convective rainbands of TCs with little CG lightning near the eyewall. An apparent paradox is thus created as research shows that vertical velocities in rainbands are weaker than those in the eyewall. It is important to note, however, that rainbands >54 nmi (100 km) outside of the eyewall remain virtually unsampled. Based upon the above findings, we hypothesize that supercooled water and charge separation occasionally occurs in the strong convection in TCs. The recent additions of the four rotating vane field mills that measure the vector electric field and an induction ring that measures the charge on individual particles to the suite of instrumentation already on board the WP-3D aircraft will help to confirm or refute this hypothesis.

Previous observational studies have shown that the primary mechanism responsible for the decay of TCs after landfall is the large reduction in latent and sensible heat fluxes. These post-landfall reductions in surface fluxes have been shown to be the result of decreases in land temperature beneath the storm. It also has been shown that these decreases in land temperature are due to the limited heat capacity of the soil subsurface. Several studies have also shown that the rate of TC decay after landfall is proportional to the landfall intensity and that the winds associated with landfalling TCs decrease rapidly within the first few km of the coastline. However, the above findings have typically relied upon a relatively sparse observational network and/or compositing techniques that assume stationarity over a considerable length of time. Clearly, collecting high resolution landfall data sets against which the above findings can be verified is a worthwhile task, particularly in light of the substantial damage and loss of life that occurred in inland regions during Hurricanes Hugo (1989), Andrew (1992), Opal (1995), and Fran (1996).

Objectives:

- Collect flight level wind data and make surface wind estimates to improve real-time and post-storm surface wind analyses in TCs.
- Collect airborne Doppler radar to combine with WSR-88D radar data in post-storm three-dimensional wind analyses.
- Document thermodynamic and kinematic changes in the storm during and after landfall.
- Determine the kinematic and thermodynamic characteristics inside (toward the eye) and outside of TC rainbands, including those that form convective rings.
- Measure the characteristics of the middle troposphere and the TC boundary layer through utilization of GPS-sonde data.
- Determine how different inflow trajectories that may pass over land, and warmer or cooler waters alter the energy content of the inflow.
- Measure the sign and magnitude of the vector electric field near the eyewall and in an outer convective rainband.
- Determine the polarity and magnitude of the charge on ice precipitation at several temperature levels above the melting level.
- Estimate the transport of electrical charge in the storm.
- Record the types and concentrations of all particle types observed in the electrically active portions of the storm.
- Document changes in microphysics and rainfall characteristics in the storm during and after landfall.
- Obtain a remote sensing database suitable for evaluation and improvement of satellite and ground validation rainfall estimation algorithms for landfalling TCs.

Mission Description: This experiment is designed to be conducted by flying one or two single aircraft missions with a NOAA WP-3D aircraft when a TC moves within 215 nmi (400 km) of the U.S. coastline. The first of these two flights will typically consist of the real-time module followed by the rainband, electrification, or post landfall module. If the storm either moves parallel to the coastline or moves slowly, inland and resources permit, the experiment may be repeated with a second flight. While the storm's location relative to the coastline will dictate which combination of these modules will be ultimately flown, the real-time module will generally precede all of the other modules. In addition, the rainband and electrification modules will only be flown while the storm is still over water.

This mission requires that the aircraft have working lower fuselage and tail radars. The HRD workstation should be on board, so we can transmit GPS sonde and radar images back to TPC/NHC. Microphysical data should be collected, to compare rainfall rates with those used in the WSR-88D precipitation products. The SFMR should be operated, to provide estimates of wind speed at the surface. If the C-SCAT is on the aircraft then it should also be operated to provide another estimate of the surface winds. The scanning radar altimeter (SRA) is desired, to measure storm surge height and the superimposed wave field at landfall. If the storm will be within 125 nmi (230 km) of a WSR-88D, arrangements must be made to ensure that Level II data are recorded.

If the portable Doppler radars (e.g., Doppler on Wheels, DOW), portable profilers and portable wind towers are able to participate in the experiment then they should be deployed between ~65 and 130 km inland in the onshore flow regime as depicted in Fig. 14. If possible, one of the DOWs should be positioned relative to the nearest WSR-88D such that the dual-Doppler lobes cover the largest area of onshore flow possible. In the schematic depicted in Fig. 14, one of the DOWs is positioned northwest of the Melbourne WSR-88D so that one dual-Doppler lobe is over the coastal waters and the other covers the inland region. The profiler is positioned in the inland dual-Doppler lobe to provide independent observations of the boundary layer to anchor the dual-Doppler analysis.

The primary module of the experiment, the "real-time module", will support real-time and post-storm surface wind analyses. A dual-Doppler option should be flown if the storm is near a WSR-88D radar. A coastal-survey option can be flown when the storm is too close to the coast to permit radial penetrations. The flight patterns will depend on the location and strength of the storm relative to surface observing platforms and coastal radars.

Real-time module:

The real-time module combines passes over marine surface platforms with one or more figure-4 patterns in the core of the TC. The aircraft flies at or below 5,000 ft (1.5 km) (ideally at 2,500 ft [750 m]), so that flight level winds can be adjusted to 30 ft (10 m) to combine with measurements from marine surface platforms. Flight-level data and GPS-sondes dropped near the platforms will be used to validate the adjustment method. Note that if the storm is outside of WSR-88D Doppler range then the figure-4 pattern could be repeated before returning home, or the electrification module could be flown.

The landfall flight pattern should take advantage of buoys or C-MAN sites nearby. The aircraft descends at the initial point and begins a low-level figure-4 pattern, modifying the legs to fly over the buoys (Fig. 11). The radar will be in F/AST mode. If time permits the aircraft would make one more pass through the eye and then fly the dual-Doppler module. In this example, the pattern would be completed in about 2.5 h. GPS-sondes would be dropped near the buoys or C-MAN sites.

If the timing is such that the storm is farther off the coast than desired for landfall, then the aircraft can execute the Rainband Module (see Fig. 12) to map the thermodynamic structure of the inflow. The flight pattern should overfly any buoys or C-MAN sites that are in high wind regimes and if possible, include legs coordinated with a WSR-88D.

Dual-Doppler Option: If the TC moves within Doppler range of a coastal WSR-88D 125 nmi (230 km), then we will fly a second module, to collect a time-series of dual-Doppler data from the storm's inner core. Note that the optimal volume scans for this pattern will be obtained when the storm is 32-80 nmi (60-150 km) from the radar, because beyond 80 nmi (150 km) the lowest WSR-88D scan will be above 5,000 ft (1.5 km) which is too high to resolve the low-level wind field. Within 32 nmi (60 km) the volume scan will be incomplete, because the WSR-88D does not scan above 19.5°.

The pattern will depend on the location of the storm relative to the coastal radar. Depending on safety and operational considerations, the aircraft could fly this portion of the experiment at a higher altitude, although 5,000 ft (1.5 km) would still be preferred. After completing the real-time module, the aircraft flies to an initial point on the track intersecting the storm center and the coastal radar (Fig. 11). The aircraft then makes several passes through the eyewall (**A-B** in Fig. 11). Depending on the size of the eyewall each pass should last 10-20 min. It is essential that these passes be flown as straight as possible, because turns to fix the eye will degrade the Doppler radar coverage. After each pass, the aircraft turns quickly and heads back along the same track, adjusted to keep the storm center and the coastal radar on the same line. In 2 h, 6-12 volume scans will be collected. The last pass should be followed by a pass through the eye perpendicular to the other legs, to provide data for EVTD and pseudo-dual Doppler analyses. If time permits, the real-time module could be repeated before returning home, or the coastal-survey, rainband, electrification, or post-landfall module could be flown.

A major objective is to obtain wind and precipitation measurements in the inner core of the storm as it makes landfall using the remote sensors on the DC-8 and ER-2 (Appendix B). These types of observations can greatly enhance the TC Wind fields at Landfall Experiment and can provide ground truth for the remote sensing instruments. The DC-8 aircraft and the ER-2 will take off 1/2 to 1- h after the WP-3D aircraft in order to coordinate the in-storm pattern. Both aircraft will fly a coordinated inner-core pattern similar to the WP-3D's initial figure-4 (Fig. 11), with slightly longer legs to accommodate their faster groundspeed, until the storm moves inland. Subject to safety and operational constraints, the DC-8 will climb to the 250-hPa level (about FL 370) and the ER-2 climbs to 65,000 ft. Both aircraft fly over the ground test facility on Andros Island on their way to the storm. The WP-3D lead scientist will pass storm position, storm motion, and a recommended IP to the DC-8 lead scientist. Both aircraft will fly a pattern similar to (Fig. 11) until the storm moves inland. Flight legs may be abbreviated at the coast at the discretion of the DC-8 crew. The DC-8 and ER-2 should fly along WSR-88D radials if dual Doppler data are desired. The inner core pattern (Fig. 11), designed to provide detailed observations of the eye and eyewall structure, can be executed in conjunction with the WP-3D repeated passes through the eyewall along **A-B** at the discretion of the DC-8 lead scientist in coordination with the WP-3D lead scientist.

Coastal Survey option: When the TC is making landfall, this module will provide information about the boundary layer in the onshore and offshore flow regimes. The WP-3D would fly a coastal survey pattern parallel to the coast, as close as safety permits, at 5,000 ft (1.5 km) or less, and drop GPS-sondes on either side of the storm track, to sample both onshore and offshore flow regimes. The Doppler radar would be in F/AST mode, to provide wind estimates on either side of the aircraft track. This module could be flown when the TC is making landfall or after the storm moves inland. The pattern could be flown in ~1 h. GPS-sonde drops could be adjusted to be near surface platforms. The track can be adjusted to maintain optimal SRA data collection.

Rainband module:

The single aircraft rainband thermodynamic structure module has been designed to be flown with other experiments in "rainbands of opportunity" and last 30-60 min (Fig. 12). The goal of the module is to gather data inside, outside, and across several rainbands of several storms over several seasons. While individual data sets will increase our understanding of the structure of rainbands, the primary objective here is to develop a database of rainband observations for future comprehensive study.

This module requires one WP-3D flying above the inflow layer (8,000 to 10,000 ft). The WP-3D deploys 6-8 GPS-sondes and an occasional AXBT along a curved track approximately 60 nmi (100 km) long that roughly mimics the inflow trajectory for air in the sub-cloud and lower cloud layers. Deployment of the GPS-sondes occurs between the eyewall outer edge and the inner edge of any convective rainband found at greater radial distance. If there are no rainbands then sonde deployment may cease at approximately 60 nmi (100 km) radial distance from the circulation center. Fig. 12a is a plan view of the experiment; Fig. 12b is a radius-height cross-section of the scheme. Note that shorter times between each GPS-sonde launch are preferred when the aircraft is near the eyewall. A sonde should also be deployed in the eye. The mission easily can be accomplished when the aircraft is conducting a reconnaissance mission for NHC. Instead of cardinal headings to and from the eye, the aircraft follows a spiral path in and out of the circulation center. A typical spiral path should be 20-40° from a tangent to a given radius. Flight time for 60 nmi (100 km) is about 15-20 min.

GPS-sondes are deployed every 6-9 nmi (10-15 km) starting from about 6 nmi (10 km) from the outer edge of the eyewall to insure that the sonde falls outside of the main updraft and rain. After four sondes are in the air and the first sonde splashes down a new one may be deployed. The design assumes that four sondes may be in the air simultaneously and that the sonde descends at about 10 m s^{-1}.

A single spiral in or out will provide a view of how energy content changes along a trajectory for one portion of the storm. If several trajectories are sampled then energy content and cyclone intensity can be studied. Judicious choice of the inflow trajectories to be flown is made by the airborne mission scientist and would likely include sampling inflow from the southeast and from the northwest as shown in Fig. 12a.

Electrification Modules:

The aircraft must be equipped with the DRI electric field instruments in addition to the standard instrumentation. The PMS probes must be the best available, and the radars must be fully operational. The experiment is composed of two options. In both options, it is desirable to have 4 to 6 GPS-sondes to obtain soundings outside the convection in the inflow near the areas of interest. The aircraft should loiter in the eye or any other suitable area when it is necessary to service equipment. If the NASA DC-8 and ER-2 are available for these modules, they will coordinate their pattern subject to safety and operational constraints. The DC-8 will climb initially to 250-hPa (about FL 370) and the ER-2 to 65,000 ft. The WP-3D lead scientist will pass storm position, storm motion, and recommended IP to the DC-8 lead scientist.

Rainband option: If a convective outer rainband is available >80 nmi (150 km) from the eye, it should first be surveyed for evidence of electric fields. The survey consists of flying along the band until the field mills register a space charge or the Doppler radar reveals the presence of vigorous convection. When an interesting area is located, the aircraft should either seek a clear area and climb to maximum altitude or descend to the 0° C (~16,000 ft [4.8 km]) altitude, whichever is closer, and start making passes downwind (Fig. 13a) through the middle of the band. Each downwind pass (**1-2** in Fig. 13a) should maintain a track along the axis of the band and be about 50 nmi (93 km) long and 1,500 ft (500 m) higher (lower) than the previous one. During this portion of the pattern, the Doppler radar should make 360° scans normal to the aircraft track. After the downwind pass is completed, the aircraft should exit the band on the outer side, climb (descend), and return (Fig. 13a, **3-4**) upwind to the start of the band. The Doppler data will be obtained on the upwind pass using the F/AST method. This pattern will require about 20 min to execute. Pass length may be altered as circumstances dictate. The DC-8 and ER-2 will fly a pattern similar to Fig. 13a. The figure-8 pattern, designed to provide detailed observations of the rainband microphysics structure, can be executed in conjunction with the WP-3D repeated passes through the convection at the discretion of the DC-8 lead scientist in coordination with the WP-3D lead scientist. Repeat this pattern until the maximum altitude is reached, or seek a new area as desired. As an alternate, a zigzag path downwind through the convective band may be flown if necessary for flight safety.

(Note: If the feature of interest is not translating, radial legs should be flown on a constant track instead of a constant heading. The length of the radial legs depends upon the diameter of the eye and the width of the rainband, respectively. Turns should be initiated into the wind.)

Landfalling storm option: The purpose of this option is to investigate the relationship between cloud physics, vertical velocity, and the occurrence and location of CG lightning. Outer convective rainbands are of primary interest since they are the most likely features to be electrified. Vertically pointing Doppler rays are used to estimate vertical air motions during passes through active convection in both tropical storms and hurricanes. Along with the vertical velocities, coincident microphysics and electric field measurements are made at heights above the melting level. Three-dimensional wind fields of the convective areas can be constructed from a Pseudo-dual Doppler technique and from the F/AST Doppler data. CG lightning data are available within 325 nmi (600 km) range of the NLDN. Together, these data sources and techniques should lead to a better understanding of the characteristics of the convective processes that lead to lightning in TCs and, possibly, to intensity changes of the storms.

If possible, the aircraft will initially fly a survey figure-4 pattern similar to the one depicted in Fig. 11 at ~18,000 ft (5.5 km) altitude. The figure-4 pattern would be completed in 1.5-2.0 h with radial legs 80 nmi (150 km) in length. The second part of this option (Fig. 13b) concentrates on rainbands that are located within the useful range of the NLDN. Upon exiting the eye at **3** (Fig 13a), the aircraft should climb as high as possible on the way to the rainband of interest (**5**). A sawtooth pattern is flown downwind (Doppler operating in standard mode) with repeated crossings of the rainband to **6**. We prefer to fly directly down the band, but for reasons of safety, a sawtooth pattern may be flown. An upwind leg, flown outside of the band, is performed with the tail radar operating in the F/AST mode. The sawtooth pattern across the band is repeated with an exit toward the eye at **7**. After entering the eye, the aircraft turns toward the second rainband at 8. The sawtooth crossings and the F/AST downwind leg are repeated as in the first rainband. A final center fix is made (time permitting) before returning to base from **10**. About one hour should be spent in each of the rainbands. The DC-8 and ER-2 will fly a pattern similar to Fig. 13b. The figure-8 pattern, designed to provide detailed observations of the rainband microphysics structure, can be executed in conjunction with the WP-3D repeated passes through the convection at the discretion of the DC-8 lead scientist in coordination with the WP-3D lead scientist. If only one rainband is present within the useful range of the NLDN, a second study of the same band can be performed after a circuit through the storm center.

Post-Landfall Module:

This single option module is designed to collect kinematic and thermodynamic data commencing ~1-2 h prior to and up to 6 h after a TC makes landfall. It is essential that ground based measurements are obtained in conjunction with those that are being made by aircraft, since the primary goal of this module is to determine the kinematic and thermodynamic changes that occur after a TC makes landfall throughout the depth of the lower troposphere.

The WP-3D will fly a coastal survey pattern followed by a figure-4 pattern (Fig. 14) over land with leg lengths of (~150 km) at an altitude of ~15,000 ft (5 km). The DC-8/ER-2 will fly the coordinated pattern shown in Fig. 14 with leg lengths of ~150 km at an altitude of ~37,000 ft (11 km) and ~67,000 ft (20 km) respectively. If feasible, the DC-8 and WP-3D should fly legs along WSR-88D radials with the PR-2 and tail Doppler data in FAST mode. These data will aid in rainfall estimation and will help document the changes in vortex and rainband structure over land that are crucial to understanding the environment that supports tornado and mesovortex development.

Over land, 12 mesonet stations, 3 profilers and 2 DOW Doppler radars should be deployed along the path of the landfalling TC to identify the changes in storm structure as the TC moves inland. The mesonet stations should be deployed in three lines of four stations each. The mesonet stations will be employed to obtain high-resolution surface wind, temperature, pressure, relative humidity, and perhaps rainfall measurements. A profiler will be placed at the center of each of the lines of mesonet stations. The profilers and collocated RASS sounder will provide wind and temperature measurements within the lowest 3 and 1 km, respectively. If possible, rain gauges should be collocated at each profiler and DOW radar site to obtain high-resolution rainfall measurements useful both for calibrating the radar rainfall algorithms and for documentation of storm rainfall.

The first of the three lines of the mesonet stations should be placed as close as possible to the coastline (<10 km) to enable accurate documentation of the surface wind field just after landfall. The other two lines should be placed ~65 and 135 km inland respectively; however, these distances will vary depending upon the intensity and speed of motion of the landfalling storm as well as safety considerations. Fig. 15 shows the estimated time after landfall that is required for the TC winds to decay to various wind threshold levels as determined using the Kaplan/DeMaria empirical inland wind decay model. The spacing between the mesonet stations located within the 3 lines themselves should be ~30 nm (50 km) to maximize the likelihood that one of the mesonet stations will be located near the radius of maximum wind of the landfalling storm.

The inland profilers should be highly mobile so that it will be possible to follow severe weather producing rainbands if safety and logistical considerations allow. The DOW Doppler radars should be placed roughly halfway between the two rear lines of mesonet and profiler stations. The DOW radars in combination with the three profilers with RASS will aid in documenting the changes in kinematic and thermodynamic structure of the TC after landfall. An accurate analysis of such changes is crucial to learning more about the development of mesovortices and/or tornadoes spawned by the landfalling TC. They will also help document the changes in winds within the PBL of a landfalling TC. Finally, the radars will aid in the measurement of the rainfall associated with the landfalling TC.

TROPICAL CYCLONE WINDFIELDS NEAR LANDFALL EXPERIMENT

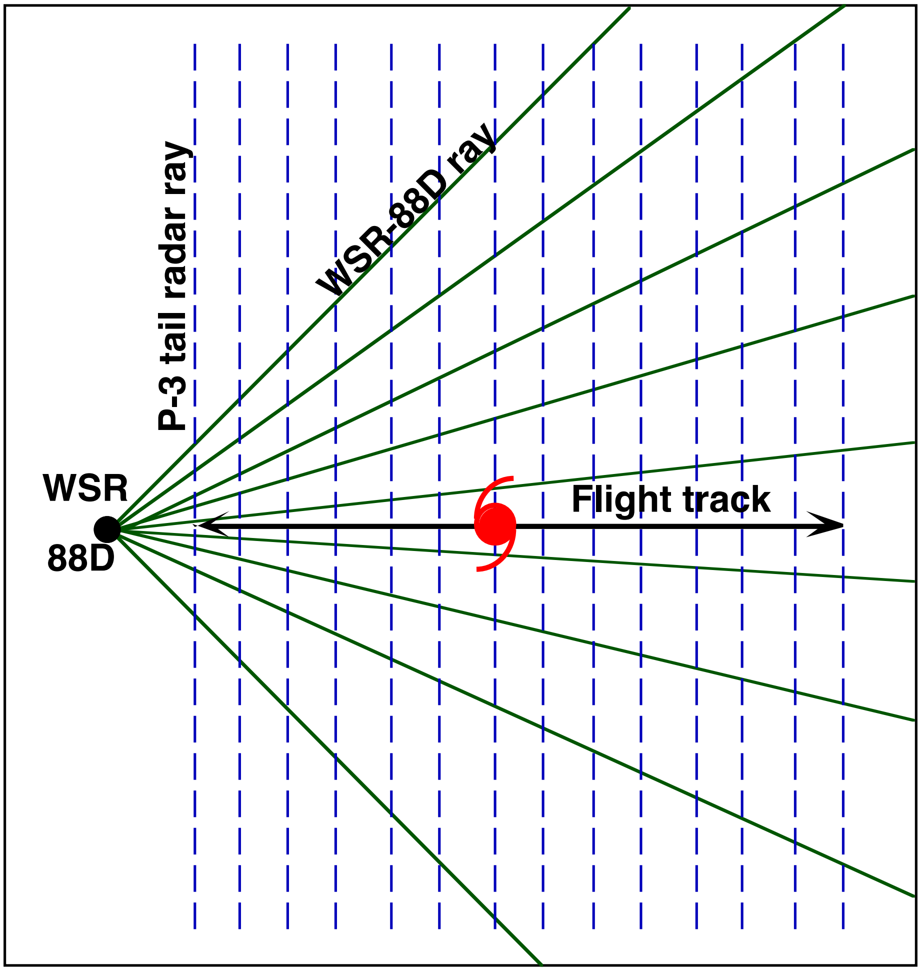

Fig. 10. Ground-based/Airborne Doppler Scanning Strategy

• Note 1.	The legs through the eye may be flown along any compass heading along a radial from the ground-based radar.
• Note 2.	Set airborne Doppler radar to scan in F/AST mode on all legs.

TROPICAL CYCLONE WINDFIELDS NEAR LANDFALL EXPERIMENT

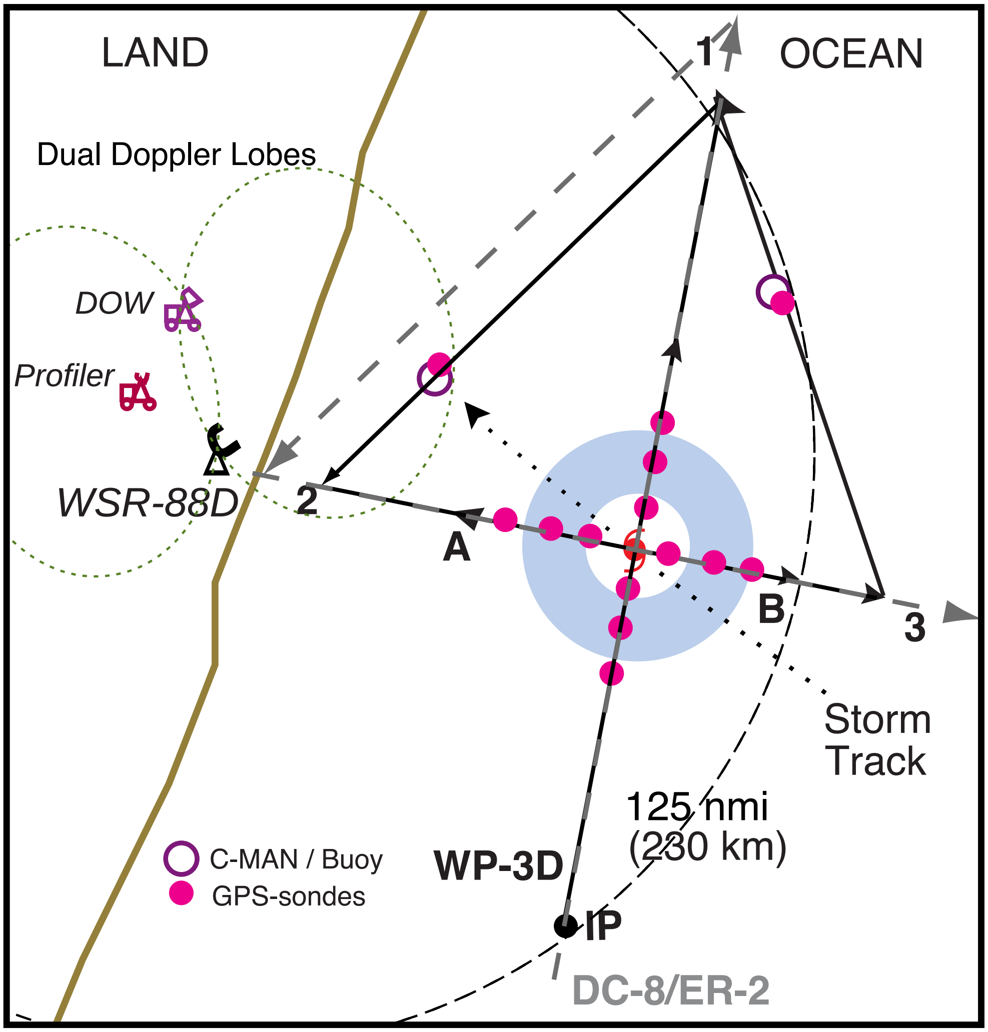

Fig. 11. Flight track for the real-time module with over flights of moored buoys for a storm passing within range of a coastal WSR-88D.

• Note 1.	True airspeed calibration required.
• Note 2.	The legs through the eye may be flown along any compass heading along a radial from the ground-based radar. The **IP** is approximately 100 nmi (185 km) from the storm center. Downwind legs may be adjusted to pass over buoys.
• Note 3.	The DC-8 and ER-2 should fly the coordinated figue-4 pattern at an altitude of ~37,000 ft (11 km) and ~67,000 ft (20 km), respectively.
• Note 4.	If possible, the DC-8 and WP-3D should fly legs along the WSR-88D radials. Set airborne Doppler radar to F/AST scanning on all legs.
• Note 5.	All aircraft should avoid penetration of intense reflectivity regions (particularly those over land). Wind center penetrations are optional.

TROPICAL CYCLONE WINDFIELDS NEAR LANDFALL EXPERIMENT

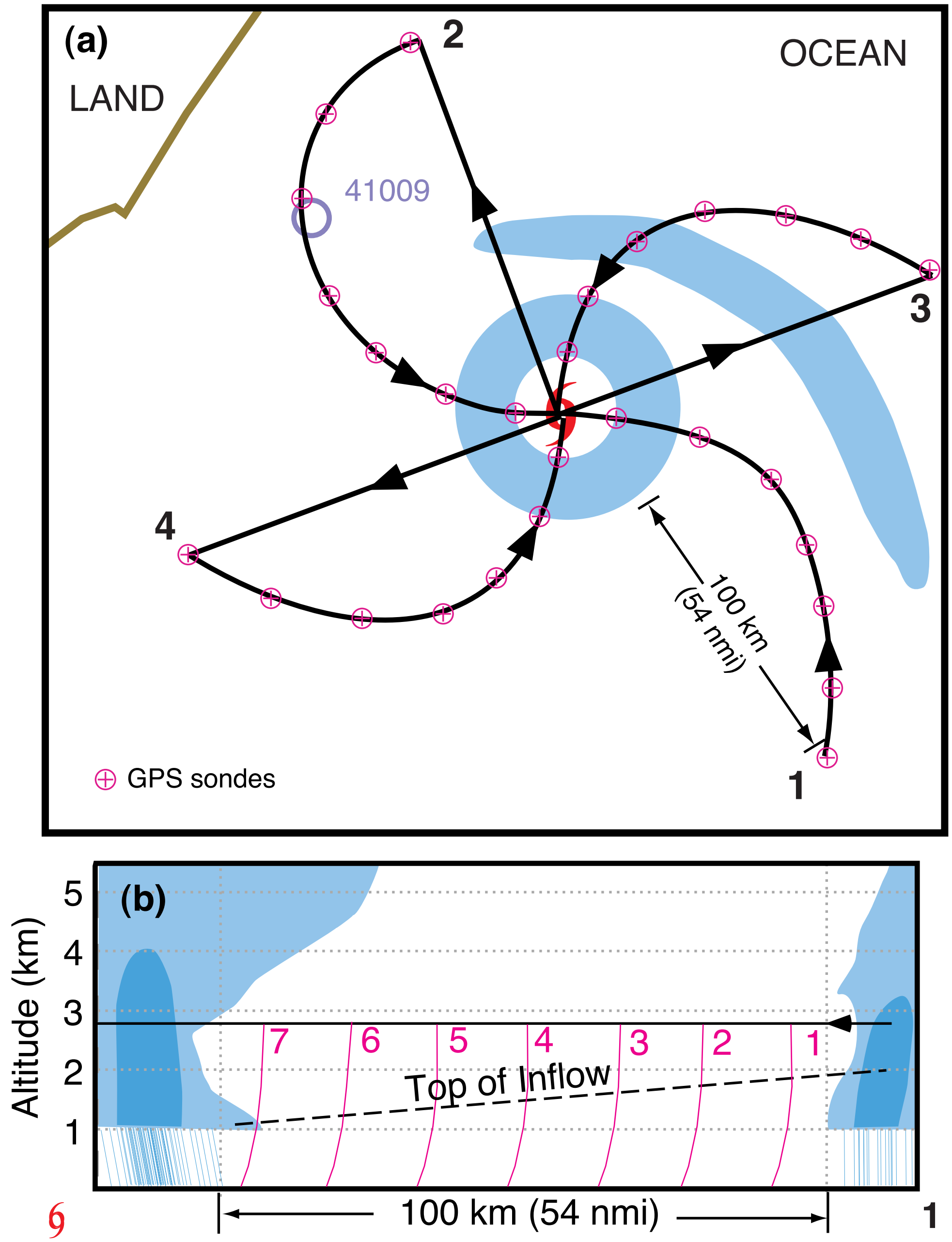

Fig. 12. Rainband Thermodynamic Structure Module (a) Plan view; and (b) track-height depiction.

• Note 1.	True airspeed calibration required.
• Note 2.	WP-3D Doppler radar should be operated in F/AST mode at a single PRF ≥2400 and 20° tilt

TROPICAL CYCLONE WINDFIELDS NEAR LANDFALL EXPERIMENT

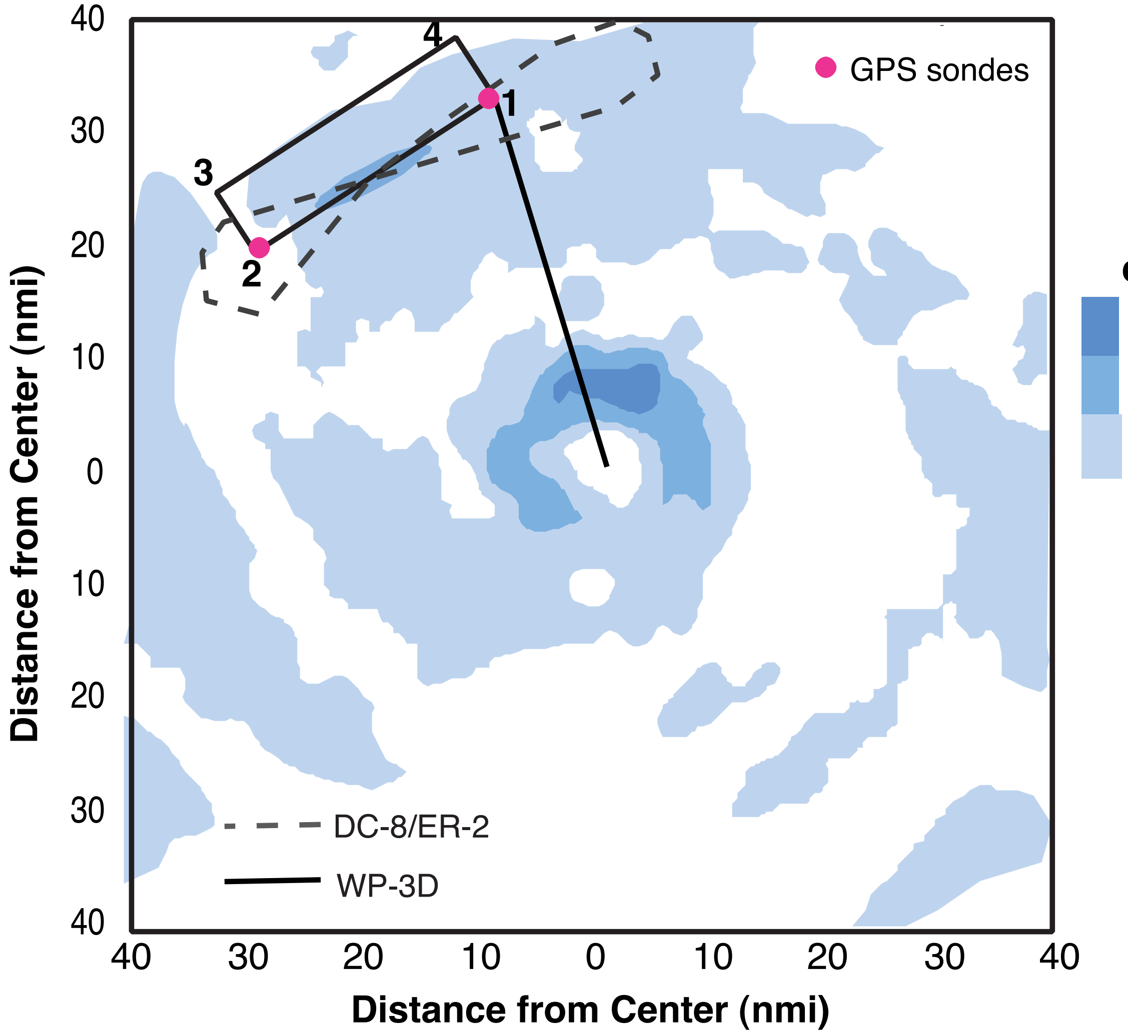

Fig. 13a. Electrification rainband module flight pattern.

• Note 1.	True airspeed calibration is required.
• Note 2.	The pattern may be flown along any compass heading.
• Note 3.	Rainband passes **1-2** are separated by 1500 ft (500 m) altitude. Climbs (descents) occur along **3-4** outside the convection.
• Note 4.	Set airborne Doppler radar to continuously scan perpendicular to the track from **1-2**, and in F/AST mode at a single PRF ≥2400 and 20° tilt on all other legs.

TROPICAL CYCLONE WINDFIELDS NEAR LANDFALL EXPERIMENT

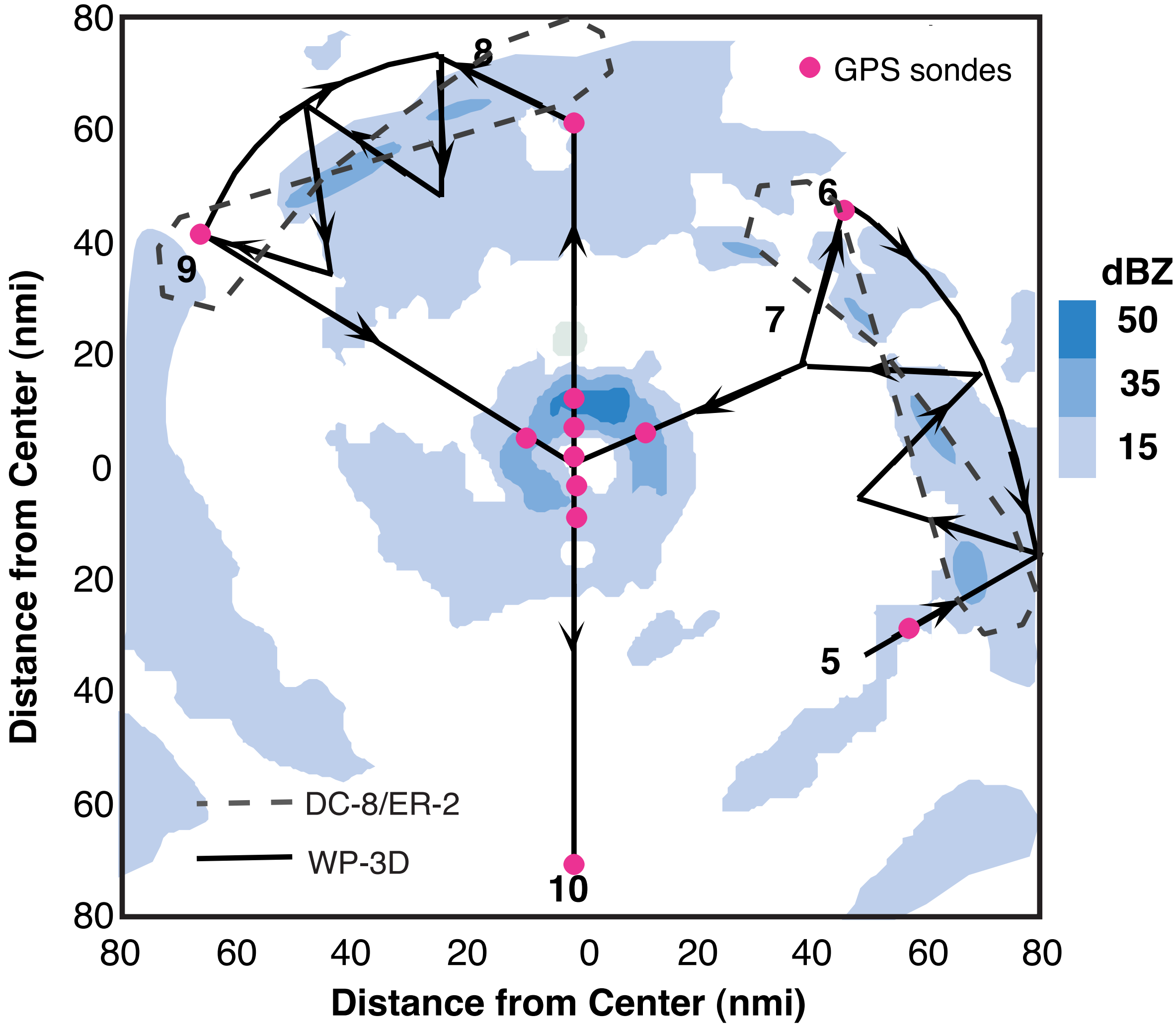

Fig. 13b. Electrification landfall module flight pattern.

• Note 1.	Fly zig-zag legs **5-6** and **8-9** at highest possible altitude. Each leg is approximately 25 nmi (45km) long. Outside turns of 270°-300° are at the end of each zig-zag leg.
• Note 2.	At **6** and **9** fly upwind leg along rainband at highest possible altitude to a point near the beginning of the zig-zag legs.
• Note 3.	Repeat pattern in different parts of the storm as time permits.
• Note 4.	Set airborne Doppler radar to scan in F/AST mode on all legs.

TROPICAL CYCLONE WINDFIELDS NEAR LANDFALL EXPERIMENT

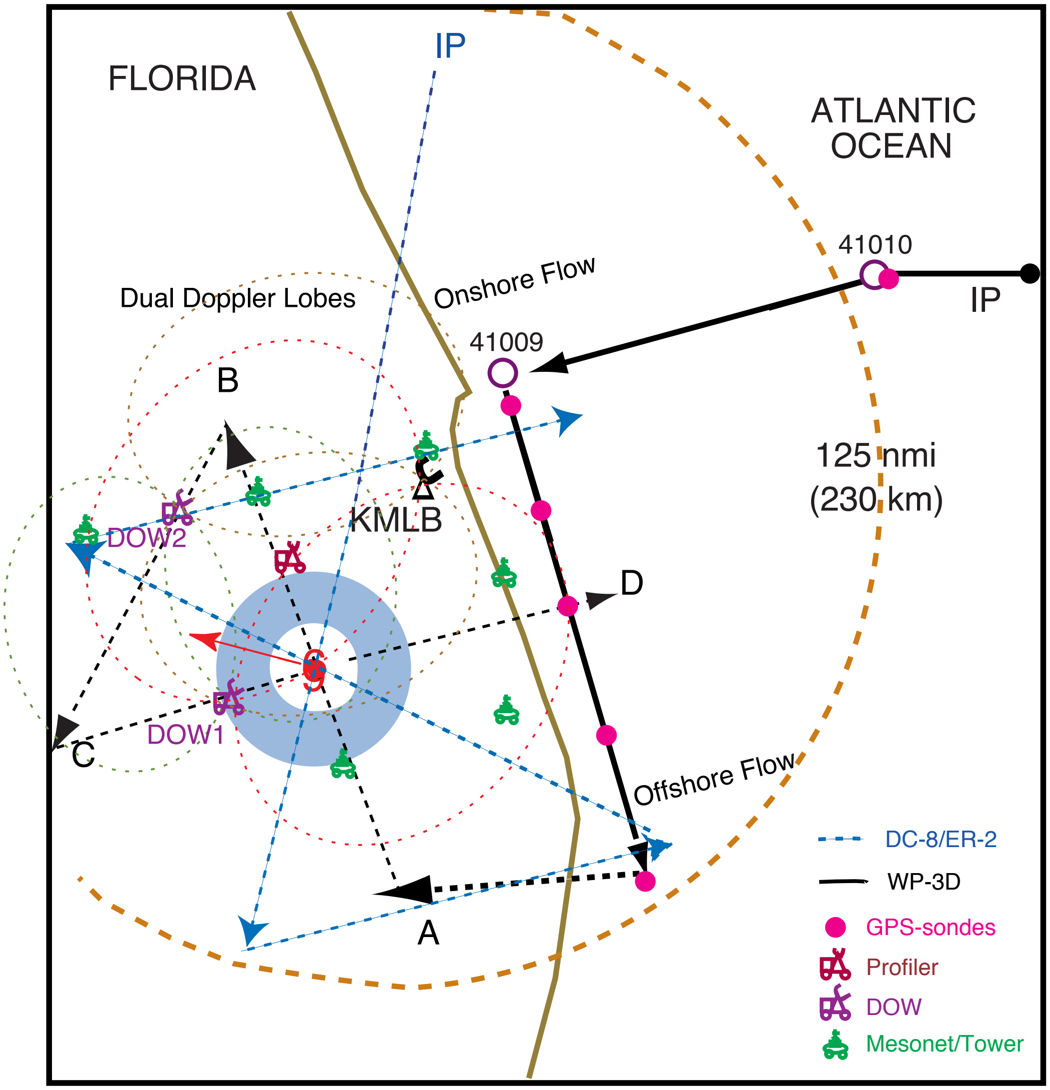

Fig. 14. Post landfall module flight pattern.

• Note 1.	The WP-3D should fly a coastal survey pattern (sold line) at an altitude of ~10,000-15,000 ft (3-4 km) dropping GPS-sondes near buoys of opportunity and within 10-20 km of the shore in both the onshore and offshore flow regimes.
• Note 2.	The WP-3D executes a figure-4 pattern (dashed line) centered on the storm with leg lengths of ~80 nm (150 km) at an altitude of ~15,000 ft (5 km).
• Note 3.	The DC-8 and ER-2 should fly the coordinated figure-4 pattern at an altitude of ~37,000 ft (11 km) and ~67,000 ft (20 km), respectively.
• Note 4.	If possible, the DC-8 and WP-3D should fly legs along the WSR-88D radials. Set airborne Doppler radar to F/AST scanning on all legs.
• Note 5.	All aircraft should avoid penetration of intense reflectivity regions (particularly those over land). Wind center penetrations are optional.

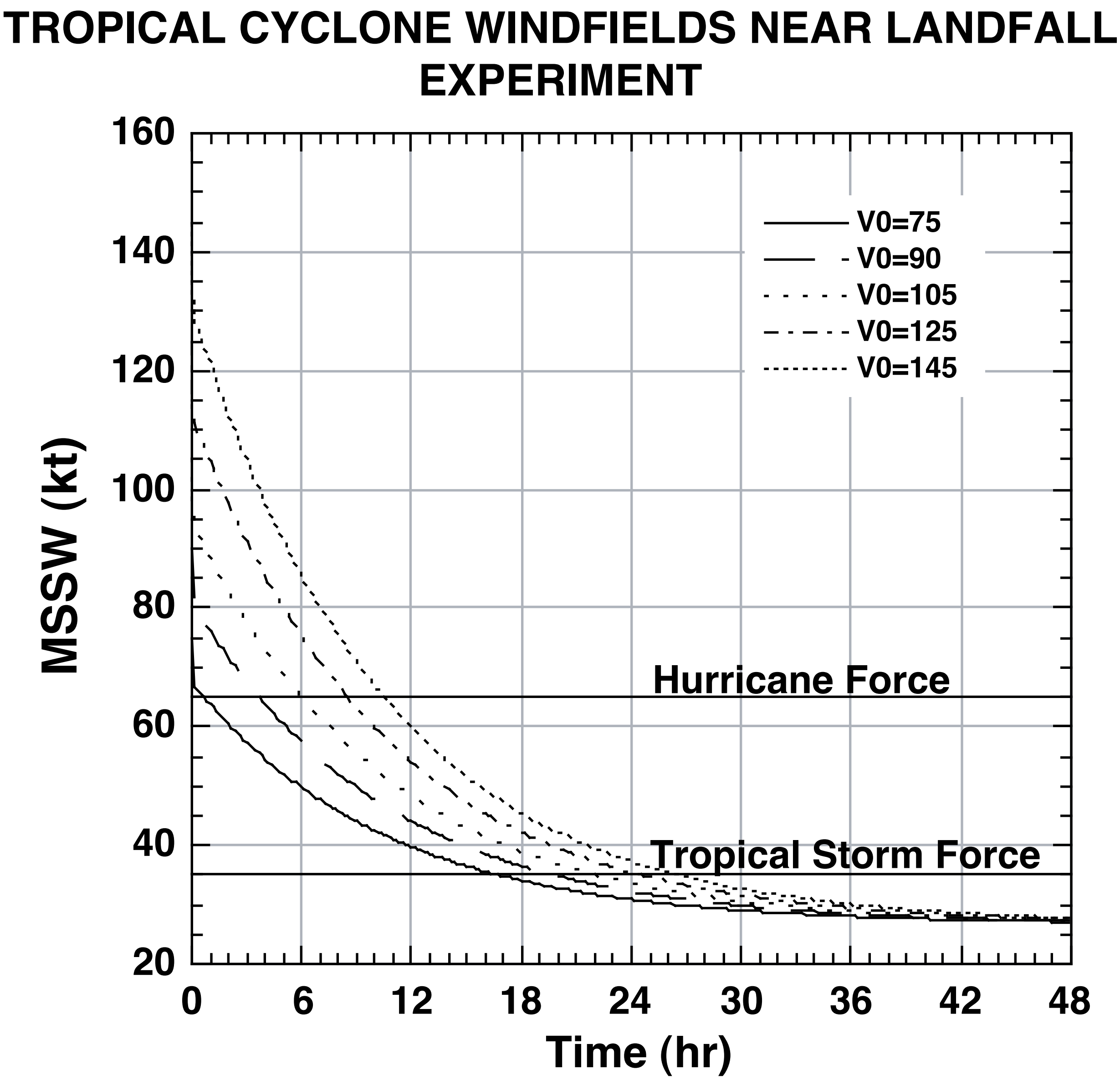

Fig. 15. Maximum sustained surface winds (MSSW) after landfall estimated using the Kaplan/DeMaria inland wind decay model for TCs with landfall intensities (V0) of 75,90,105,120, and 145 kt.

12. Hurricane Synoptic-Flow Experiment

Program Significance: Accurate numerical TC forecasts require the representation of meteorological fields on a variety of scales, and the assimilation of the data into realistic models. Omega dropwindsonde (ODW) observations from WP-3D aircraft obtained between 1982 and 1996 during the Hurricane Synoptic Flow Experiment produced significant improvement in the guidance for official track forecasts. Since 1997, fifty operational "Synoptic Surveillance" missions have been flown with the NOAA G-IV jet in the environments of TCs threatening the United States coastline; almost half of these have been supplemented with dropwindsonde observations from one or two WP-3D aircraft during Hurricane Synoptic Flow Experiments. An improved dropwindsonde based on the Global Positioning System has been developed by the National Center for Atmospheric Research and has replaced the ODW. With further operational use of the G-IV aircraft, and as other mobile observing platforms become available, optimal sampling and utilization techniques must be devised to provide the greatest possible improvement in initial condition specification.

Objectives: The goal of the HRD synoptic flow experiment is to improve landfall predictions of TCs by releasing GPS sondes in the environment of the TC center. These data will be used by TPC/NHC and NCEP to prepare objective analyses and official forecasts through their assimilation into operational numerical prediction models. Because the atmosphere is known to be chaotic, very small perturbations to initial conditions in some locations can amplify with time. However, in other locations, perturbations may result in only small differences in subsequent forecasts. Therefore, targeting locations in which the initial conditions have errors that grow most rapidly may lead to the largest possible forecast improvements. Locating these regions that impact the particular forecast is necessary. When such regions are sampled at regularly-spaced intervals the impact is most positive. The optimal resolution of these intervals is an ongoing area of research.

A number of methods to find targets have been investigated, mainly in the wintertime extratropics. Potential vorticity diagnosis can help to find the cause of forecast failure. Singular vectors of the linearized equations of motion can estimate the growth of small perturbations in the model. This method is relatively expensive, and full implementation in the Tropics where adiabatic processes dominate has proven difficult, and the linear assumption tends to break down at the 72 h forecast time necessary for the posting of hurricane watches and warnings. Related strategies involve the sensitivity vector, and quasi-inverse linear method. All these methods may depend on the accuracy of the initial conditions determined without the supplemental data.

A fully nonlinear technique uses the breeding method, the operational NCEP perturbation technique in which initially random perturbations are repeatedly evolved and rescaled over a relatively short cycling time. These vectors are related to local Lyapunov vectors and, therefore, define the fastest growing modes of the system. Changes to initial conditions due to dropwindsonde data obtained from operational synoptic surveillance missions during the 1997 and 1998 hurricane seasons grow (decay) in regions of large (small) perturbation in the operational NCEP Ensemble Forecasting System. Therefore, these bred-modes provide a good estimate of the locations in which supplemental observations are likely to have the most impact. However, though the breeding method can find locations of probable error growth in the model globally, it does not distinguish those locations which impact the particular forecast from those which do not.

A more generalized method which can use any dynamical ensemble forecast system is the ensemble transform. This method transforms an ensemble of forecasts appropriate for one observational network into one appropriate for other observational networks. Ensemble forecasts corresponding to adaptations of the standard observational network are computed, and the expected prediction error variance at the observation time is computed for each potential network. The prediction error variance is calculated using the distances between the forecast tracks from all ensemble members and the ensemble mean. This method has shown promise during previous synoptic flow experiments.

Mission Description: To assess targeting strategies a relatively uniform distribution of GPS-sonde soundings will be collected over a minimum period of time by both NOAA/AOC WP-3D aircraft operating *simultaneously within and surrounding the TC, and in coordination with operational surveillance missions of the G-IV.* Specific flight tracks will vary depending on such factors as the location of the storm, relative both to potential bases of operation and to particular environmental meteorological features of interest, and the operational pattern being flown by the G-IV.

A sample mission is shown in Fig. 16. The two WP-3D aircraft and the G-IV will begin their missions at the same time. Subject to safety and operational constraints, each WP-3D will climb to the 500-hPa level (about FL 180) or above, then proceed, step-climbing, along the routes assigned during preflight. *It is particularly important that both aircraft climb to and maintain the highest possible altitude as early into the mission as aircraft performance and circumstances allow, and attain additional altitude whenever possible during the mission.*

GPS-sondes are released in one of two modes. Beyond 40 nmi (75 km) from the storm center, drops are made at pre-assigned locations, generally every 25 min or 120 nmi (222 km). These drop locations are provided with the particular mission flight tracks 2 h before blockout. Within 40 nmi (75 km) of the TC's center, drop locations are specified relative to the center's position (e.g., 40 nmi (75 km) north of the eye). During in-storm portions of the mission, drops will be made with possible spacing <8 min or 40 nmi (75 km). GPS sondes should generally be released *after the turn is complete*.

At least one aircraft will fly through the TC center and execute a figure-4 pattern. This aircraft's Doppler radar should be set to scan perpendicular to the aircraft track. *"Hard" center fixes are not desirable*. On the downwind leg of the figure-4, the Doppler should be set to record forward and aft (F/AST) continuously. If both aircraft penetrate the storm, the figure-4 pattern will generally be executed by the *second* aircraft through the storm, and the first aircraft through will collect vertical incidence Doppler data. Coordination with potential USAF reconnaissance is necessary to ensure adequate aircraft separation. The in-storm portion of the missions is shown schematically in Fig. 17, although the actual orientation of these tracks may be rotated.

Of paramount importance is the transmission of the GPS-sonde data to NCEP and TPC/NHC for timely incorporation into operational analyses, models, forecasts, and warnings. Operational constraints dictate an 0600 or 1800 UTC blockout time, so that the GPS-sonde data will be included in the 1200 or 0000 UTC analysis cycle. Further, limiting the total block time to 9 h allows adequate preparation time for aircraft and crews to repeat the mission at 24-h intervals. These considerations will ensure a fixed, daily real-time data collection sequence that is synchronized with NCEP and TPC/NHC's analysis and forecasting schedules.

A CAMEX-4 objective is to obtain water vapor profiles around the storm's environment using the LASE instrument on the DC-8 (Appendix B). This mission is best when coordinated with a multi-plane Synoptic Flow Experiment, whose GPS-sondes will provide ground truth for the water vapor profiles. A sample mission is shown in Fig. 18. The DC-8 aircraft and the ER-2 will begin their missions at the same time as the two WP-3D and G-IV aircraft. Subject to safety and operational constraints, the DC-8 will fly as high as possible between 20,000 ft (FL200) and 40,000 ft (FL400) and at an altitude low enough to minimize cloud interference with nadir lidar (LASE) water vapor measurements. *G-IV GPS sondes may pose a hazard to the DC-8 aircraft. If a simultaneous G-IV surveillance mission is conducted it is particularly important that the DC-8 mission avoid conflicts with the operational requirements.*

HURRICANE SYNOPTIC FLOW EXPERIMENT

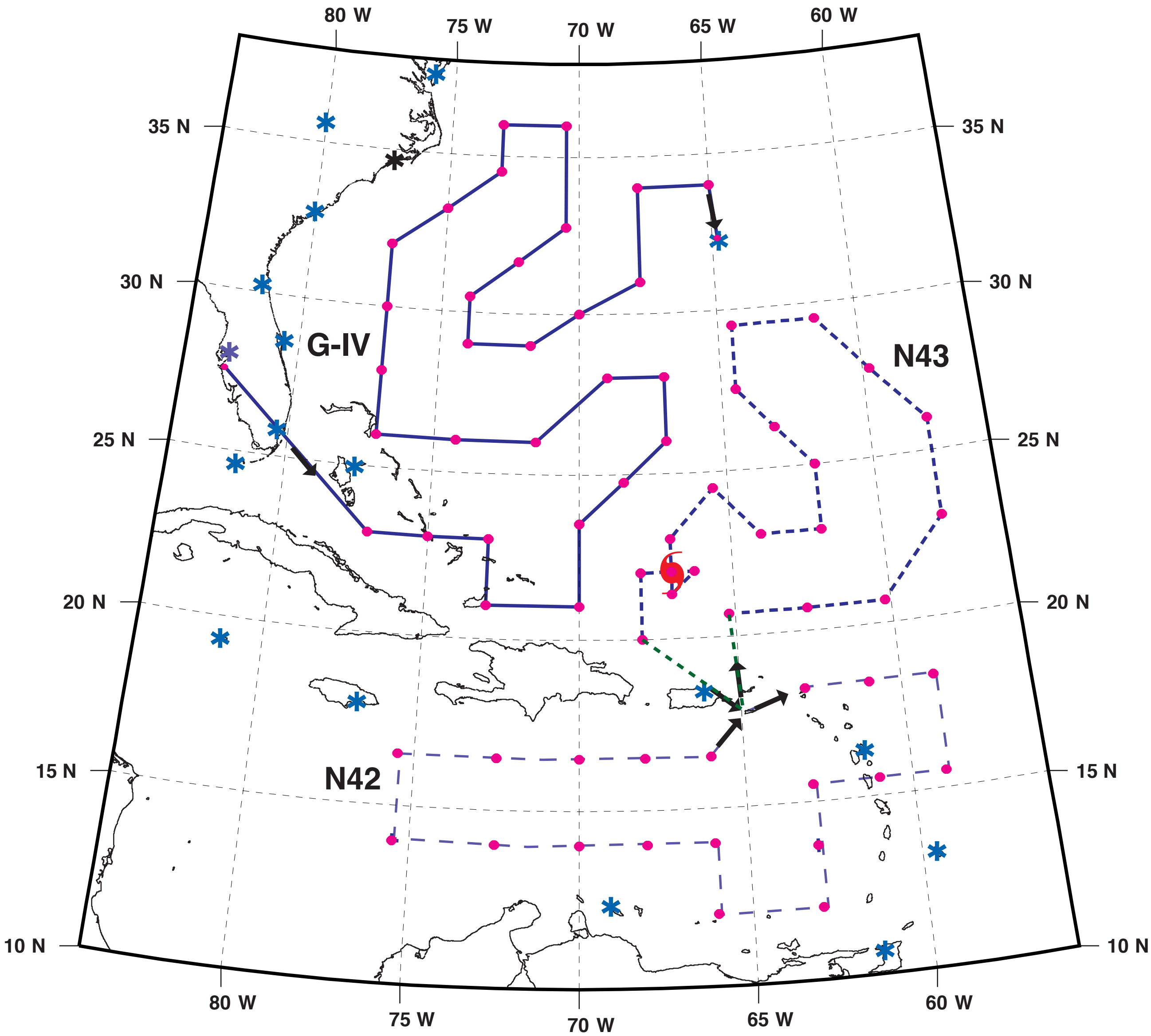

Fig. 16. Sample Environmental Patterns

• Note 1.	During the ferry to the **IP**, the WP-3D aircraft will climb to the 500 hPa level (about FL 180). The 400-hPa level (about FL 250) should be reached as soon as possible and maintained throughout the remainder of the pattern, unless icing or electrical conditions require a lower altitude.
• Note 2.	During the ferry to the **IP**, The G-IV should climb to the 41,000 ft (200 hPa) as soon as possible and climb as feasible to maintain the highest altitude for the duration of the pattern.

HURRICANE SYNOPTIC FLOW EXPERIMENT

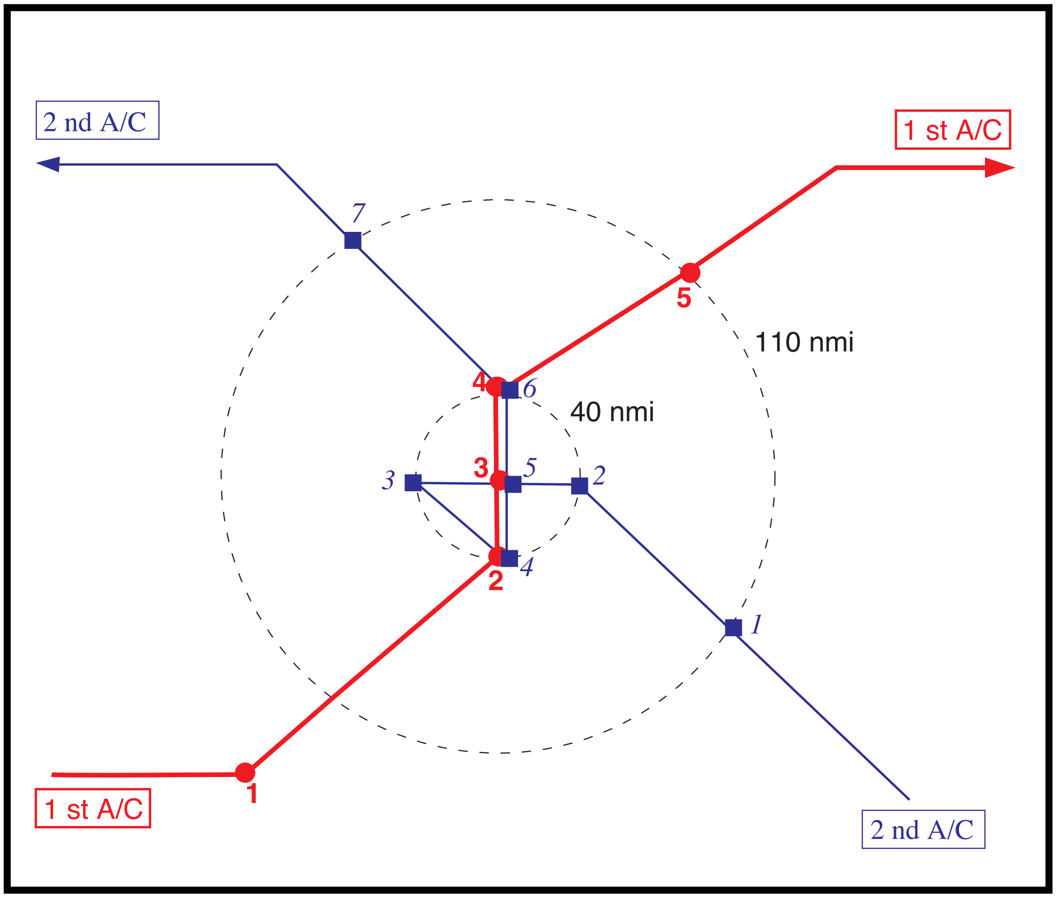

Fig. 17 In-Storm Patterns

• Note 1.	Within the 40 nmi (75 km) range ring, all legs are on cardinal tracks.
• Note 2.	The second aircraft through the storm will execute the Doppler "figure-4" pattern. The Doppler radar should be set to continuously scan perpendicular to the track during radial penetrations and to F/AST on the downwind leg.
• Note 3.	Numbered symbols (◆, ■) reflect scheduled drops for each aircraft.
• Note 4.	Drop #5 in the "figure-4" pattern occurs on the second pass through the eye.
• Note 5.	A/C 1 should collect vertical incidence Doppler data during storm penetration.
• Note 6.	If missions are not repeated, then block times may exceed 9 h. In addition to the GPS-sonde data, *3-4 RECCO's h^{-1} should be transmitted during each mission.*

Special Notes: Missions similar to the Synoptic Flow missions may be flown in non-hurricane conditions to collect GPS-sonde data sets for satellite sounding evaluations. These missions differ from the normal experiment as follows:

- Block times are 10 h, and the experiment is not repeated on the following day.
- In-storm portion of the pattern (Fig. 17) is omitted and no Doppler data are collected.
- The G-IV does not participate in the mission

HURRICANE SYNOPTIC FLOW EXPERIMENT

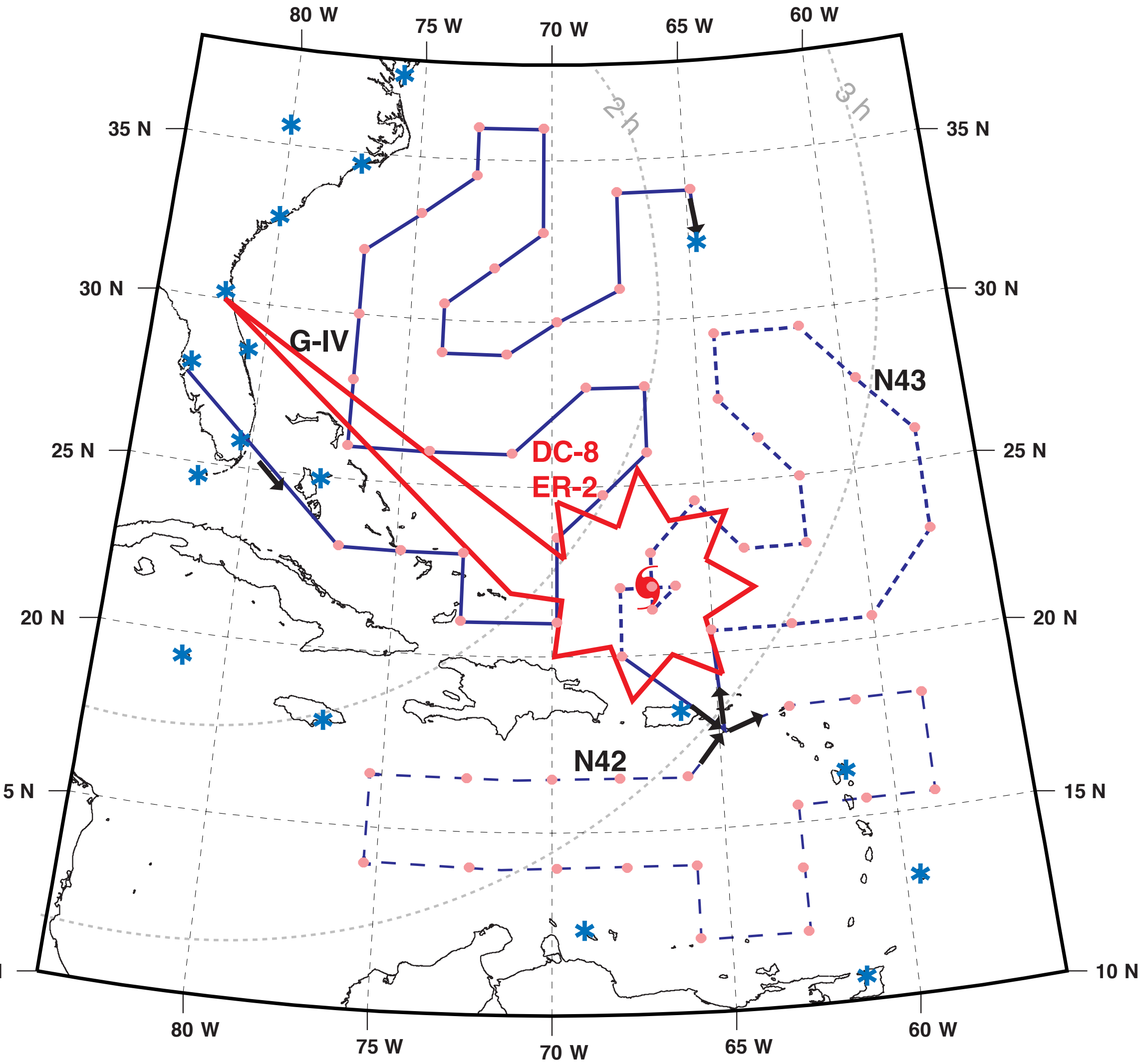

Fig. 18. DC-8 and ER-2 Sample Surveillance Pattern

- Note 1. Aircraft should begin pattern at approximately the same time as the two WP-3D aircraft, but precise coordination is not required.
- Note 2. Subject to safety and operational constraints, the DC-8 will fly as high as possible between 20,000 ft (FL200) and 40,000 ft (FL400) and at an altitude low enough to minimize cloud interference with nadir lidar (LASE) water vapor measurements
- Note 3. GPS sondes and the downward-pointing lasers may pose a hazard to the WP-3D or WC-130 aircraft. Hence, positive communication with these aircraft must be obtained before the laser is operated or sondes released.
- Note 4. If a G-IV surveillance mission is conducted simultaneously care must be taken by the DC-8 crew to coordinate with the operational G-IV mission. G-IV GPS sondes may pose a hazard to the DC-8 aircraft. Therefore, the DC-8 mission should avoid conflicts with the operational requirements.

13. Extratropical Transition Experiment

Program Significance: The poleward movement of a TC initiates complex interactions with the midlatitude environment such that the nearly symmetric distributions of winds, clouds, and precipitation that are concentrated about the mature TC circulation center develop asymmetries that expand greatly in area. The asymmetric expansion of areas of high wind speeds and heavy precipitation may cause severe impacts over land without the TC center making landfall. Due to interactions between the TC and midlatitude circulation, regions of heavy precipitation may be embedded in large cloud fields that extend far ahead of the TC center. If the heavy precipitation associated with the primary structure of the TC then falls over the same region as the pre-storm precipitation, the potential for flooding is increased. Over water, the poleward movement of a TC may produce extremely large surface wave fields due to the high wind speeds and increased translation speed of the decaying TC that results in a trapped-fetch phenomenon. The relatively small scale of the TC and the complex physical processes that occur during the interactions between the TC and the midlatitude environment make it very difficult to specify the exact evolution of winds, clouds, and precipitation during the initial stage of extratropical transition.

Based on satellite imagery and numerical analyses from global- and regional-scale numerical models, four primary physical processes associated with the initial stage of extratropical transition have been identified: (i) environmental advection of relatively cold, dry (warm, moist) air on the western (eastern) side of the TC center, (ii) interaction with the midlatitude baroclinic environment to produce ascent over tilted isentropic surfaces, (iii) systematic decay and tilt of the warm core aloft in response to increased vertical wind shear, and (iv) evolution of the outer circulation into an asymmetric pattern that implies lower-tropospheric frontogenesis. All of these processes contribute to the evolution from purely TC characteristics to midlatitude cyclone characteristics. However, important questions remain as to the rate at which these changes occur, the importance of the TC size, intensity, and structure characteristics, and to what the roles of the remaining TC features are relative to the characteristics of the midlatitude circulation into which the TC is moving. Additional questions are related to the influence of the boundary layer environment (e.g., surface fluxes, surface roughness, sea-surface temperature gradients associated with the Gulf Stream) on the evolution of the precipitation, wind, and wave fields during the initial stage of extratropical transition.

Because of the lack of high resolution (in space and time) observations, and due to the inability to adequately resolve the horizontal and vertical structure of the TC with numerical model analyses or forecasts, diagnoses of the changes in the TC structure due to interaction with the midlatitude baroclinic zone are often inconclusive. Furthermore, development of isolated regions of high winds and heavy precipitation are not fully identified. For example, interactions between the TC and midlatitude circulation may contribute to localized regions of conditional symmetric instability (CSI) that enhance frontogenesis and heavy rainfall far ahead of the TC center.

The multiple aircraft platforms and suite of sensors available during the combined CAMEX-4 and HRD field experiment provide the ideal capability for achieving a detailed observational description of the characteristic changes associated with the initial stage of the extratropical transition of a TC. Improved understanding of these changes will contribute to the development of conceptual models that will lead to improved warnings associated with these potentially dangerous systems.

Objectives Study the interactions between a TC and midlatitude baroclinic environment. Specific objectives are to identify the physical mechanisms associated with the asymmetric expansion of wind, cloud, precipitation, and ocean surface wave fields during the initial stage of extratropical transition. To examine the relative roles of the TC and midlatitude circulation, aircraft will be used to monitor the changes in TC structure and the interface between the TC and midlatitude circulation into which it is moving.

Other goals are:

- To examine the development of an asymmetric precipitation distribution during the transformation stage of extratropical transition.

- To examine the development of warm frontogenesis in the forward portion of the transforming TC.
- To examine the development of heavy precipitation in conjunction with the pre-storm baroclinic zone.
- To use *in situ* observations of the thermodynamic and dynamic structure of the forward portion of the transforming TC to determine whether conditional symmetric instability is important for enhancing precipitation in the warm frontal region.
- To examine the interface between the upper-level outflow from the TC and the midlatitude jet stream.
- To quantify the influence of the TC outflow on the enhancement of dynamical factors favorable for enhanced precipitation in the pre-storm environment.
- To measure the influence of the increased vertical wind shear associated with the midlatitude baroclinic environment on the structural characteristics on the TC circulation.
- To measure the influence of low-level atmospheric temperature gradients and sea-surface temperature gradients on the evolution of the primary TC characteristics during transformation.
- To identify processes associated with the expansion of maximum winds, precipitation rates, and ocean surface waves away from the TC center.
- To examine the forcing of ocean waves in a possible trapped-fetch environment.
- To study the roles of surface roughness, air-sea interaction, exchange of heat, momentum, and mass, and the interaction with the ocean during transformation into a region of enhanced boundary-layer gradients.
- To compare wind speed distribution with measured sea-level pressure during transformation.
- To examine and validate numerical forecasts of the transformation stage of extratropical transition with observations.
- To understand the dynamical and physical processes that contribute to poor numerical weather forecasts of extratropical transition.
- To improve data assimilation into numerical analyses with emphasis on incorporation of special observation types.
- To examine cloud microphysical properties to determine how they impact the development and decay of areas of heavy precipitation.
- To identify the precipitation formation mechanisms in the pre-storm precipitation region.
- To examine the precipitation efficiency of the pre-storm precipitation region.
- To validate remotely-sensed data sets of various parameters during the transformation stage of extratropical transition.
- To use new observation data sets for development of a conceptual model of the transformation stage of extratropical transition. The conceptual model will address the expansion of asymmetric rainfall and wind distributions away from the decaying TC center.

Mission Description: The mission is designed to use multiple aircraft to monitor the TC structural changes and the interactions between the TC and midlatitude circulation. The ideal storm will be a poleward-moving TC that is offshore of the mid-Atlantic coastline of the United States and has entered the transformation stage of extratropical transition. In the transformation stage, the primary structural characteristics are contained in three regions (Fig. 19): (i) the pre-storm precipitation area; (ii) the TC/midlatitude interface; and (iii) the TC core. The optimal mission is designed to examine each of these regions. A list of primary structural characteristics in each region is provided in Table 1 together with critical observation parameters. Table 1 can be used to determine asset coordination in the event that optional scenarios are required due to limited aircraft availability, storm characteristics, etc. The experiment requires:

- GPS Sondes should be available on all aircraft.
- AXBT instrumentation should be available on the NOAA WP-3Ds.
- The lower fuselage and tail Doppler radars should be operational on both WP-3Ds.

- The C-SCAT and microphysical instruments should be operational on the WP-3D that will fly at upper levels.
- The SRA should be operational on the WP-3D that will fly at low levels.
- Cloud microphysics instruments should be operational on the Convair 580.
- Doppler radar and scanning radiometers should be operational on the ER-2.

Flight-level and dropwindsonde data from the U. S. Air Force WC-130s will be used to monitor the TC core. Typically, the WC-130s are on station for 4-6 h flying figure-4 patterns along the cardinal. Nominal leg lengths are 150 nmi at an altitude between 850 hPa and 700 hPa (5,000 to 10,000 ft). There may be a gap of 6-7 h when no WC-130 is on station. However, if there is a threat of landfall that gap may be reduced to 3 h.

In an optimal setting, five aircraft will participate in staggered missions to observe the physical characteristics listed in Table 1. The changes in the primary TC core characteristics will be examined by the NASA ER-2 and one NOAA WP-3D, which should be N42RF since the SRA will be required to examine surface wave spectra especially in the right front quadrant of the decaying TC. Due to the interaction with the midlatitude baroclinic environment, the structural characteristics of the TC change rapidly. Aircraft missions will be staggered to provide continuous coverage of the primary features associated with the decaying TC. Because a decaying TC often translates rapidly poleward, an optional flight plan is supplied for a TC core region only mission. Other options provide for unavailability of various aircraft. Flight plans for these options are a matter of substituting available aircraft for those unavailable, or eliminating the observation of one of the regions associated with extratropical transition.

1) **TC CORE REGION**: The NASA ER-2 will fly a modified figure-4 pattern at an altitude of 65,000 ft in which three passes through the TC center will be made (Fig. 20). The pattern will be skewed such that the legs to the north of the center will be longer than those to the south. Also, the pattern will be oriented such that one approach to the center will be from the north to compliment the pattern of the WP-3D that will fly patterns (Fig. 21) rotated to be in the northeast and northwest quadrants of the decaying TC. The northeast quadrant is an area of strong warm advection and warm frontogenesis that often contains organized rain bands. The northwest quadrant is an area of cold advection and frontolysis associated with sinking cold air. Therefore, the processes occurring in these quadrants are thought to be important in production of kinetic energy during the transformation of the decaying TC to an extratropical cyclone.

   If the ER-2 and WP-3D depart their respective bases at nearly the same time, the decaying TC center will be observed from 65,000 ft at 1.25, 3.25, and 5 h after takeoff time and from lower levels at 2.25, 4.5, and 6 h after takeoff time. Furthermore, the NASA DC-8 departure will be two hours after the ER-2 takeoff time to provide a 40,000 ft pass through the center near 6.5 h (Fig. 22) after the ER-2 departure time. Therefore, the evolution of the warm core and deep convection near the TC center will be sampled nearly once an hour during this period of often rapid transformation.

   Both the ER-2 and WP-3D will deploy GPS sondes once they have entered their respective patterns. GPS sondes will be deployed at the end of each leg, and at evenly spaced intervals along each leg with optimal spacing near 60 nmi for the WP-3D (22 GPS sondes) and 100 nmi for the ER-2 (20 GPS sondes). Furthermore, AXBTs will be deployed from the WP-3D at the midpoint of each leg that is north of the TC center (12 AXBTs).

   Due to a trapped fetch phenomenon, the ocean surface wave heights can reach extreme levels immediately ahead of a TC undergoing extratropical transition. Therefore, primary importance for the WP-3D in the northeast quadrant of the decaying TC will be use of the scanning radar altimeter to observe the ocean surface wave spectra. Flight level will be chosen to accommodate use of this instrument.

   TC Core Only Option: This option is best suited if the TC core region is translating rapidly northward such that the pre-storm precipitation region will not be in range of either the NASA or NOAA aircraft.

In this option, the NASA ER-2, DC-8, and NOAA WP-3D (N42RF) aircraft will be used as discussed above. However, N43RF will fly a pattern (Fig. 22) concentrated ahead of the TC center to gather more detailed information on the development of regions of heavy precipitation on the poleward side of the decaying TC. The N42RF departure time will be 1 h after the departure of N42RF such that arrival at **7** will be approximately one hour after N43RF arrived at the same leg end point. The flight plan for N43RF is designed to be a "lawnmower" pattern across the poleward semi-circle of the decaying TC. If the target TC is farther east such that the interface between the midlatitude jet stream and TC outflow is located over water, then **7** in Fig. 21 and **7** and **4** in Fig. 22 should be placed within the interface region. Although both aircraft operate at levels that are below the primary interface, they will be able to gather data over the lower region of the outflow/jet interface. The over water requirement is necessary for the deployment of the GPS-sondes. GPS sondes will be deployed at the end of each leg, and at approximately 60 nmi spacing between end points. AXBTs will be deployed at the end of each leg and at appropriately spaced intervals between end points such that two equally-spaced AXBTs are placed between **3-4** and **6-7**, and one AXBT is placed at the midpoint between **4-5**.

2) **TC/MIDLATITUDE INTERFACE:** Immediately ahead of the decaying TC there are important interactions between the midlatitude jet stream and the outflow from the TC. This region will be investigated primarily by the NASA DC-8 (Fig. 22). To coordinate passage through the center of the decaying TC after the final pass by the ER-2, the DC-8 will depart between 1.5 and 2 h after the ER-2. The DC-8 will enter the pattern in the northwest quadrant of the decaying TC. Deployment of GPS sondes will begin when the DC-8 enters the environment of the decaying TC (**D** in Fig. 22). In the TC/midlatitude interface region, the DC-8 will fly a south-to-north leg at 40,000 ft across the midlatitude jet and TC outflow regions. If the target TC is farther east such that the interface between the midlatitude jet stream and TC outflow is located over water, then the leg **D-2** should be flown to allow at least one cross from the east to west side of the interface region before crossing back to **2**. The over water requirement is necessary for the deployment of the GPS-sondes. The next leg will be oriented to be nearly perpendicular to the start of the pre-storm precipitation region. Leg **4-5** is oriented north-south in the northeast quadrant of the decaying TC where warm frontogenesis and heavy precipitation are often located. Leg **5-2** is oriented across the TC/midlatitude interface with a final leg to the TC center from the north. This leg will be approximately 1.5 h after a similar leg by the ER-2. At this time, the ER-2 will be flying a northeast-southwest leg (**4-2** in Fig. 20) similar to the initial leg of the DC-8 pattern several hours earlier. With the staggered departure, both NASA aircraft will recover at nearly the same time.

3) **PRE-STORM PRECIPITATION REGION:** Pre-storm precipitation regions that typically form ahead of the TC near the primary interface with the midlatitude circulation will be investigated (Figs. 23-24) by the second WP-3D (preferably N42RF) and the Canadian Convair-580 aircraft. Initially, the WP-3D will pass through the decaying TC center from the west. If N42RF departs approximately one hour prior to N43RF and the ER-2, it will provide the first center observation about 0.5 h prior to the first ER-2 observation. Following the pass through the center, N42RF will proceed to the east then turn to the north along a path across the region of warm frontogenesis and potential significant wave heights. Of importance on this leg are observations of surface winds with the C-band scatterometer. Near the pre-storm precipitation area, N42RF will enter a rotated figure-4 pattern at an altitude near 20,000 ft to examine the lower portion of the TC/midlatitude interface and the microphysical and dynamical characteristics of the pre-storm precipitation area. Two passes along leg **4-5** are planned to observe the lower-levels across the midlatitude jet and TC outflow as the entire system translates northward.

The N42RF aircraft will deploy its first GPS dropwindsonde in the TC center. No GPS sondes will be required along leg **2-3** since this will be well sampled by the ER-2 and N43RF aircraft. Starting at **3**, GPS sondes will be deployed at approximately 60 nmi intervals (20-25 GPS sondes) through the second pass along leg **4-5**. The ocean thermal profile will be observed ahead of the decaying TC via AXBTs that will deployed starting at **3** then at 150 nmi intervals (approximately 9 AXBTs). Recovery will be at Boston, MA or Providence, RI.

For a typical poleward-moving TC along the eastern North American coastline, the pre-storm precipitation region will be within range of the Canadian aircraft, which will operate out of Greenwood, Nova Scotia (Fig. 25a). Flight level will be between 20,000-23,000 ft. The pattern is designed such that there is one out and back leg. On the outbound leg, the aircraft will cross the pre-storm precipitation region at and altitude between 20,000 and 25,000 feet. On the return leg, the aircraft will do several descents (Fig. 25b) to an appropriate altitude, climb back to altitude. The vertical patterns will provide important microphysical information on the precipitation formation mechanisms and the precipitation efficiency of the storm. GPS sondes, radar, and detailed microphysical properties of the pre-storm precipitation region will be obtained by this aircraft.

Typically, a decaying TC that has entered the transformation stage of extratropical transition may translate northward at speeds in excess of 30 kt. If a typical translation speed is observed, the second set of missions will only include the WP-3D that recovered in either Boston, MA or Providence, RI and the Canadian Convair 580. It is anticipated that the WP-3D aircraft will fly a modified TC core mission similar to that flown by N42RF the previous day when the TC was farther south. The plan will be modified to allow for recovery back to MacDill AFB.

The EC Convair 580 will fly a mission similar to its previous plan that concentrates on the microphysical and structural characteristics of the pre-storm precipitation area. Depending on the location of the decaying TC relative to Greenwood, NS, the EC Convair plan will provide for a second flight to examine the decaying TC core region. It is anticipated that the flight plan for the second Convair 580 flight would be similar to the previous day's flight (Fig. 25), except that the out and back leg will traverse t he decaying TC core rather than the pre-storm precipitation region.

4) **Limited Aircraft Availability Option:** In the case when one or more aircraft are unavailable, altitude and distance considerations will determine the mission priority. Using Table 1, scenarios may be devised to eliminate or concentrate on specific regions or characteristics.

   i) **NASA ER-2 Unavailable:** Priority will be placed on observation of the decaying TC core structure rather than TC/midlatitude interface. Therefore, the NASA DC-8 will fly the ER-2 pattern defined in Fig. 20 with appropriate altitude modification and the pattern in Fig. 22 will not be flown. No change will be required for the N42RF pattern (Fig. 23) while N43RF may fly the pre-storm precipitation pattern (Fig. 23) unless the TC Core Only Option is taken in which N43RF will fly the pattern defined in Fig. 22.

   ii) **NASA DC-8 Unavailable:** If the NASA DC-8 is unavailable, the observation of the TC/midlatitude interface will be deleted from the mission plans. The ER-2 will fly the TC core pattern (Fig. 19) since there is a requirement for observations of the decaying TC structure in the upper troposphere. Since the TC/midlatitude interface is concentrated at the outflow/jet stream level, neither NOAA WP-3D will be diverted to fly the TC/midlatitude interface pattern (Fig. 23). No change will be required for the N42RF pattern (Fig. 20) while N43RF may fly the pre-storm precipitation pattern (Fig. 23) unless the TC Core Only Option is taken in which N43RF will fly the pattern defined in Fig. 22.

   iii) **Both NASA aircraft Unavailable:** Mission priority will be placed on observation of the decaying TC core structure as defined in the TC Core Region Option above. Aircraft N2RF will fly the pattern in Fig. 21 while N43RF will fly the pattern in Fig. 22.

   iv) **High altitude WP-3D unavailable:** The pre-storm precipitation area will only be observed by the EC Convair 580. The available WP-3D will fly the TC core pattern (Fig.. 21) due to the importance of observing the transformation of the warm core during interaction with the midlatitude baroclinic environment, observations of precipitation patterns ahead of the decaying TC, and observations of wave spectra with the SRA poleward of the decaying TC center.

   v) **Low altitude WP-3D unavailable:** N42RF will fly the TC core pattern (Fig. 21) with emphasis on the low-level wind field, precipitation patterns poleward of the decaying TC center, and decay of the warm core.

Table 1. Physical characteristics to be observed in each area of a TC that is in the transformation stage of extratropical transition plus optimal aircraft flight level, instrumentation, and aircraft.

Pre-Storm Precipitation Area

Purpose	Vertical Level	Instrumentation	Aircraft
Examine thermodynamic structure of pre-storm environment to assess the presence of potential instability and conversion to slantwise or gravitational instability.	Middle troposphere (20,000-30,000 ft) and below	GPS sondes Microwave radiometer (SFMR) Doppler radar	WP-3D N42RF (high-level aircraft)
Examine microphysical characteristics of the pre-storm precipitation area	Middle troposphere (20,000-30,000 ft) and below	Cloud physics package	WP-3D N42RF (high-level aircraft)
		Cloud physics package	Convair 580

TC/Midlatitude Interface

Purpose	Vertical Level	Instrumentation	Aircraft
Examine interactions between the TC outflow and the midlatitude environment into which the decaying TC is moving	Upper troposphere (40,000 ft) and below	GPS sondes Doppler radar (PR-2)	NASA DC-8
Examine oceanic temperature profile ahead of the decaying TC core	Middle troposphere and below	AXBTs	WP-3D (either aircraft)
Examine surface wind field	Middle troposphere and below	C-band scatterometer (C-SCAT)	WP-3D N42RF
Examine surface wave spectra ahead of the decaying TC	Lower troposphere (5,000 ft) and below	Radar altimeter (SRA)	WP-3D N43RF

TC Core

Purpose	Vertical Level	Instrumentation	Aircraft
Examine decay and tilt of the warm core aloft in response to increased vertical wind shear associated with the midlatitude environment. Examine interactions between the TC core and upper-level synoptic-scale features	Upper troposphere (65,000 ft) and below	GPS sondes Doppler radar Visible and IR sensors, scanning radiometer	NASA ER-2
Examine evolution of deep convection in response to increased vertical wind shear in the environment	Upper troposphere (65,000 ft) and below	GPS sondes Doppler radar Scanning visible and IR sensor and scanning radiometer	NASA ER-2

Examine evolution of extratropical cyclone characteristics such as frontogenesis, asymmetric wind distribution, and warm and cold temperature advection	Middle troposphere and below	GPS sondes Doppler radar Cloud physics package	WP-3D N43RF at mid levels until SRA is needed
Examine ocean thermal properties	Middle troposphere and below	AXBTs	WP-3D N43RF, low-level aircraft

EXTRATROPICAL TRANSITION EXPERIMENT

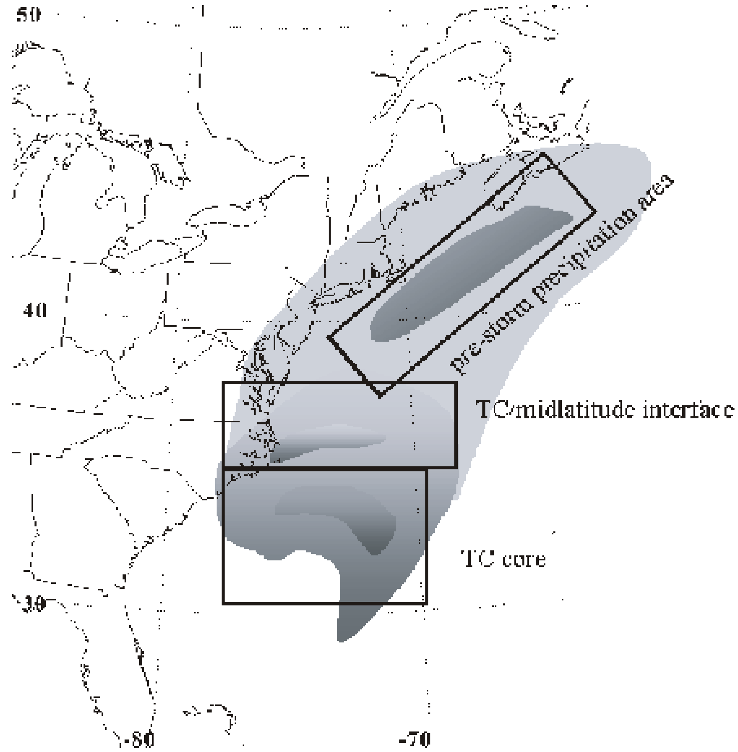

Fig. 19. Schematic of TC undergoing extratropical transition

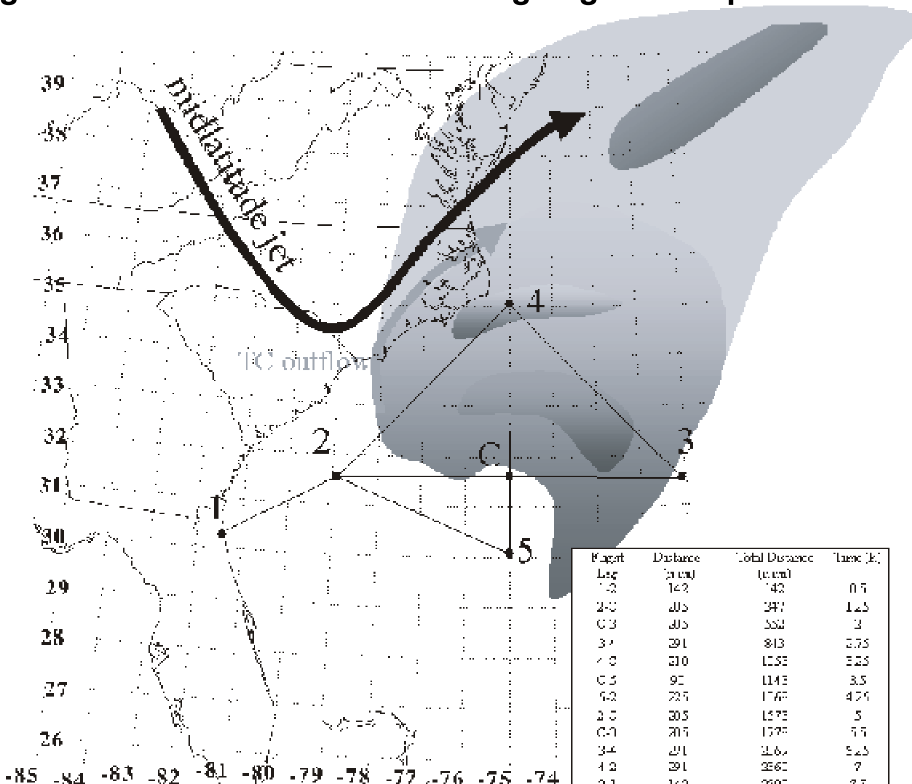

Flight Leg	Distance (n mi)	Total Distance (n mi)	Time (h)
1-2	142	142	0.5
2-C	205	347	1.25
C-3	205	552	2
3-4	291	843	2.75
4-C	210	1053	3.25
C-5	90	1143	3.5
5-2	225	1368	4.25
2-C	205	1573	5
C-3	205	1778	5.5
3-4	291	2069	6.25
4-2	291	2360	7
2-1	142	2502	7.5

Fig. 20. ER-2 Extratropical Transition Pattern

EXTRATROPICAL TRANSITION EXPERIMENT

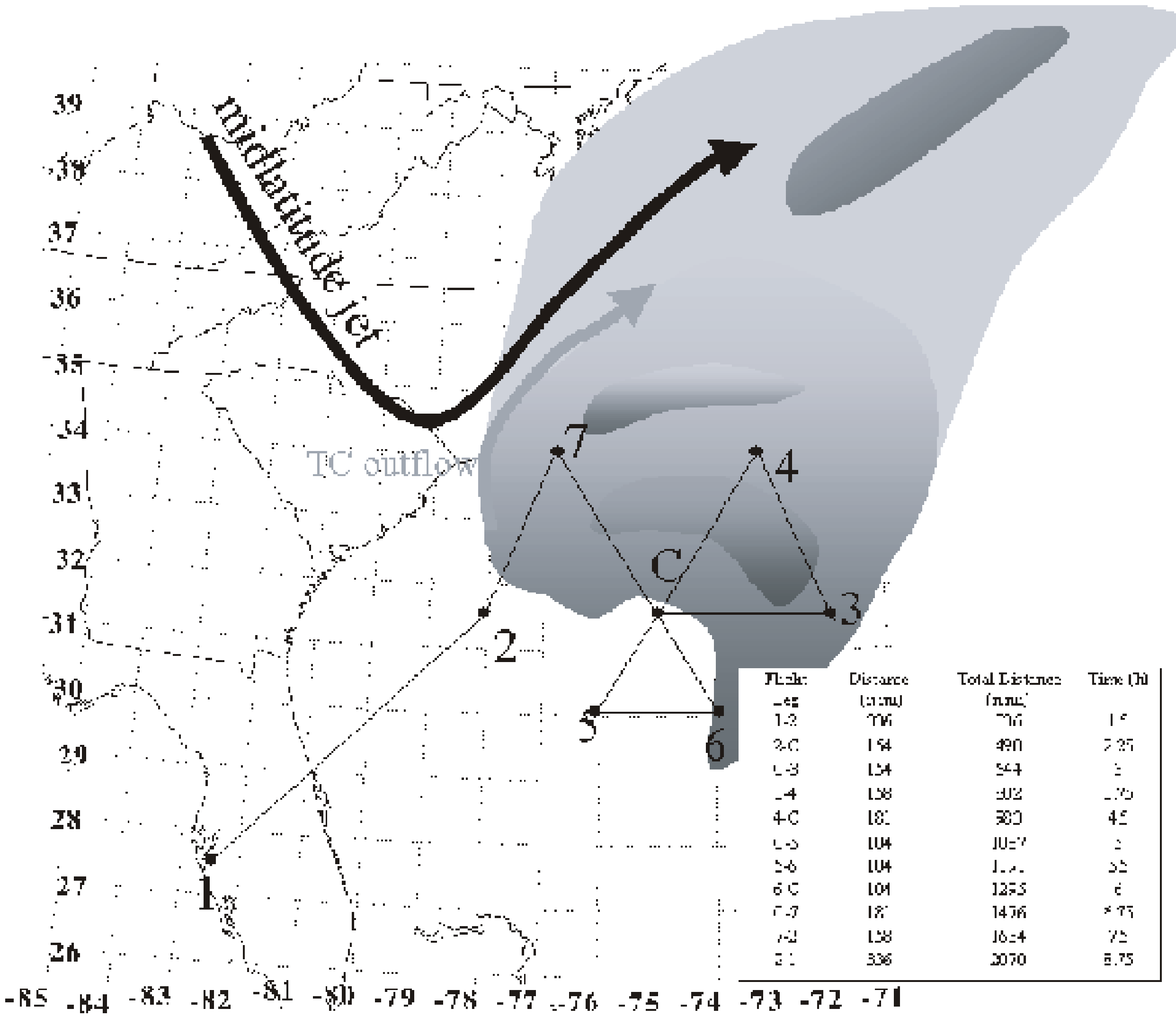

Flight Leg	Distance (nm)	Total Distance (nm)	Time (h)
1-2	[illegible]	[illegible]	[illegible]
2-C	154	490	[illegible]
C-3	154	544	[illegible]
3-4	158	[illegible]	[illegible]
4-C	[illegible]	[illegible]	[illegible]
C-5	104	[illegible]	[illegible]
5-6	104	[illegible]	[illegible]
6-C	104	[illegible]	[illegible]
C-7	[illegible]	1476	[illegible]
7-2	158	[illegible]	[illegible]
2-1	336	2070	[illegible]

Fig. 21. WP-3D (N42RF) Core Pattern

• Note 1.	Set airborne Doppler radar to F/AST on all legs.

EXTRATROPICAL TRANSITION EXPERIMENT

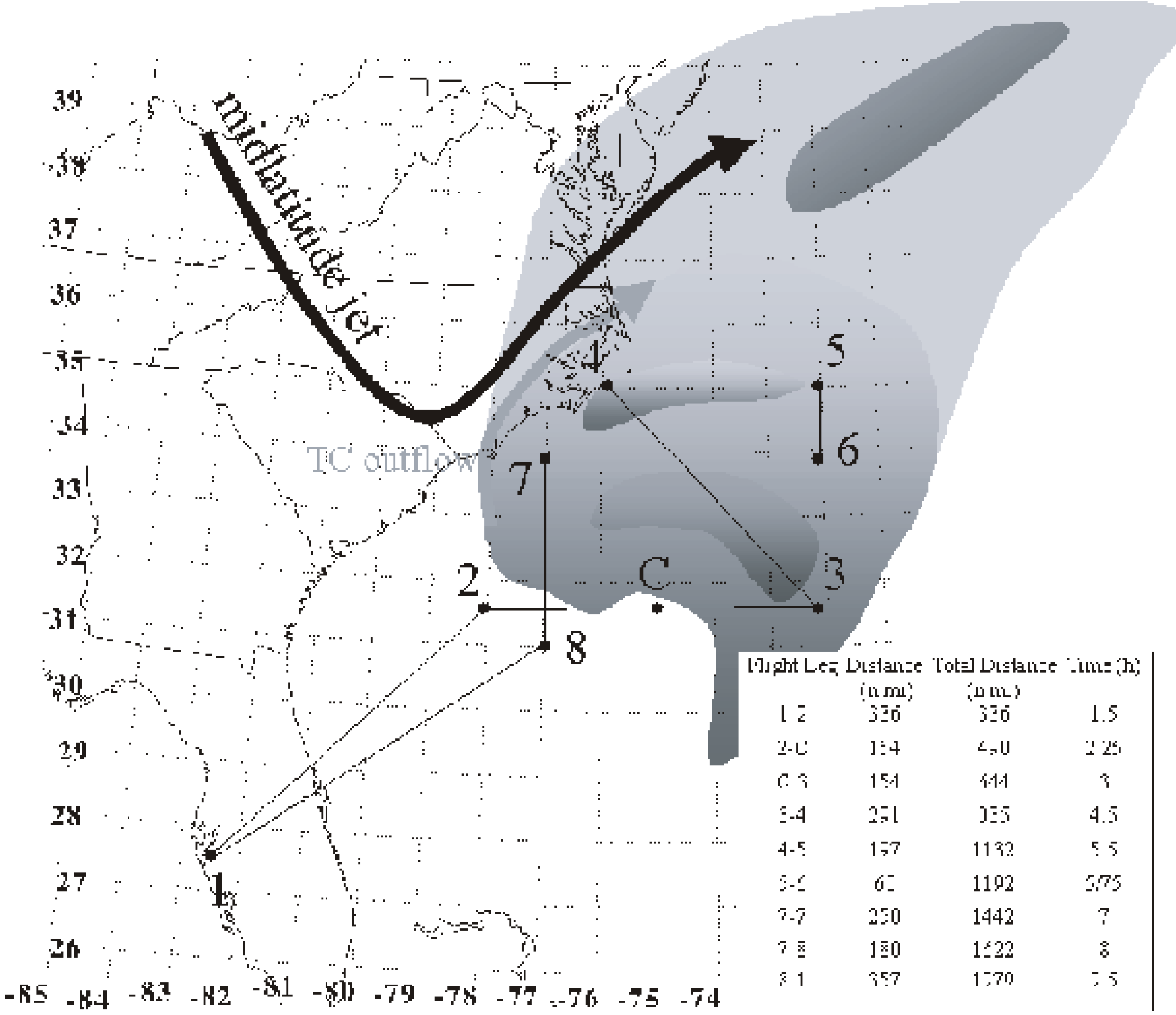

Flight Leg	Distance (n mi)	Total Distance (n mi)	Time (h)
1-2	336	336	1.5
2-C	154	490	2.25
C-3	154	644	3
3-4	251	895	4.5
4-5	157	1132	5.5
5-6	60	1192	5.75
6-7	250	1442	7
7-8	180	1622	8
8-1	357	1970	9.5

Fig. 22. WP-3D (N43RF) TC Core only option

• Note 1.	Set airborne Doppler radar to F/AST on all legs.

EXTRATROPICAL TRANSITION EXPERIMENT

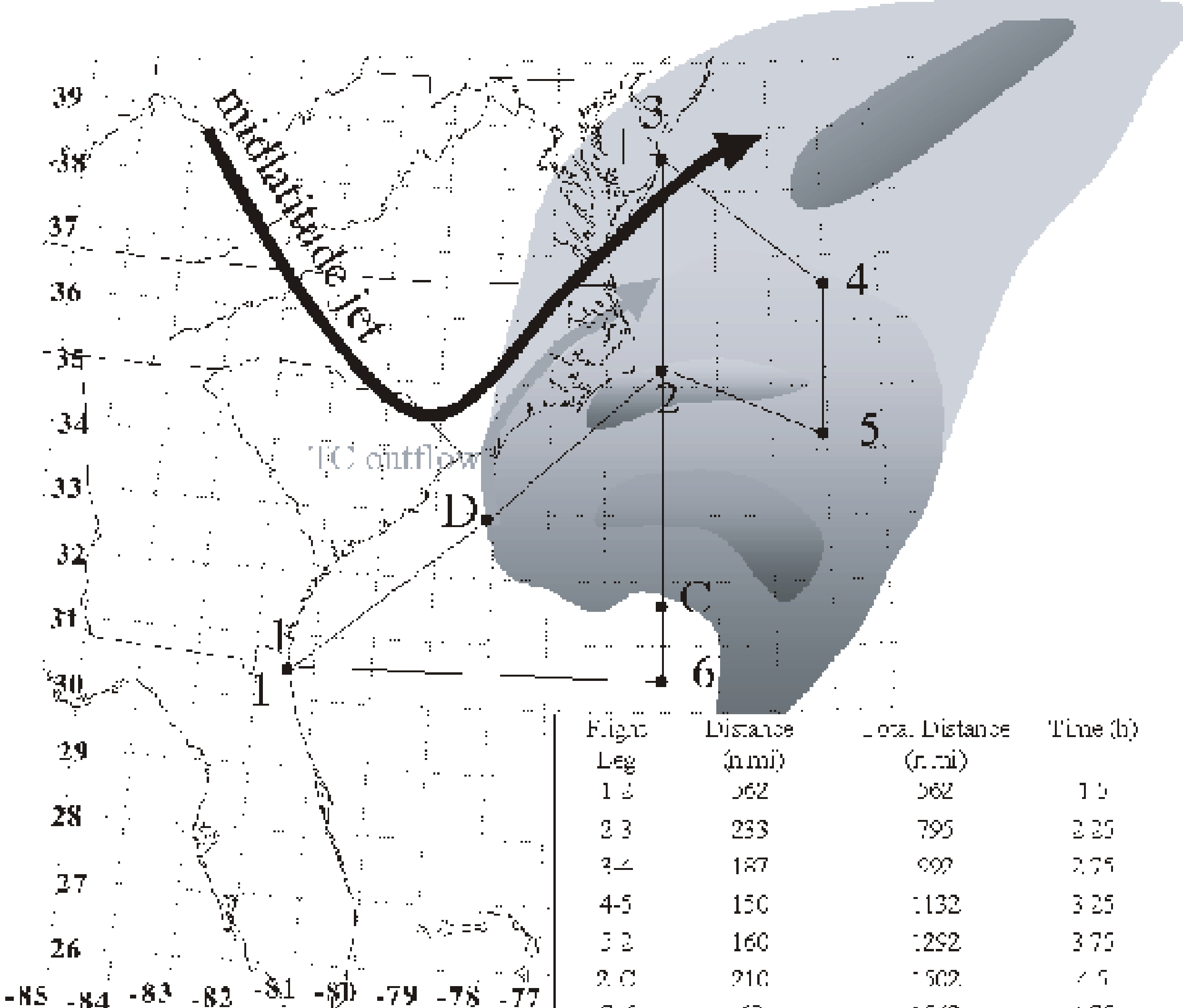

Flight Leg	Distance (n mi)	Total Distance (n mi)	Time (h)
1-2	562	562	1.5
2-3	233	795	2.25
3-4	187	982	2.75
4-5	150	1132	3.25
5-2	160	1292	3.75
2-C	210	1502	4.5
C-6	60	1562	4.75
6-1	337	1899	6

Fig. 23. DC-8 Extratropical Transition Pattern

EXTRATROPICAL TRANSITION EXPERIMENT

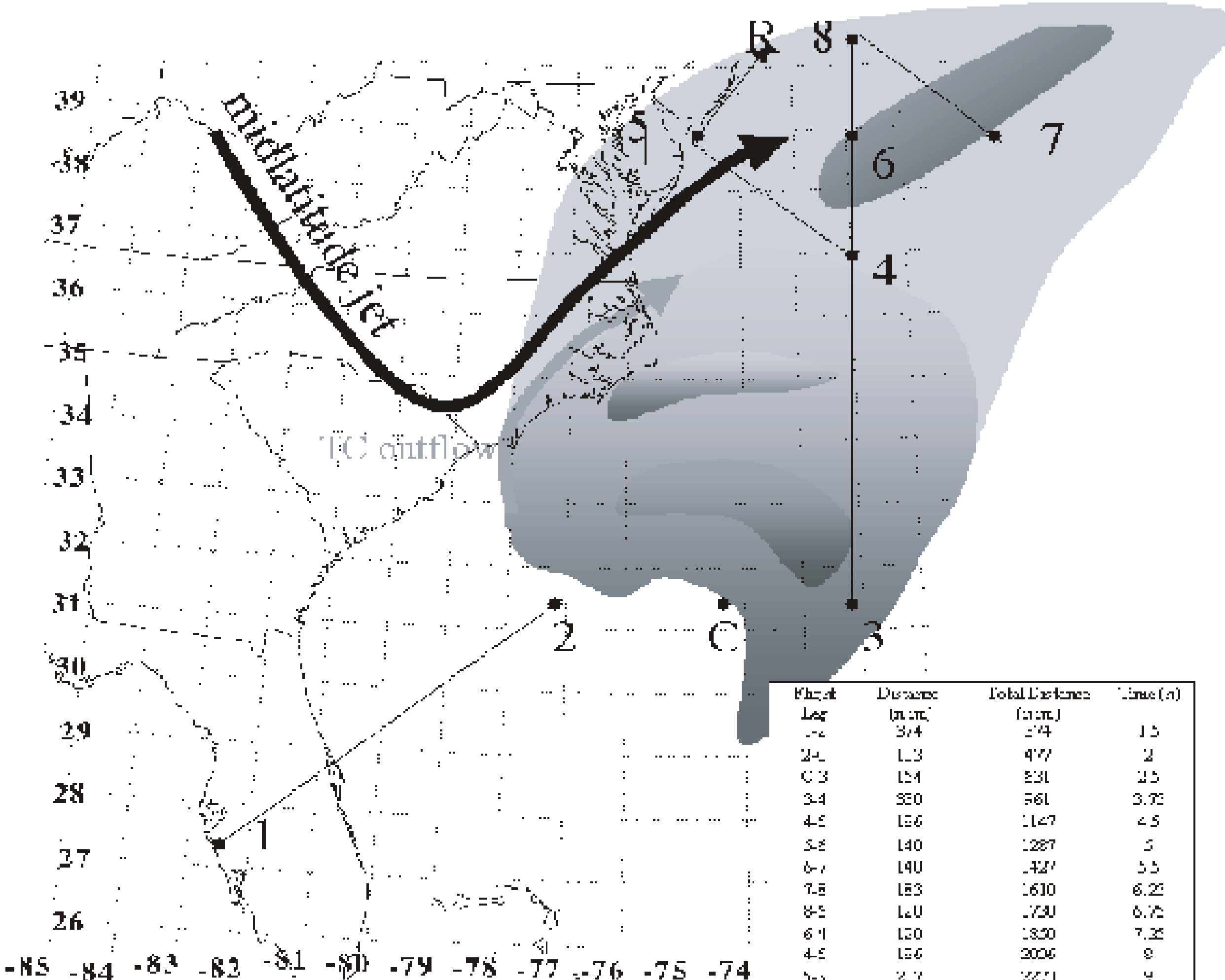

Flight Leg	Distance (n.mi.)	Total Distance (n.mi.)	Time (h)
1-2	374	374	1.5
2-C	123	497	2
C-3	134	631	2.5
3-4	330	961	3.75
4-5	186	1147	4.5
5-8	140	1287	5
6-7	140	1427	5.5
7-8	183	1610	6.25
8-6	120	1730	6.75
6-4	120	1850	7.25
4-5	156	2006	8
5-R	[illegible]	[illegible]	9

Fig. 24. WP-3D (N43RF) Extratropical Transition Pattern

EXTRATROPICAL TRANSITION EXPERIMENT

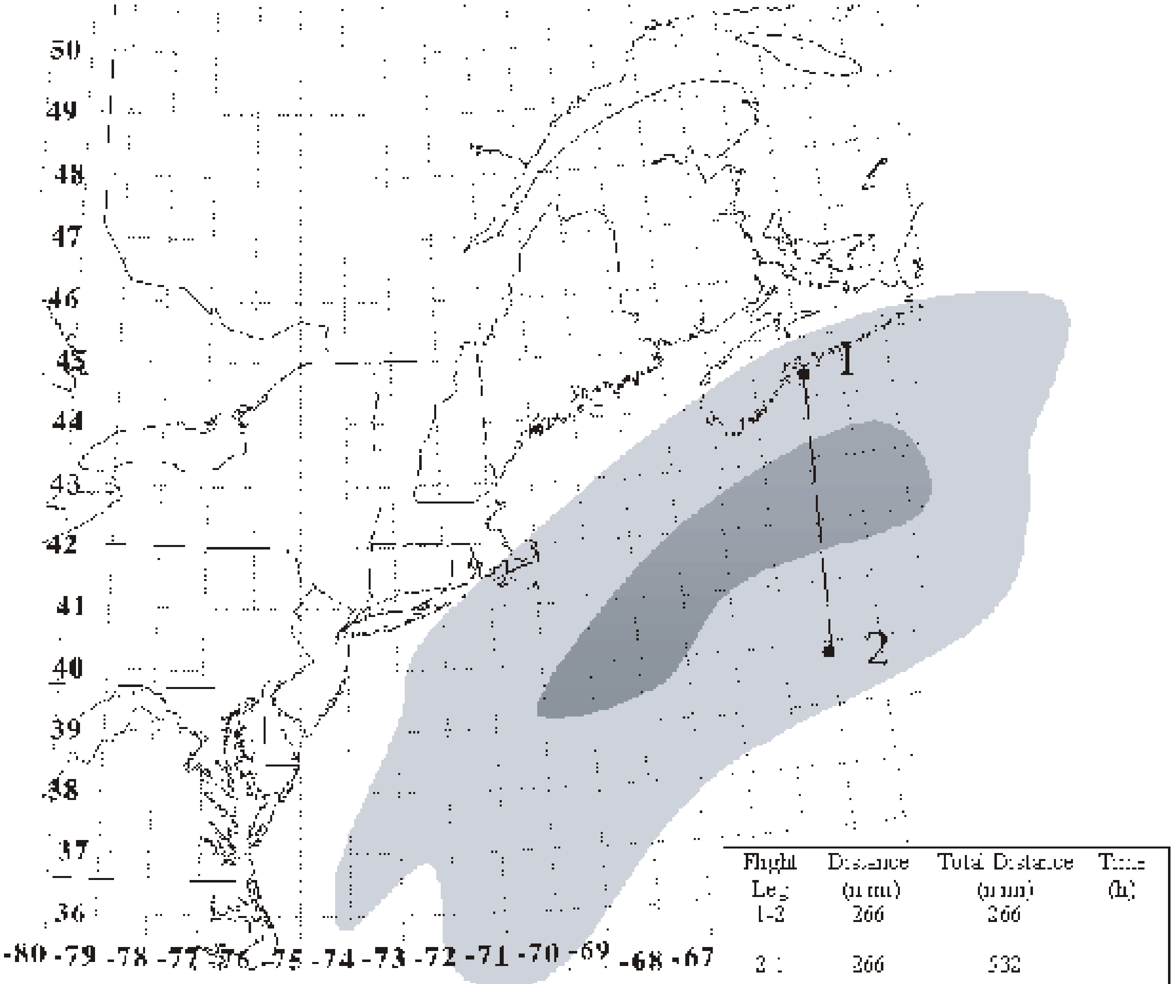

Flight Leg	Distance (n mi)	Total Distance (n mi)	Time (h)
1-2	266	266	
2-1	266	532	

Fig. 25. (a) Convair 580 Extratropical Transition Pattern

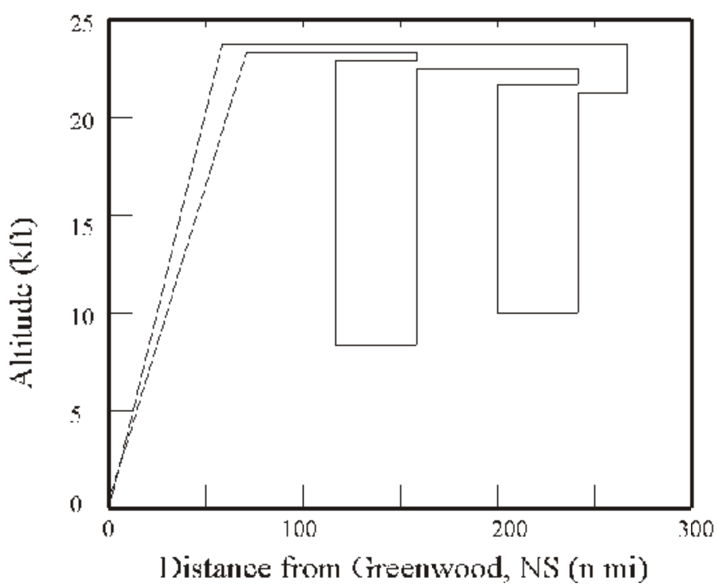

Fig. 25. (b) Vertical profile of Convair 580 pattern

14 Tropical Cyclogenesis Experiment

Program Significance: Tropical cyclogenesis can be viewed as a rapid increase of low-level cyclonic vorticity organized on the mesoscale within a region of enhanced convective activity. Numerous hypotheses have been advanced in the literature to explain how this vorticity develops and amplifies. In many of these genesis hypotheses an incipient midlevel (e.g., 850-500 hPa) cyclonic vortex is required for development of the low-level cyclonic circulation. Where these hypotheses differ is in the role that the midlevel vortex plays in genesis. In one theory, downdrafts driven by evaporational cooling advect the vorticity of the midlevel vortex downward, enhancing convection and low-level vorticity production. Observations of multiple midlevel vortices prior to genesis have led some to view the genesis process as a stochastic one whereby chance merger and axisymmetrization of these midlevel vortices leads to growth of the circulation to the surface. Another hypothesis emphasizes the role of the midlevel vortex in axisymmetrizing nearby low-level convectively-generated cyclonic vorticity, leading to spin-up of the surface circulation. Yet, another hypothesis emphasizes the role the midlevel vortex plays in providing a favorably reduced local Rossby radius of deformation to retain the heating from convective bursts and spin up low-level vorticity through low-level stretching caused by the convective heating. The purpose of the proposed experiment is to identify what role, if any, midlevel vortices play in organizing and amplifying low-level cyclonic vorticity.

Since the onset of deep, moist convection is a crucial component in tropical cyclogenesis, the identification of large-scale environments favorable for such convective activity is an important step in identifying likely candidates for genesis. Environments favorable for genesis in the Atlantic Ocean have been revealed by composites of operational analyses and case studies of genesis and lysis events. Western and eastern Atlantic composites have shown the dynamical importance of ascent forced through cyclonic vorticity advection (CVA) in the incipient storm environment. Over the eastern Atlantic, this vorticity advection is generally found equatorward of a 200 hPa zonally-oriented ridge axis in association with an upper-level easterly jet, while over the western Atlantic the CVA occurs downstream (upstream) of a 200 hPa trough (ridge). In both composites the low-level disturbance is located beneath an area of CVA and near a minimum in vertical wind shear (200 hPa-ATOLL level). Developing disturbances in both regions of the Atlantic are found downstream of a 700-hPa southeasterly jet along the equatorward side of a ridge axis. The conditions important in the Atlantic basin are similar to those found to be important in other basins, where conditions of weak vertical shear, low-level positive vorticity, and the repeated development of convective bursts are all necessary conditions for tropical cyclogenesis.

Recent observations from airborne Doppler radar have identified important processes on the mesoscale that contribute to tropical cyclogenesis. For example, results obtained from a WP-3D aircraft investigation of Dolly (1996) indicate its genesis was strongly influenced by persistent, deep convection in the form of mesoscale convective systems (MCSs) that developed in association with an easterly wave over the Caribbean. Within this deep convection an eye-like feature formed, after which time the system was declared a depression. The initial development of the low-level circulation in both Dolly (1996) and Guillermo (1991) occurred in the presence of multiple midlevel vortices. The close proximity of the low- and mid-level vorticity maxima (often within 50-100 km horizontally) observed in these two genesis cases supports a further examination of the aforementioned vortex merger ideas. To adequately diagnose the role of the midlevel vortex, it is vital that it be sampled in its entirety (which will invariably depend on the distribution of precipitation scatterers) and with a temporal resolution that allows time continuity of the vortex to be established. For a complete picture detailed observations of the mid- and low-level thermal and moisture fields are also necessary.

Since both tropical cyclogenesis and TC intensity change can be defined by changes in low- and mid-level vorticity, knowledge of the processes that play a significant role in genesis will also advance our understanding of intensity change. A better understanding of the processes that lead to an increase in low- and mid-level cyclonic vorticity will also allow NHC to better monitor and forecast tropical cyclogenesis and intensity change, improvements that would be especially valuable for those events that threaten coastal areas. Data obtained by aircraft investigating potential genesis events will positively impact operations and research in other ways as well. The ingestion of this data into the NCEP model analysis and initialization schemes will permit an improvement in NCEP model forecast performance based upon a better representation of the mesoscale and synoptic-scale structure near the incipient disturbance. In addition to improving the understanding and forecasting of tropical cyclogenesis and intensity change, the proposed experiment will yield useful insight into the structure, growth and ultimately the predictability of the systems responsible for almost all of the weather-related destruction in the tropical Atlantic. Investigation of systems that fail to complete the genesis process will also result in a better understanding and prediction of easterly disturbances in general, so that distinction can be better made between developing and non-developing tropical disturbances.

Objectives: In keeping with the discussions above, the objectives of this experiment are as follows:

- Develop means for identifying likely candidates for tropical cyclogenesis and techniques for finding and tracking midlevel vortices within these candidates.
- Investigate role, if any, that midlevel vortex plays in organizing deep convection.
- Document the development of low-level vorticity in the presence of a midlevel vortex center.
- Study the interactions between low- and mid-level vortices in pre-genesis environments.

Mission Description: This experiment may be executed with aircraft from NOAA alone, or NOAA in cooperation with the USAF flying into pre-genesis and incipient tropical disturbances over the Atlantic Ocean, Caribbean Sea, Gulf of Mexico, and tropical eastern North Pacific Ocean. The primary mission will require two WP-3Ds flying back-to-back with the G-IV aircraft flying a coordinated pattern. The two WP-3Ds will fly mesoscale patterns in close proximity to any suspected mid-level vortices while the G-IV simultaneously flies at upper levels (200-300 hPa) and collects observations to a distance of ~1500 km from the center of the disturbance. Crucial to a complete understanding of the genesis process is the collection of observations with high temporal and spatial resolution. Therefore, the staggered WP-3D missions are designed to commence on station at 0300 LT and again on station at 1500 LT. The G-IV mission would occur coincident with the afternoon flight and consistent with synoptic missions centered on the 00 GMT synoptic time. If available, the USAF WC-130 aircraft can be used to enhance flight-level observations.

The main aircraft for the mesoscale flights will be the two WP-3Ds. Doppler radar observations, GPS-sondes, and flight level observations obtained during these flights will help locate low- and mid-level vortices and help document their structures and life cycles. A primary aspect of this experiment will be to observe the complete life cycle and interaction of low- and mid-level vortices and understand how these vortices are influenced by the diurnal cycle of convection. The location of persistent areas of deep convection and candidate vortices will be determined using high-resolution visible and infrared GOES-winds produced at HRD and rapid-scan and super-rapid-scan visible satellite imagery provided by CIRA/Colorado State University. Additionally, favorable large-scale environments for deep convection and vortex development, such as those described in the Introduction, will be identified using water vapor loops, model analysis fields enhanced by satellite winds, and QuickSCAT imagery, all available at HRD.

Staggered missions with the two WP-3D aircraft will begin with the first aircraft flying a low-level diamond pattern at 700-500 hPa (10,000-18,000 ft) shown in Fig. 26. Leg lengths will be 325-430 nmi (600-800 km), and the pattern will be centered approximately on the vortex as identified from satellite analyses. The benefit of this pattern is that it covers a relatively broad horizontal area, while the return flight allows for some temporal continuity (on the order of 3 hours) to the data. The primary purpose of these aircraft missions will be to collect F/AST Doppler radar and GPS-sonde data in the area of deep convection in order to map the evolution of the three-dimensional wind and thermodynamic structure of the deep convection and incipient vortex. Once a mid-level vortex is identified the aircraft will fly a pattern centered on the vortex (Fig. 27). Flight legs will be significantly reduced in length [100-135 nmi (180-250 km)] to allow for the collection of data with high temporal and spatial resolution near the vortex. The length of these flight legs is designed to completely include any low-level vortex within about 50-100 km of the midlevel vortex center. This will be important in documenting any interaction between the midlevel and low-level vortices.

If available, the G-IV will be most beneficial flying a synoptic-scale pattern. It will fly at maximum altitude observing the upper and lower troposphere with GPS-sondes in the pre-genesis and incipient tropical disturbance environment. A potential genesis event occurring in conjunction with primarily an upper tropospheric anticyclone will require a flight pattern similar to that given in Fig. 28a. The aircraft will dispense 20-25 GPS-sondes mostly on the poleward side of the incipient disturbance during the flight to help define wind, temperature and moisture patterns near the ridge axis. Should a potential genesis event occur in association with an upper-tropospheric trough-ridge couplet, a flight pattern similar to that shown in Fig. 28b will be required. This flight pattern will collect observations near both the trough and ridge with upwards of 20-25 GPS-sondes. These flight patterns are designed to define those regions where large-scale forcing for ascent exists and persistent deep convection is favored.

An enhancement of the data collected during genesis by the three NOAA aircraft may be accomplished by adding observations from investigative AFRES WC-130 aircraft. Should a AFRES WC-130 aircraft be available it would be requested to fly at maximum altitude dispensing GPS-sondes in the southern and eastern quadrants of the incipient disturbance. This aircraft would be requested to fly a saw-tooth pattern centered on asymptotes of confluence, convective inflow bands, and/or thermal boundaries within ~300 nmi (500 km) of the incipient disturbance.

In addition to the satellite and airborne data described above, temperature soundings of the mid- and upper-level thermodynamic environment of the system will be obtained using the GOES satellite and the AMSU instrument aboard the polar-orbiting NOAA-15 satellite. These observations will yield important information about the response of the vortex's thermal structure to the convective bursts complementing the GPS-sondes dropped from the aircraft. SSM/I imagery, available from the World Wide Web, will also be used to infer the intensity of incipient disturbances during times when the aircraft are not flying.

The possible availability of multiple aircraft during this experiment leads to several different scenarios. A summary of the potential combinations of aircraft during genesis experiments follows:

- Option 1 (lesser experiment):

The two core NOAA WP-3D aircraft alone will fly staggered figure-4 or grid patterns (Figs. 26-27) centered on the area of persistent deep convection and/or any low level vortex over a 2-4 day period.

- Option 2 (primary experiment):

Option 1 augmented with large-scale upper- and lower-tropospheric observations obtained by the G-IV or NASA DC-8 aircraft flying patterns similar to those given in Fig. 26.

- Option 3 (optimal experiments):

A) Option 2 with AFRES WC-130 flying a standard reconnaissance mission.

B) Option 2 with AFRES WC-130 flying a targeted mission to sample asymptotes of confluence, convective inflow bands, and/or thermal boundaries within ~300 nmi (500 km) of the incipient disturbance.

C) Option 2 with the G-IV or NASA DC-8 aircraft to collect quasi-continuous observations in the upper and lower troposphere within ~900 nmi (1500 km) of the disturbance.

D) Option 3B with the G-IV or NASA DC-8 aircraft to collect quasi-continuous observations in the upper and lower troposphere within ~900 nmi (1500 km) of the disturbance.

TROPICAL CYCLOGENESIS EXPERIMENT

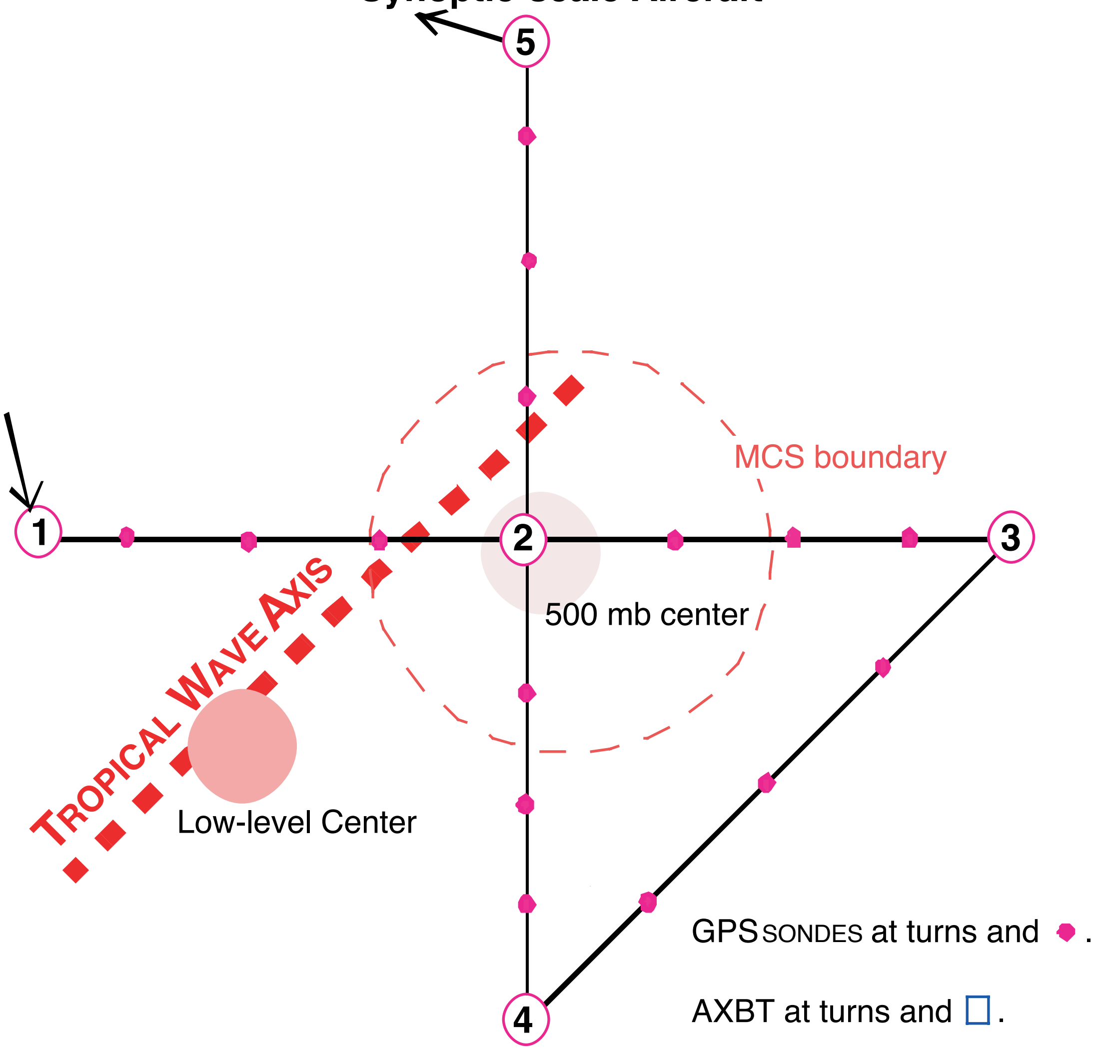

Fig. 26. Synoptic-scale Aircraft Flight Track

• Note 1.	True airspeed calibration is required.
• Note 2.	The pattern may be entered along any compass heading.
• Note 3.	Fly **1—2—3—4—2—5** at 18,000 ft (5.5 km or ~500 hPa), 325–430 nmi (600-800 km) leg length, depending on ferry distance.
• Note 4.	Point 2 is near the moving apex of the trough axis.
• Note 5.	Set airborne Doppler radar to continuously scan perpendicular to the track on radial penetrations, and F/AST on downwind legs.

TROPICAL CYCLOGENESIS EXPERIMENT

Mesoscale Aircraft

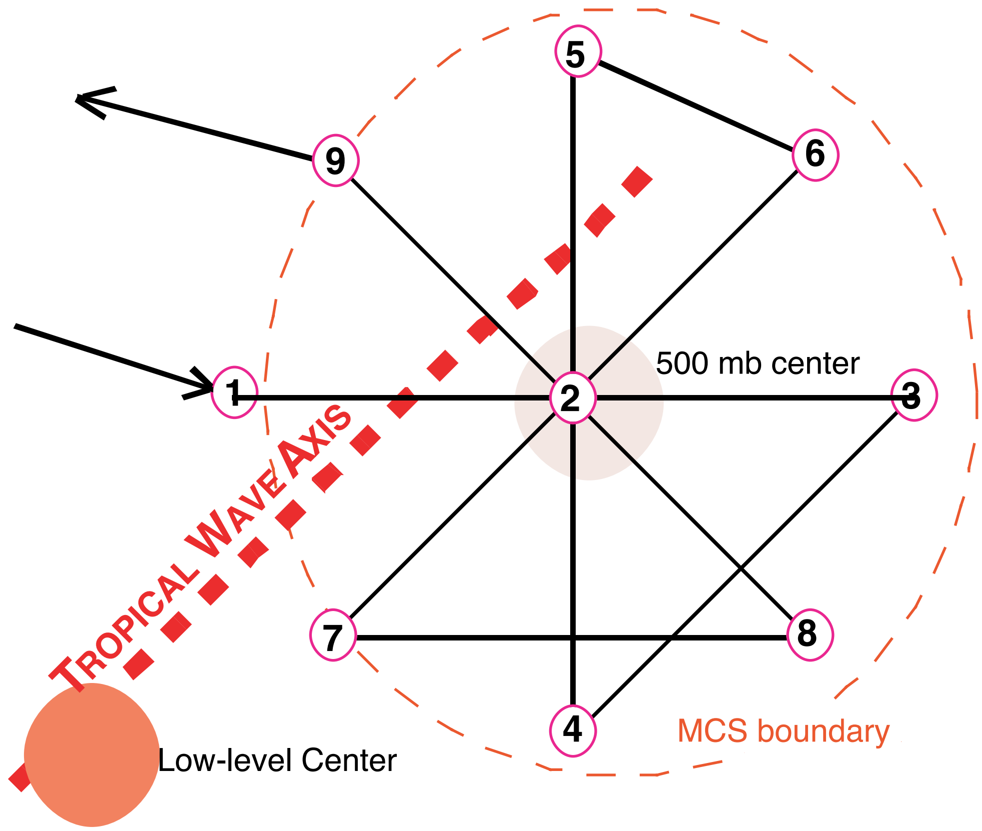

Fig. 27. Mesoscale Aircraft Flight Track

• Note 1.	True airspeed calibration is required.
• Note 2.	The pattern may be entered along any compass heading.
• Note 3.	Fly **1—2—3—4—2—5—6—2—7—8—2—9** at 600 or 700 hPa (PA), 100–135 nmi (185-250 km) leg length.
• Note 4.	Point **2** is near the moving apex of the trough axis.
• Note 5.	Set airborne Doppler radar to continuously scan perpendicular to the track on radial penetrations, and F/AST on downwind legs.

TROPICAL CYCLOGENESIS EXPERIMENT

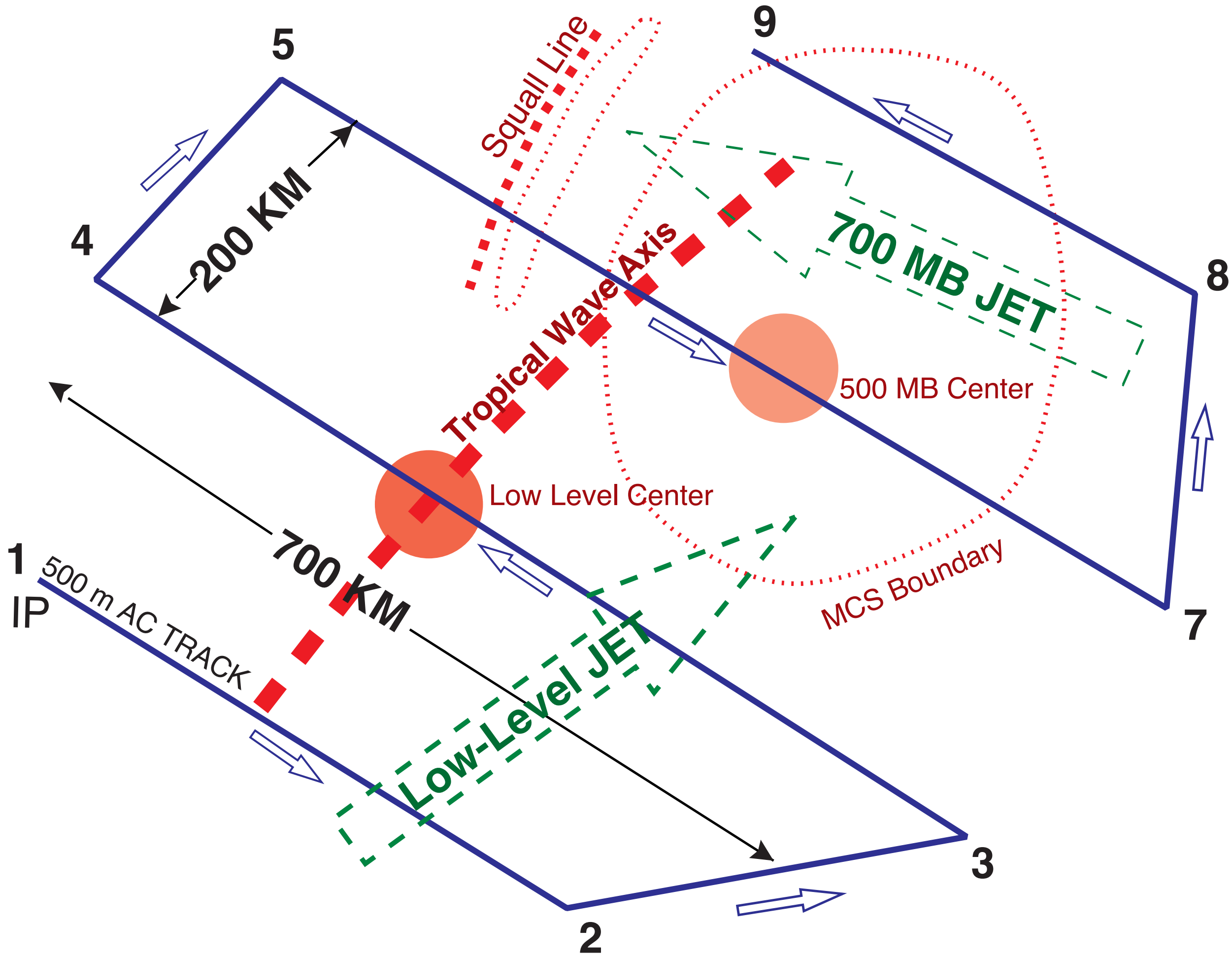

Fig. 28. (a) Low-level Grid Flight Track

• Note 1.	True airspeed calibration is required.
• Note 2.	The pattern is flown with respect to the wave axis, typically inclined at 30°–40° from N, or relative to circulation or vorticity centers.
• Note 3.	Fly **1—2—3—4—5—6—7—8—9** at 1,000 ft (300 m) or 10,000 ft (3.0 km) altitude, passing through the low–level jet, low–level circulation center (if it exists), MCS and associated mid–level center, or across mid–level jet.
• Note 4.	Set airborne Doppler radar to F/AST on all legs.

TROPICAL CYCLOGENESIS EXPERIMENT

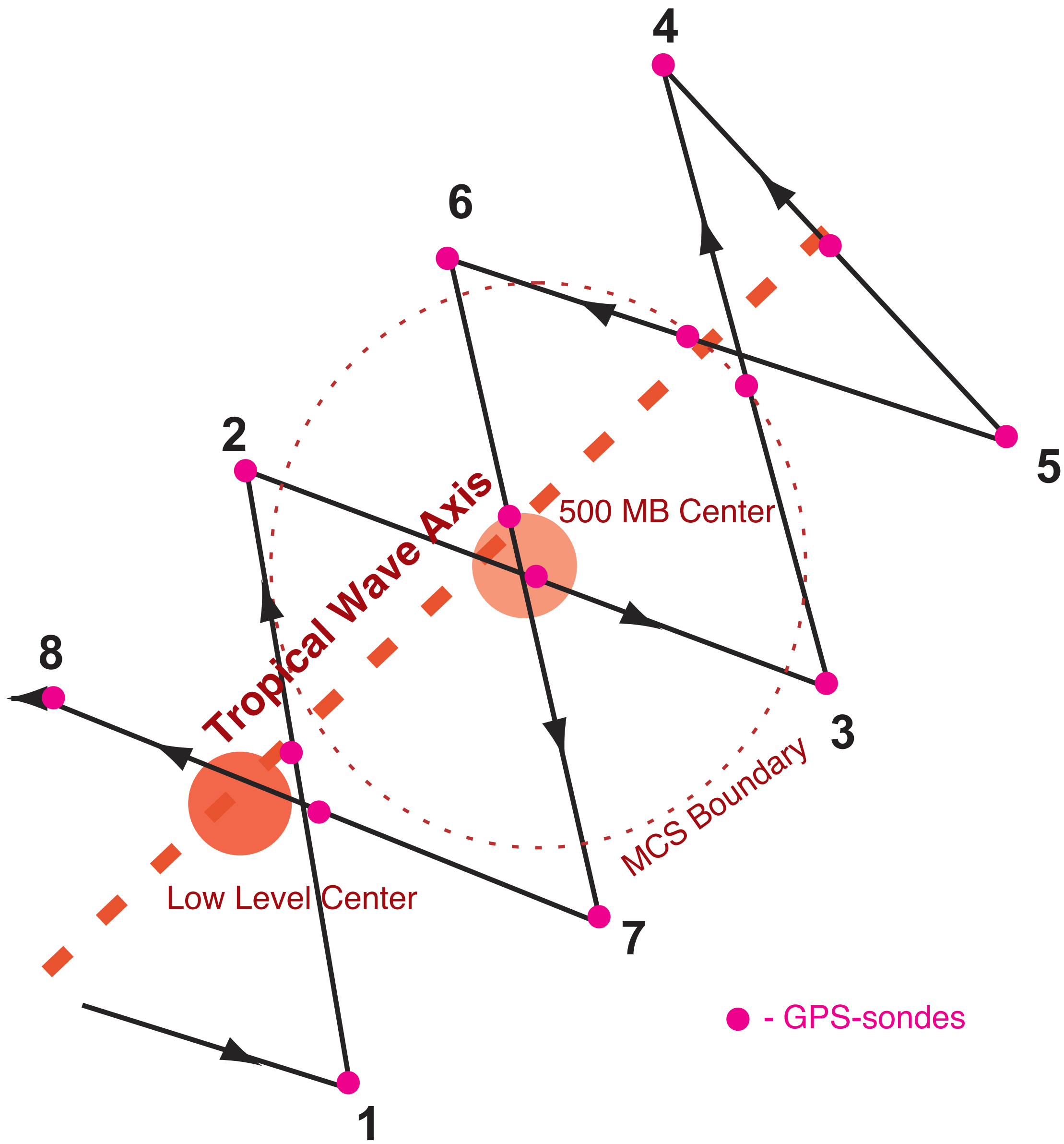

Fig. 28. (b) Alternate Grid Pattern

• Note 1.	True airspeed calibration is required.
• Note 2.	The pattern is flown with respect to the wave axis, typically inclined at 30°–40° from N, or relative to circulation or vorticity centers.
• Note 3.	Fly **1—2—3—4—5—6—7—8** at 3,000 ft (1.0 km) or 10,000 ft (3.0 km) altitude, passing through the low–level jet, low–level circulation center (if it exists), MCS and associated mid–level center, or across mid–level jet.
• Note 4.	Set airborne Doppler radar to F/AST on all legs.

15. Clouds and Climate

Program Significance: It has become widely recognized that the physics of clouds and precipitation must be considered in any realistic study of climate change. Clouds and water vapor play a pivotal role in the Earth's heat and radiation budgets. They control the amount of solar energy absorbed by the climate system as well as the infrared radiation emitted to space, and they strongly influence the redistribution of heat throughout the climate system, particularly in the tropics. Tropical clouds and cloud systems, because they lie in the zone of maximum solar input into the atmospheric system, have an important and probably direct climatic effect. Together with the release of latent heat, the radiative heating of layered clouds in the upper tropical troposphere is a significant source of energy for driving the global circulation. A wide spectrum of tropical cloud types and sizes are important from a climate viewpoint. In some instances, the very small-scale microphysical characteristics of the clouds, and interactions with the cloud dynamics, are important on the climate scale.

Small precipitating tropical cumuli, even though their fraction of active convective updrafts may be rather small at any given instant, have an aggregate fraction of total cloud cover, including decaying clouds that is in the range of 20-30%. Hence, they have a direct effect on the radiative transfer in the tropics. In addition, they have an effect on the turbulent mixing in the upper ocean through changes in radiative heating of the sea surface, and through precipitation into the sea surface. The behavior of these small clouds is linked to the ocean, and the ocean to the behavior of these clouds. As sea surface temperature influences the atmosphere on various time and space scales, clouds and upper ocean dynamics are inextricably linked.

The aerosol environment of the cloud is also very important to the evolution and climatic feedback of the clouds. The radiative properties, and the microphysical behavior of many clouds are strongly influenced by the aerosol environment of the cloud, largely through the activity spectrum of cloud condensation nuclei (CCN) (the number of CCN is effective as a function of increasing supersaturation). The size and number densities of cloud droplets and hydrometeors directly affect the radiative properties of the clouds. Thus, the tropospheric aerosol is particularly important because it affects the microphysics, and strongly influences the subsequent evolution of the radiative properties of a cloud.

The precipitation processes are also modulated by the CCN, aerosol concentrations, and the initial liquid water contents of the clouds. Clouds with lower CCN concentrations rain much more easily. So, the aerosol, besides exerting strong control on radiative effects of clouds, controls the course of the microphysics of clouds and precipitation development, and thus assumes a central role in the atmospheric water cycle and the atmospheric heating profiles due to latent heat. Besides the feedbacks on cloud radiative properties and latent heating profiles, the aerosols also have direct climatic effects of their own; e.g., large changes in optical depth across the Atlantic due to dust outbreaks from Africa. A number of issues concerning aerosol-cloud interactions remain uncertain and require further investigation. An inventory of the principal sources and nature of CCN, and CCN spectra, are required. The CCN characteristics over tropical ocean areas are particularly important from a climate standpoint, and adequate observations are particularly scant.

This study is complimentary to our continuing work on studies of the dynamics and microphysics of TC convection. The oceanic cumulus provides a simple, easily observed convective entity that has more similarities to TC convective clouds than differences. One advantage is that the precise stage of an oceanic cumulus in its life cycle is usually definable. Thus answering questions about this simpler entity will complement the TC observation program, and greatly aid in the interpretation of more complex data sets from large international field programs. We can exploit our extensive observational capability in the natural convective laboratory at our doorstep (Florida Bay, Bahamas, and the Caribbean Sea) for a relatively meager investment of resources. The result will be an increased understanding of principles that are applicable to convection in general.

The detailed microphysical measurements will also be useful to studies of the characteristics of precipitation in the tropics. We plan to measure the CCN characteristics in the subcloud layer, as well.

The precipitation characteristics derived from this proposed experiment will provide a data base for statistical rainfall studies underway in support of the Florida Bay Restoration Act, the Climate and Global Change Initiative, TOGA COARE, and TRMM. In particular this year the experiment will be coordinated with other TRMM validation experiments under the auspices of CAMEX-4. This data set will provide data on isolated topical convective clouds.

Objectives: The experiment will document the kinematics and microphysics of a representative sample of convection, with the initial emphasis being on small precipitating convective cells. We are particularly interested in these clouds` life cycle evolving from first condensation to a precipitating stage (glaciated or not). The specific scientific objectives of this experiment include:

- Building a database, or census, of small precipitating cumulus; e.g., dimensions (top height, diameter, and depth) and precipitation characteristics that has potential uses in several facets of climatic analysis.
- Documenting the thermodynamic and wind environment of the clouds. Mapping the three dimensional flow field within an active convective feature, and computing the hydrometeor trajectories into the region surrounding the storm using the airborne Doppler radar.
- Collecting rainfall statistics of oceanic convection for use in statistical rainfall studies.
- Measure the CCN concentrations in the cloud environments.
- Perform underflights of the TRMM satellite to obtain a data base suitable for evaluation and improvement of satellite and ground validation rainfall estimation algorithms.
- Testing the capability of determining the hydrometeor distributions from the reflectivity and Doppler mean velocity data at, or near, vertical incidence.
- Documenting the initial electrification and the evolution of the electric field within a sample of clouds.
- Documenting the characteristics of significant convective updrafts-water mass flux, the evolution of ice particles in the updrafts and the conversion rates to ice.
- Studying the relationship between initial and subsequent precipitation formation and the interaction between precipitation loading and the dynamics of the convective cell.
- Studying the interactions between warm cloud and ice microphysics at different stages of cloud development. Emphasis will be placed on the warm rain development versus rain from glaciation.

Mission Description: The experiment calls for a basic one-aircraft cloud structure and evolution sampling module (Fig. 29). This simple module could be executed during dedicated flights over Florida Bay or the Keys, or on targets of opportunity during deployments. Sampling during dedicated flights will emphasize combinations of remote sensing and cloud penetrations, while remote sensing will be used during deployments. These missions can be conducted in conjunction with NASA DC-8 and ER-2 flights in support of CAMEX-4.

The basic cloud-sampling module utilizes one WP-3D aircraft, equipped with the airborne Doppler radar and microphysics instrumentation, to investigate maritime convective clouds. Desired candidates for study should be convective clouds that can be followed through nearly their entire life cycle. The flight patterns of the basic cloud sampling module are shown in Fig. 29, and are relatively straightforward. Early in cloud development, the aircraft will make rapid repeated penetrations of the cloud, to sample the microphysical and electric field development at a constant distance below the cloud top (Fig. 29a). The attempt will be to document the microphysics and electric field development near cloud top from first condensation through a mature cloud stage. At each pass through the cloud, vertical incidence Doppler data will be collected to document the evolution of the vertical velocity field as the cloud matures. These patterns, or penetrations, will be oriented based upon the environmental wind shear vector. The aircraft will release a GPS-sonde or perform an aircraft sounding in the environment of each cloud sampled (in the clear, upwind of the cloud). The DC-8 and ER-2 should fly a butterfly pattern over the target of opportunity collecting remote sensing data.

As the cloud system matures the aircraft will attempt to sample the boundary layer airflow, CCN, rainfall characteristics, the warm cloud microphysics, and photo-document the cloud behavior. The basic pattern for this phase of cloud system development is shown in Fig. 29b. The WP-3D aircraft will mix circumnavigations of the cloud system to collect CCN and airborne Doppler radar observations, with low-level penetrations to collect rain and vertical incidence Doppler radar data. During this stage the DC-8 and ER-2 fly a butterfly pattern over the target region collecting remote sensing data. If it is deemed safe the DC-8 will penetrate the top of the cloud system to collect in situ microphysics data.

When the cloud system reaches the mature stage, with an extensive stratiform anvil, the WP-3D penetrates the stratiform rain region to collect microphysics and airborne Doppler radar data, interspersed with spiral descents from just above the bright band to 3,000 ft (1 km) altitude to document the microphysical changes as the precipitation particles melt and fall as rain (Fig. 29c). The spiral descents, done at a near constant bank angle of 15-20°, have varying descent rates to match the typical precipitation fall speeds (e.g., 200 ft min^{-1} in snow to 1800 ft min^{-1} in heavy rain). The DC-8 and ER-2 fly a butterfly pattern over the target region collecting remote sensing data. If it is deemed safe the DC-8 will also do a spiral descent from the top of the cloud system to the bright band altitude (16,000 ft) to collect in situ microphysics data. Spiral descents need to be closely coordinated between aircraft.

CLOUDS AND CLIMATE EXPERIMENT

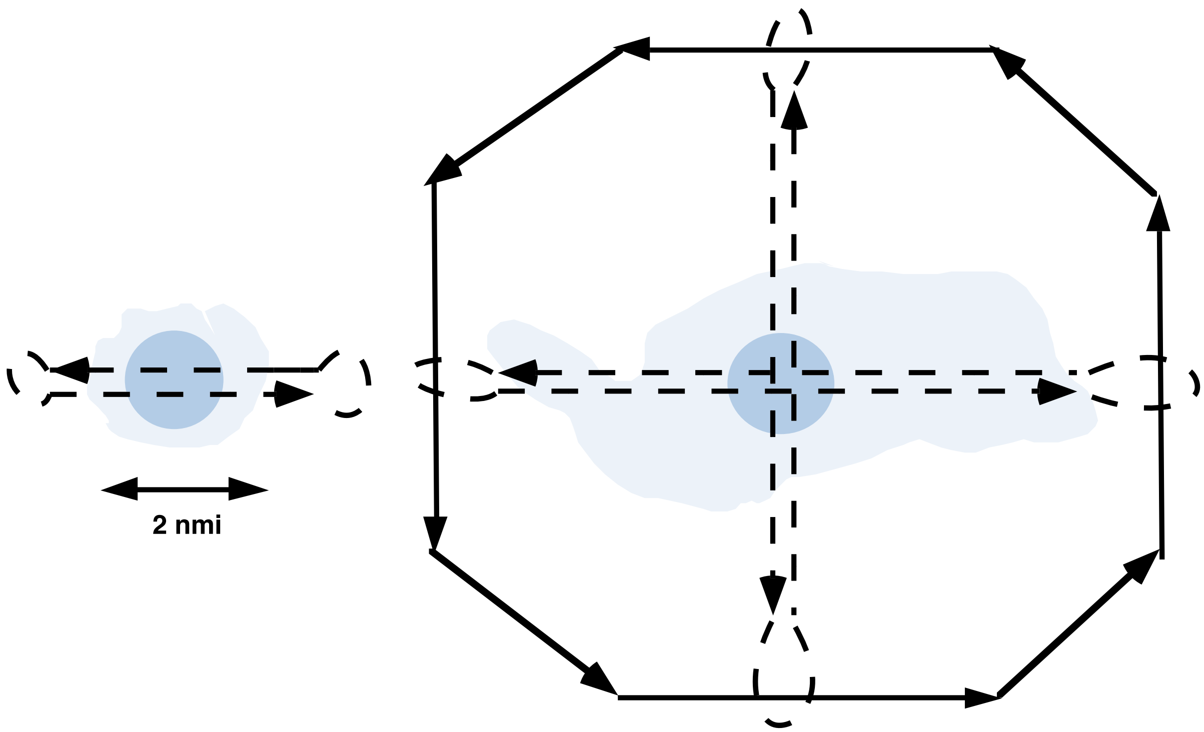

Fig. 29. (a) Initial Cloud Stage **Fig. 29. (b) Growing Stage**

• Note 1.	True airspeed calibration is required.
• Note 2.	The pattern may be flown along any compass heading.
• Note 3.	During initial cloud stage the aircraft conducts rapid penetrations climbing with cloud top from 12,000 ft (3.5 km), climbing with the cloud top on each successive pass. Passes are separated by 1,500 ft (500 m) altitude. Climbs occur away from the convection.
• Note 4.	During the growing stage the aircraft conducts circumnavigation at 5,000 ft (1.5 km) with 5-6 nmi (10-12 km) legs centered on cell to provide F/AST Doppler mapping. The circumnavigation is followed by penetration of the cell at 3,000 (1 km) or 5,000 ft (1.5 km).
• Note 5.	Set the airborne Doppler radar to F/AST scan on all circumnavigation legs, and to scan perpendicular to the track on all penetration legs.

CLOUDS AND CLIMATE EXPERIMENT

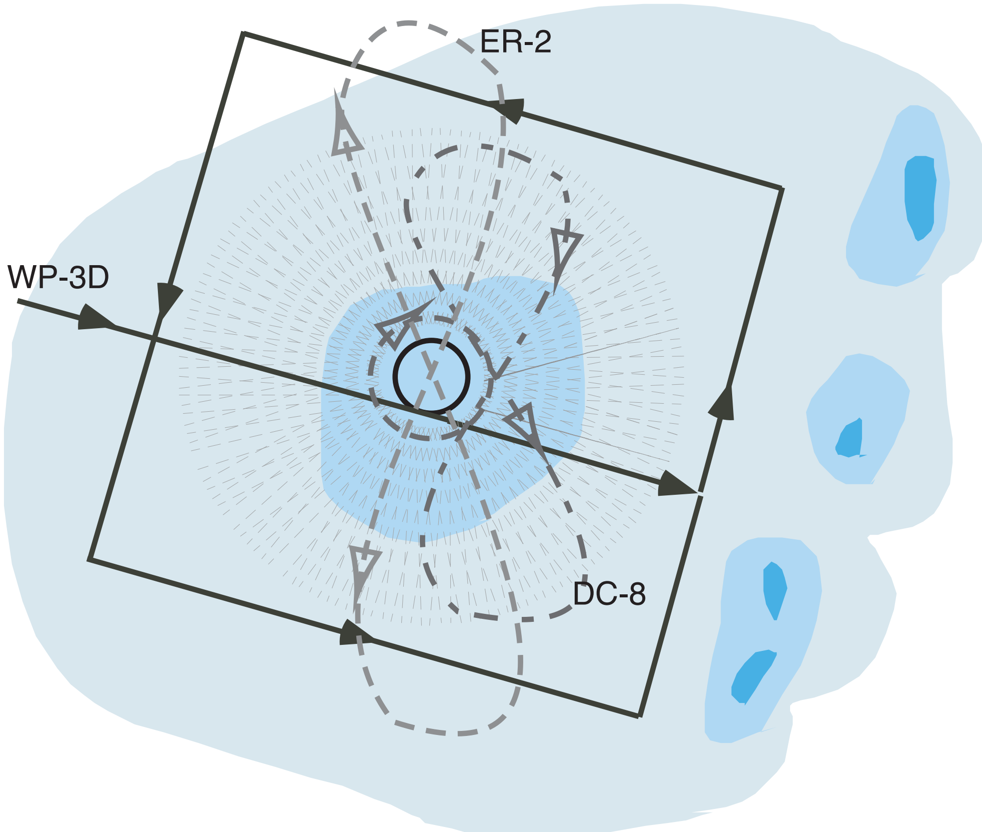

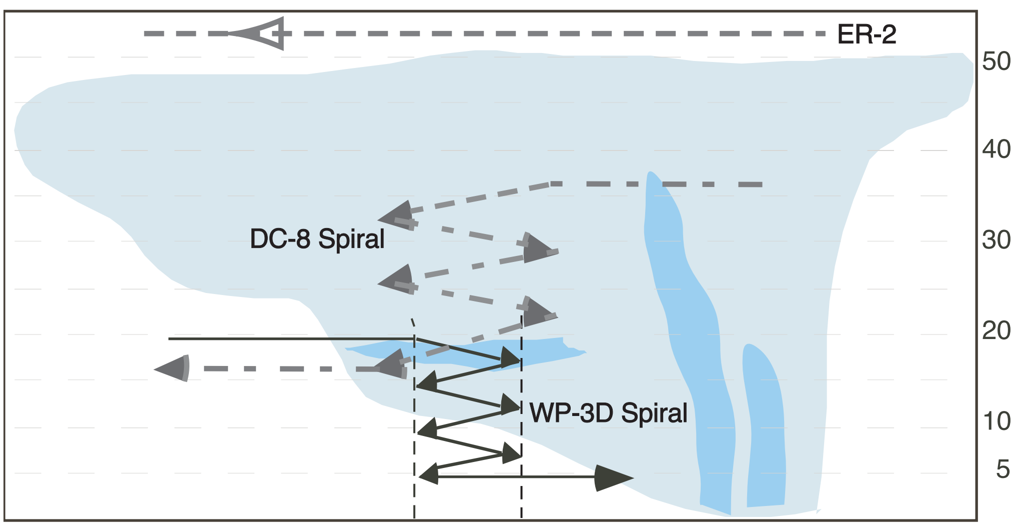

Fig. 29 (c) Mature Stage:

• Note 1.	The pattern may be flown along any compass heading.
• Note 2.	WP-3D aircraft flies a circle (~5-10 km radius) within the selected area making dual-Doppler radar scans and precipitation measurements in a slow spiral descent from 23,000 ft to cloud base.
• Note 3.	Set the airborne Doppler radar to F/AST scan on all legs.

APPENDIX A

DECISION AND NOTIFICATION PROCESS

DECISION AND NOTIFICATION PROCESS

The decision and notification process is illustrated in Fig. A-1. This process occurs in four steps:

1) A research mission is determined to be probable within 72 h [field program director]. Consultation with the director of HRD, the AOC Project Manager, and the CAMEX-4 Lead Mission Scientist (Hood) (or designee) determines: flight platform availability, crew and equipment status, and the type of mission(s) likely to be requested.

2) The Field Program Advisory Panel [Director, HRD, Marks, M. Black, P. Black, R. Black, Cione, Dodge, Gamache, Kaplan, Powell, Landsea, White, and McFadden (or AOC designee) meets to discuss possible missions and operational modes. Probable mission determination and approval to proceed is given by the HRD director (or designee) and the CAMEX-4 Lead Mission Scientist (or designee).

3) Primary personnel are notified by the field program director [Marks] and CAMEX-4 Lead Mission Scientist (or designee).

4) Secondary personnel are notified by their primary affiliate (Table A-2).

General information, including updates of program status, are provided continuously by tape. Call (305) 221-3679 to listen to the recorded message. During normal business hours, callers should use (305) 361-4400 for other official inquiries and contacts. During operational periods, an MGOC team member is available by phone at (305) 229-4407 or (305) 221-4381. MGOC team leader, and the HRD field program director, and the CAMEX-4 Principal Scientist will have telepager units. (Appropriate telepager phone numbers will be provided to program participants before the start of the field program.)

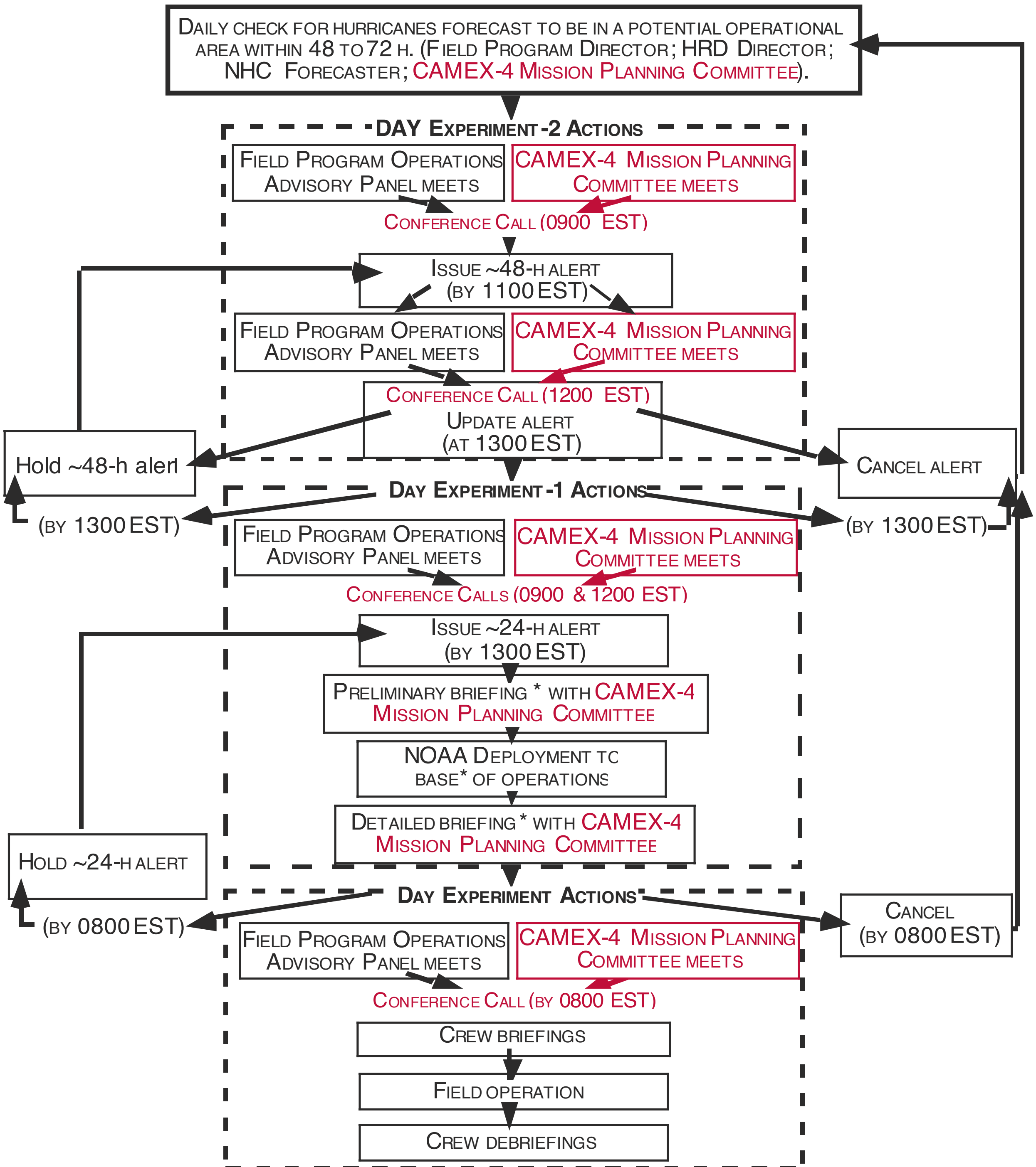

* Time of briefings and deployments are dictated by the crew, scientist, aircraft and storm locations and conditions.

Fig. A-1. Decision and notification process.

Table A-1. Primary Contacts

Name	Agency/title	Home phone	Work phone
H. Willoughby	HRD/Director	305-665-4080	305-361-4502
F. Marks	HRD/Field Program Director	305-271-7443	305-361-4321
P. Black	HRD/Assistant Field Program Director	305-859-7784	305-361-4320
H. Friedman	HRD/MGOC Senior Team Leader	954-962-8021	305-361-4319
J. McFadden	AOC/Project Manager for Hurricane Research	305-666-3622 813-839-7550	813-828-3310 x3076
J Parrish	AOC/Project Manager for Hurricane Surveillance	813-933-2302	813-828-3310 X3077
J. Pavone	CARCAH/Liaison	305-248-3422 434-3420[1]	305-229-4474
R. Hood	CAMEX-4 Lead Mission Scientist	TBA	256-961-7959
G. Heymsfield	CAMEX-4 Mission Scientist	TBA	301-614-6369
E. Zipser	CAMEX-4 Mission Scientist	TBA	801-585-9482
R. Kakar	CAMEX-4 Program Manager	TBA	202-358-0240
S. Hipskind	CAMEX-4 Project Manager	TBA	650-604-5076
J. Abraham,	AES/Canada Convair 580	TBA	
P. Bowyer		TBA	(902) 426-9181
Synoptic Analysis Branch	NESDIS/Liaison		301-763-8444 301-763-8445
K. Katsaros	AOML/Director	305-361-5543	305-361-4302 305-361-4300
J. Goldman	OAR/PA		301-713-2483
F. Lepore	TPC/NHC/PA	305-235-6670	305-229-4404
MacDill Global[2]			813-828-3109 813-828-3356 813-828-3881

1 DSN: Defense Switched Network (replaced Autovon).
2 MacDill Global phone patch; used to contact the NOAA aircraft during missions.

Table A-2. Secondary Contacts

Name/group	Home phone	Work phone	Contacted by
HRD participants			F. Marks/MGOC
AOC participants			J. McFadden
Deputy Dir./AOC			J. McFadden
FAA			AOC
LT.COL Gale Carter	601-928-7681	601-377-3207	CARCAH
53rd Wea. Reconnaissance. Squadron		597-3207[1]	
M. Mayfield/TPC/NHC		305-229-4402	F. Marks/MGOC
C. Burr/TSAF/TPC/NHC	305-667-9932	305-229-4430	F. Marks/MGOC
Sr. Duty Meteorologist/NCEP	--	301-763-8298	F. Marks/MGOC
		301-763-8364	
		301-763-8076	
E. Walsh	303-447-1694	303-497-6357	F. Marks
W.-C. Lee/NCAR	303-939-8281	303-497-8814	F. Marks
P. Harr	831-647-9883	831-656-3787	F. Marks
S. Lord/NCEP	301-249-7713	301-763-8005	S. Aberson
C. Velden/U. Wisconsin	608-274-5500	608-262-9168	S. Aberson
Craig Bishop/PSU		814-865-9500	S. Aberson
Julian Heming/UKMO		44-0-1344-854494	S. Aberson
Rolf Langland/NRL		831-656-4786	S. Aberson
Zoltan Toth/NCEP		301-763-8545	S. Aberson
J. Carswell/ U. Massachusetts	413-549-7467	413-545-4867	P. Black
P. Chang/NESDIS	703-670-8285	301-763-8231x167	P. Black
T. Gobel/OFCM	301-589-5771	301-427-2002	P. Black
	717-637-1284		
H. Selsor/NRL	504-641-5674	601-688-4760	P. Black
P. Vachon/AES	613-825-8425	613-995-1575	P. Black
E. Meindl/NDBC	228-466-9529	228-688-1717	M. Powell
M. Burdett/NDBC	601-798-1151	228-688-2868	M. Powell
T. Reinhold/Clemson University	--	864-656-5941	M. Powell
J. Schroeder/TTU	--	806-742-3476x288	M. Powell
J. Straka/U. Oklahoma	--	405-325-6561	M. Powell
R. Jensen/USACE	--	601-634-2101	M. Powell
S. Gill/NOS	--	301-713-2840	M. Powell
K. Knupp/U. Alabama/Huntsville	--	256-961-7762	P. Dodge
B. McCaul/U. Alabama/Huntsville	--	256-961-7837	P. Dodge
J. Wurman/U. Oklahoma	--	405-325-7689	P. Dodge

1 DSN: Defense Switched Network (replaced Autovon).

APPENDIX B

Aircraft Scientific Instrumentation

Aircraft Scientific Instrumentation

Table B1. NOAA/AOC WP-3D (N42RF, N43RF) instrumentation

	N42RF	N43RF
NAVIGATIONAL		
Position, position update	INE and GPS	INE and GPS
Radar and pressure altitude	Radar and pressure altimeters	Radar and pressure altimeters
METEOROLOGICAL		
Free air temperature (derived)	Rosemount total temperature	Rosemount total temperature
Static and dynamic pressure	Rosemount	Rosemount
Dew point temperature	General Eastern	General Eastern
Horizontal wind (computed)	INE/TAS (computed); GPS	INE/TAS (computed); GPS
Vertical wind (computed)	High-resolution angle of attack, pitch angle, vertical acceleration	High-resolution angle of attack, pitch angle, vertical acceleration
Temperature and momentum flux	Radome-mounted gust probe and fast-response total temperature	Radome-mounted gust probe and fast-response total temperature
RADIATION		
Sea surface temperature	AOC modified PRT-5	AOC modified PRT-5
CO_2 air temperature	AOC modified PRT-5	AOC modified PRT-5
CLOUD PHYSICS		
Small cloud droplet spectrum	FSSP forward scattering probe	FSSP forward scattering probe
Cloud droplet spectrum	PMS Knollenberg 2-D Gray probe	PMS Knollenberg 2-D Gray probe
Hydrometeor size spectrum	NASA High Volume Particle Spectrometer (HVPS)	PMS Knollenberg 2-D mono probe
Cloud liquid water	Johnson-Williams hot wire	Johnson-Williams hot wire
Total liquid water	PMS King probe	
Cloud Condensation Nuclei	DRI CCN counter	
Electric Field (3 axis)e	5 field mills	
RADAR		
Radar reflectivity	C-band PPI lower-fuselage (LF), 360° scan (horizontal)[1]	C-band PPI lower-fuselage (LF), 360° scan (horizontal)[1]
Radar reflectivity and radial velocity	Doppler X-band RHI tail (TA), 360° scan (vertical)[1] (AOC antenna)	Doppler X-band RHI tail (TA), 360° scan (vertical)[1] (AOC antenna)
MISCELLANEOUS		
Cloud structure; surface wind	Video photography (3 axis)	Video photography (3 axis)
Vertical atmospheric sounding	GPS Dropwindsonde system	GPS Dropwindsonde system
Oceanic temperature, current and salinity profile	AXBT receiver	AXBT, AXCP, AXCTD receivers and laptop
Stable water isotope ratio		University of Houston water collection device
Ozone concentration	AOML O_3 instrument	
Data transmission	Aircraft-satellite-data-link (ASDL)[2], IMARSAT Mini-M	Aircraft-satellite-data-link (ASDL) [2], IMARSAT Mini-M
Clear-air winds	Chaff sondes	Chaff sondes
Surface wind speed & direction	Ku/C-SCAT, SFMR[3]	SFMR[3]
Surface wave spectra & altimetry		SRA[4]

[1] LF radar data recorded every other scan. TA radar recorded every scan.
[2] An HRD airborne workstation will be installed on each NOAA/AOC WP-3D.
[3] U. MASS Ku/C-band scatterometer and Stepped frequency microwave radiometer
[4] NASA Scanning radar altimeter

Table B-2. NASA DC-8 (NA817) instrumentation

Instrument Acronym	Instrument Type	Temporal Resolution	Spatial Resolution	Data Volume/ Mission
MTP	Radiometer (fixed) Microwave temperature profiler	1 Hz	~1-2 km @ surface	
PR-2	Dual-frequency 13.8 and 35 GHz Doppler radar (Thru-nadir scanning) (multi-polarization)	1.8 s/scan; 10 MHz sample rate; 5 kHz PRF	800 m at surface; 80 m range resolution (after averaging)	10 GB (raw), 200-600 MB (processed)
Microphysics	• 2DC, 2DP, FSSP 300 • HVPS • CPI and CVI	1 Hz	10-200 m	2 MB at 1 Hz
AVAPS	NCAR/GPS-sonde	Simultaneously track 4 sondes	10 m (vertical)	<50 KB per sonde release
JPL laser hygrometer	Microhygrometer	TBD (<0.1 s)	Single point measurement	10 MB
LASE	Differential Absorption Lidar	3 s/profile; 2 min (averaged)	*Water profiles*: 0.2 km (vertical), 5 km (horizontal), 100 m to tropopause *Relative Absorption Lidar aerosol scattering profiles*: 30 m (vertical), 200 m (horizontal), ground to 20 km	200 MB
ACLAIM	Coherent lidar Maps clear air turbulence	Continuous		
C-STAR	Radiometer 37 GHz, multi-polarization conical scanning, fore and aft	Continuous		
LIP	Electric Field Mills	Conductivity:10 Hz; Waveforms: 100 kHz	~20m	30-50 MB
ICATS	Navigation and in situ pressure, temperature and wind data	Continuous		
MMS	High resolution winds, temperature, pressure	Continuous		

Table B-3. NASA ER-2 (NA809) instrumentation

Instrument Acronym	Instrument Type	Temporal Resolution	Spatial Resolution	Volume/ Mission
AMPR	Scanning radiometer (10, 19, 37, 85 GHz)	One 50-element scan every 3 s	0.6 km at 85 GHz; 1.5 km at 37 GHz; 2.8 km at 10, 19 GHz, (surface footprint)	20-30 MB
EDOP	Doppler Radar (9.3 GHz)	2 Hz (~100m along-track)	Vertical: 37.5 m; Horizontal: ~1.1 km at surface and ~0.55 km at 10 km	~3.5 GB
EHAD	Dropsondes	Variable	Vertical: 5-10 s	< 1 MB
LIP	Electric Field Mills	Conductivity:10 Hz; Waveforms: 100 kHz	~20m	30-50 MB
MTP	Forward-looking microwave temperature profiler	Continuous		
MAS	Scanning spectrometer	Continuous	50 m, at nadir	
HAMSR	microwave temperature and moisture profiler- cross track, AMSU frequencies	Continuous		
NOAA Ozone and water vapor	Ozone and water vapor concentration	Continuous		

Table B-4: Convair 580 Instrumentation

Particle measuring system (PMS) laser spectrometers
Systems for sampling air, cloud water and precipitation
Upward- and downward-looking radiometers
Electric field mills
Dual dropsonde system for wind, temperature and humidity profiling
Nd-YAG upward/downward-looking lidar
Multi-camera video recording system
Multiple navigation sensors (GPS, INS, Doppler, Loran C)

APPENDIX C

Calibration; Scientific Crew Lists; Data Buoys; DOD/NWS RAWIN/RAOB and NWS Coastal Land-based Radar Locations/Contacts

Calibration; Scientific Crew Lists; Data Buoys; DOD/NWS RAWIN/RAOB and NWS Coastal Land-based Radar Locations/Contacts

C.1 En-Route Calibration of Aircraft Systems

Instrument calibrations are checked by flying aircraft intercomparison patterns whenever possible during the hurricane field program or when the need for calibration checks is suggested by a review of the data. In addition, an over flight of a surface pressure reference is advisable en route or while on station when practicable. Finally, all flights enroute to and from the storm are required to execute a true airspeed (TAS) calibration pattern. This pattern is illustrated in Fig. C-1.

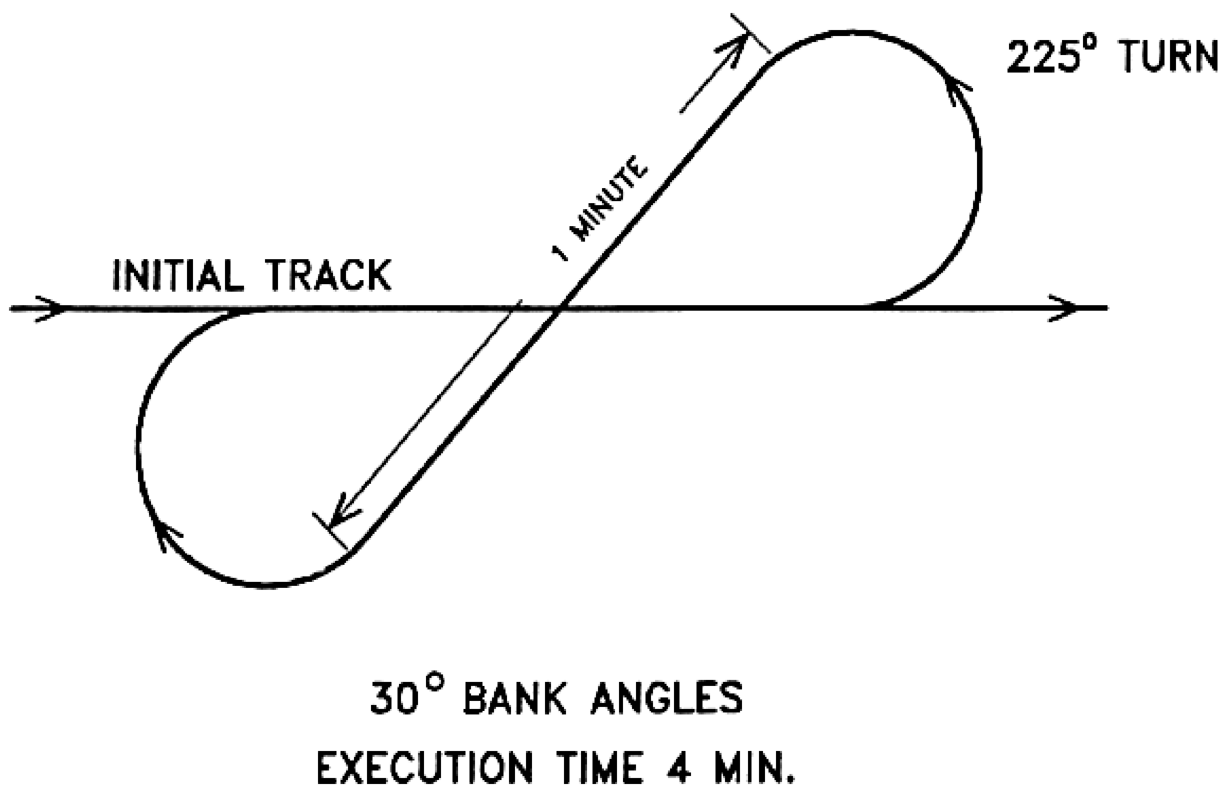

Fig. C-1 En-Route TAS calibration pattern.

C.2 Aircraft Scientific Crew Lists

Table C-2.1 Coordinated Observations of Vortex Evolution and Structure (COVES) Experiment (single-option, dual-aircraft mission)

Position	N42RF	N43RF
Lead Project Scientist	J. Gamache	P. Black
Cloud Physics Scientist	R. Black	(radar scientist)
Radar Scientist	F. Marks	M. Black
Dropsonde Scientist	S. Feuer or S. Aberson	J. Cione
Workstation Scientist	P. Dodge	P. Leighton
Ku/C-SCAT/SFMR/SRA Scientist	J. Carswell	E. Walsh

Table C-2.2 Extended Cyclone Dynamics Experiment (single-option, single-aircraft mission)

Position	N42RF or N43RF
Lead Project Scientist	H. Willoughby
Cloud Physics Scientist	R. Black
Radar Scientist	M. Black
Dropsonde Scientist	S. Goldenberg
Workstation Scientist	P. Leighton
Ku/C-SCAT/SFMR/SRA Scientist	J. Carswell or E. Walsh

Table C-2.3 Tropical Cyclone Wind fields Near Landfall Experiment (dual-option, single-aircraft mission)

Position	N42RF or N43RF
Lead Project Scientist	P. Dodge
Cloud Physics Scientist	(radar scientist)
Radar Scientist	J. Gamache
Dropsonde Scientist	C. Landsea
Workstation Scientist	P. Leighton
Ku/C-SCAT/SFMR/SRA Scientist	J. Carswell or E. Walsh

Table C-2.4 Hurricane Synoptic-Flow Experiment (single-option, single-aircraft mission)

Position	N42RF or N43RF
Lead Project Scientist	S. Aberson
Cloud Physics Scientist	(radar scientist)
Radar Scientist	F. Marks
Dropsonde Scientists	J. Kaplan
Workstation Scientist	P. Dodge
Ku/C-SCAT/SFMR/SRA Scientist	J. Carswell or E. Walsh

Table C-2.5 Extratropical Transition Experiment (multi-option, dual-aircraft mission)

Position	N42RF	N43RF
Lead Project Scientist	M. Black	P. Black
Cloud Physics Scientist	R. Black	(radar scientist)
Radar Scientist	J. Gamache	N. Dorst
Dropsonde Scientist	C. Landsea	J. Cione
Workstation Scientist	P. Leighton	P. Dodge
Ku/C-SCAT/SFMR and SRA Scientists	J. Carswell	E. Walsh

Table C-2.6 Tropical Cyclogenesis Experiment (single-option, dual-aircraft mission)

Position	N42RF	N43RF
Lead Project Scientist	F. Marks	P. Black
Cloud Physics Scientist	R. Black	(radar scientist)
Radar Scientist	N. Dorst or P. Reasor	J. Gamache
Dropsonde Scientist	M. Black	J. Cione
Workstation Scientist	P. Leighton	P. Dodge
Ku/C-SCAT/SFMR and SRA Scientists	J. Carswell	E. Walsh

Table C-2.7 Clouds and Climate Study: (single-option, single-aircraft mission)

Position	N42RF
Lead Project Scientist	R. Black
Cloud Physics Scientist	N. Dorst
Radar Scientist	P. Dodge
Dropsonde Scientist	(radar scientist)
Workstation Scientist	P. Leighton

C.3 Buoy/Platform Over flight Locations[1]

Table C-3.1 Moored Buoys

Station Identifier	Type of Station[2]		Location Lat. (N)	Lon (W)	Area	Special Obs/ Comments[4]
44007*	3D	/D	43.53	70.14	PORTLAND	A
44005*	6N	/D	42.90	68.89	GULF OF MAINE	A
44013*	3D	/D	42.35	70.69	BOSTON	--
44011*	6N	/D	41.08	66.58	GEORGES BANK	A
44008*	3D	/V	40.50	69.43	NANTUCKET	A
44025*	3D	/D	40.25	73.17	LONG ISLAND	DW
44004*[3]	6N	/D	38.46	70.69	HOTEL	--
44009*	3D	/V	38.46	74.70	DELAWARE BAY	--
44014[3]	3D	/D	36.58	74.83	VIRGINIA BEACH	DW
41001[3]	6N	/D	34.68	72.64	E. HATTERAS	A
41004*	3N	/D	32.51	79.10	EDISTO	DW
41002*[3]	6D	/D	32.28	75.20	S. HATTERAS	--
41008*	3D	/V	31.40	80.87	GRAYS REEF	--
42007*	3D	/V	30.10	88.77	OTP	A
42035*	3D	/V	29.25	94.41	GALVESTON	--
42040	3D	/D	29.18	88.29	MOBILE SOUTH	A
41010	6N	/D	28.89	78.55	CANAVERAL EAST	--
42039	3D	/V	28.78	86.04	PENSACOLA S.	A
42036*[3]	3D	/D	28.51	84.51	W. TAMPA	DW
41009	6N	/V	28.50	80.18	CANAVERAL	--
42019*[3]	3D	/D	27.92	95.35	FREEPORT	--
42041[3]	3D	/D	27.23	90.43	N. MID GULF	A
42020*	3D	/D	26.92	96.70	CORPUS CHRISTI	--
42054	LNB	/M	26.00	87.76	E. GULF	--
42002*	10D	/V	25.89	93.57	W. GULF	A
42003*	10D	/V	25.94	85.91	E. GULF	A
42001*	10D	/V	25.93	89.65	MID GULF	A

[1] Tables C-3.1 and C-3.4 were updated with information from the **Data Platform Status Report (May 3, 2001)**, NOAA/National Data Buoy Center (NDBC), Stennis Space Center, MS 39529-6000, for the period **April 29 – May 3, 2001**. (Also, the NDBC report lists the location of drifting buoys o/a **April 29 – May 3, 2001**). See subsequent editions of this weekly NDBC report for later information. Tables C-3.2, C-3.3, and portions of C-3.4 were updated with information from **National Weather Service Offices and Stations** (May 2001), NOAA/NWS, W/MB31, Silver Spring, MD.

[2]

Hull Type		Anemometer Height	
10D	-	10-m discus buoy	10.0 m
6N	-	6-m NOMAD buoy	5.0 m
3D	-	3-m discus buoy	5.0 m
LNB	-	12-m discus buoy	8.5 m

Payload types: /G = GSBP; /D = DACT; /V = VEEP; /M = MARS.

[3] Note remarks section of NDBC report (**May 3, 2001**); see latest edition of NDBC **Data Platform Status Report** for current status.

[4] A = 10-min data (continuous); R = rainfall; DW = directional wave spectra.

* Base funded station of the National Weather Service (NWS); however, all stations report data to NWS.

Table C-3.2 C-MAN sites[1]

Station Identifier	Station Name/ Payload Type	Location Lat. (N)	Location Lon (W)	Area	Comments[3]	Height (m)
MDRM1*[2]	Mt. Desert Rock, ME/D	43.97	68.13	ME COAST	--	22.6
MISM1*[2]	Matinicus Rock, ME/D	43.78	68.86	ME COAST	--	16.5
IOSN3*	Isle of Shoals, NH/D	42.97	70.62	NH COAST	--	19.2
BUZM3*[2]	Buzzards Bay, MA/V	41.40	71.03	MA COAST	A	24.8
ALSN6*[2]	Ambrose Light, NY/V	40.46	73.83	NY COAST	--	49.1
TPLM2*	Thomas Point, MD/V	38.90	76.44	MD COAST	--	18.0
CHLV2*[2]	Chesapeake Light, VA/D	36.90	75.71	VA COAST	A	43.3
DUCN7*[2]	Duck Pier, NC/V	36.18	75.75	NC COAST	A	20.4
DSLN7*[2]	Diamond Shoals Light, NC/D	35.15	75.30	NC COAST	A, DP	46.6
CLKN7*[4]	Cape Lookout, NC/V	34.62	76.52	NC COAST	A	9.8
FPSN7*[2]	Frying Pan Shoals, NC/D	33.49	77.59	NC COAST	A	44.2
FBIS1*[2,4]	Folly Island, SC/D	32.68	79.89	SC COAST	A	9.8
SPGF1*	Settlement Point, GBI/M	26.70	78.99	GR BAHAMA	A	9.8
SAUF1*	St. Augustine, FL/V	29.86	81.26	FL COAST	A	16.5
LKWF1*[2]	Lake Worth, FL/M	26.61	80.03	FL COAST	A	13.7
FWYF1*[4]	Fowey Rocks, FL/V	25.59	80.10	FL COAST	A	43.9
MLRF1*[2]	Molasses Reef, FL/V	25.01	80.38	FL COAST	--	15.8
SMKF1*[2]	Sombrero Key, FL/M	24.63	81.11	FL COAST	--	48.5
SANF1*[4]	Sand Key, FL/V	24.46	81.88	FL COAST	A	13.1
LONF1*	Long Key, FL/M	24.84	80.86	FL COAST	--	7.0
DRYF1*	Dry Tortugas, FL/M	24.64	82.86	FL COAST	--	5.7
VENF1*	Venice, FL/V	27.07	82.45	FL COAST	A	11.6
CDRF1*	Cedar Key, FL/V	29.14	83.03	FL COAST	A	10.0
CSBF1*[4]	Cape San Blas, FL/M	29.67	85.36	FL COAST	A	9.8
KTNF1*	Keaton Beach, FL/M	29.82	83.59	FL COAST	A	10.0
DPIA1*[2]	Dauphin Island, AL/V	30.25	88.07	AL COAST	--	17.4
BURL1*	Southwest Pass, LA/M	28.90	89.43	LA COAST	A	30.5
GDIL1*[4]	Grand Isle, LA/M	29.27	89.96	LA COAST	A	15.8
SRST2*[4]	Sabine, TX/M	29.67	94.05	TX COAST	A	12.5
PTAT2*[2]	Port Aransas, TX/M	27.83	97.05	TX COAST	A	14.9

[1] Coastal-Marine Automated Network (C-MAN) stations are located on coastal headlands, piers, or offshore platforms. Payload types, shown next to the station's name (after the "/") are: D = DACT; V = VEEP; M=MARS; and I = Industry-supplied. C-MAN anemometer heights are listed in the **C-MAN User's Guide**.

[2] Note remarks section of NDBC report (**May 3, 2001**); see latest edition of NDBC **Data Platform Status Report** for current status.

[3] A = 10-min data (continuous); DP = dew point; R = rainfall; DW = directional wave spectra.

[4] Hurricane Landfall (HL) Systems whose exposure characteristics are stored on the HRD Surface Wind Analysis database and on NCDC's website.

* Primarily for National Weather Service (NWS) support; however, all stations report data to NWS.

Table C-3.3 NOS next generation meteorological-tide stations*

Station Name	Location Lat. (N)	Lon (W)
Eastport Bay, ME	44.90	66.98
Bergen Point West, NY	40.63	74.14
Sandy Hook, NJ	40.47	74.01
Solomons Island, MD	38.32	76.45
Tolchester Beach, MD	39.21	76.25
Kiptopeke, VA	37.17	75.98
Lewisetta, Potomac River, VA	37.99	76.45
Sewells Point, VA	36.95	76.32
Chesapeake Bay Bridge, VA	36.97	76.10
Duck, FRF Pier, NC	36.18	75.74
Cape Hatteras Fishing Pier, NC	35.22	75.63
Mayport, FL	30.39	81.42
St. Augustine Beach, FL	29.85	81.25
Trident Pier, FL	28.42	80.59
Virginia Key, FL	25.72	80.15
Naples, FL	26.12	81.80
Fort Myers, FL	26.65	81.87
St. Petersburg, FL	27.75	82.62
McKay Bay, FL	27.90	82.42
Clearwater Beach, FL	27.97	82.43
Apalachicola Bay, FL	29.72	85.00
Panama City Beach, FL	30.20	85.87
Waveland, MS	30.28	89.37
Grand Isle, LA	29.26	89.95
Morgans Point, TX	29.47	94.92
Eagle Point, TX	29.35	94.77
Port Bolivar, TX	29.30	94.79
Galveston Pier, TX	29.28	94.78
Galveston (offshore), TX	29.12	94.50
Freeport, TX	28.94	95.30
Corpus Christi, TX	27.57	97.22
Port Isabel, TX	26.06	97.21

* Quality controlled data from these platforms can be obtained from NDBC's **Seaboard Bulletin Board Service** soon after the fact. For information contact NDBC .

Table C-3.4 Automated Surface Observing System (ASOS) sites

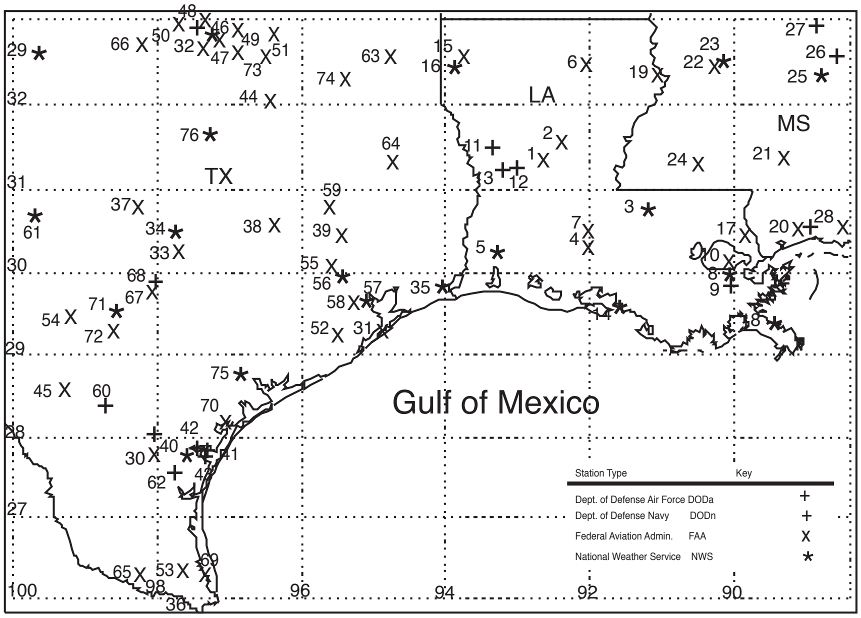

#	ID	Agency	Site Name	Lat. (N)	Lon (W)	#	ID	Agency	Site Name	Lat. (N)	Lon (W)
1	KAEX	FAA	Alexandria, LA	31.33	92.56	39	KCXO	FAA	Conroe, TX	30.36	95.41
2	KESF	FAA	Alexandria, LA	31.40	92.29	40	KCRP	NWS	Corpus Christi, TX	27.77	97.51
3	KBTR	NWS	Baton Rouge, LA	30.54	91.95	41	KNGP	DODn	Corpus Christi, TX	27.68	97.29
4	KLFT	FAA	Lafayette, LA	30.20	91.99	42	KNGW	DODn	Corpus Christi, TX	27.72	97.44
5	KLCH	NWS	Lake Charles, LA	30.12	93.23	43	KNVT	DODn	Corpus Christi, TX	27.63	97.31
6	KMLU	FAA	Monroe, LA	32.51	92.03	44	KCRS	FAA	Corsicana, TX	32.03	96.40
7	KARA	FAA	New Iberia, LA	30.29	91.99	45	KCOT	FAA	Cotulla, TX	28.45	99.22
8	KMSY	NWS	New Orleans, LA	29.99	90.02	46	KDAL	FAA	Dallas, TX	32.85	96.86
9	KNBG	DODn	New Orleans, LA	29.84	90.02	47	KRBD	FAA	Dallas, TX	32.68	96.86
10	KNEW	FAA	New Orleans, LA	30.05	90.03	48	KDFW	NWS	Dallas/Fort Worth, TX	32.90	97.02
11	FTPK1	DODa	Fort Polk, LA	31.41	93.30	49	KFTW	FAA	Fort Worth, TX	32.83	97.36
12	FTPK2	DODa	Fort Polk, LA	31.11	92.97	50	KNFW	DOD	Fort Worth, TX	32.77	97.43
13	FTPK3	DODa	Fort Polk, LA	31.12	93.16	51	KAFW	FAA	Fort Worth, TX	32.97	97.32
14	KP92	NWS	Salt Point, LA	29.56	91.53	52	KGLS	FAA	Galveston, TX	29.27	94.86
15	KDTN	FAA	Shreveport, LA	32.54	93.74	53	KHRL	FAA	Harlingen, TX	26.23	97.66
16	KSHV	NWS	Shreveport, LA	32.45	93.82	54	KHDO	FAA	Hondo, TX	29.36	99.17
17	KASD	FAA	Slidell, LA	30.34	89.82	55	KDWH	FAA	Houston, TX	30.07	95.56
18	K7R1	NWS	Venice, LA	29.26	89.36	56	KIAH	NWS	Houston, TX	29.99	95.36
19	KTVR	FAA	Vicks./Tallulah, LA	32.35	91.03	57	KHOU	NWS	Houston, TX	29.64	95.28
20	KGPT	FAA	Gulfport, MS	30.41	89.08	58	KT02	FAA	Houston, TX	29.52	95.24
21	KHBG	FAA	Hattiesburg, MS	31.27	89.26	59	KUTS	FAA	Huntsville, TX	30.74	95.59
22	KHKS	FAA	Jackson, MS	32.34	90.22	60	KNMT	DODn	Ingleside, TX	28.24	98.72
23	KJAN	NWS	Jackson, MS	32.32	90.08	61	KJCT	NWS	Junction, TX	30.51	99.77
24	KMCB	FAA	McComb, MS	31.18	90.47	62	KNQI	DODn	Kingsville, TX	27.50	97.81
25	KMEI	NWS	Meridian, MS	32.34	88.75	63	KGGG	FAA	Longview, TX	32.39	94.71
26	KNMM	DODn	Meridian, MS	32.55	88.54	64	KLFK	FAA	Lufkin, TX	31.23	94.75
27	KNJW	DODn	Meridian Range, MS	32.80	88.83	65	KMFE	FAA	McAllen, TX	26.18	98.24
28	KPQL	FAA	Pascagoula, MS	30.46	88.53	66	KMWL	FAA	Mineral Wells, TX	32.78	98.06
29	KABI	NWS	Abilene, TX	32.41	99.68	67	K3R5	FAA	New Braunfels, TX	29.71	98.05
30	KALI	FAA	Alice, TX	27.74	98.02	68	KNOG	DODn	Orange Grove, TX	27.89	98.04
31	KLBX	FAA	Angelton/L. Jack., TX	29.12	95.46	69	KT31	FAA	Port Isabel, TX	26.16	97.34
32	KF54	FAA	Arlington, TX	32.66	97.10	70	KRKP	FAA	Rockport, TX	28.08	97.04
33	KBSM	FAA	Austin, TX	30.18	97.68	71	KSAT	NWS	San Antonio, TX	29.53	98.46
34	KAUS	NWS	Austin, TX	30.29	97.70	72	KSSF	FAA	San Antonio, TX	29.34	98.47
35	KBPT	NWS	Beau./Port Art., TX	29.95	94.02	73	KTRL	FAA	Terrel, TX	32.71	96.27
36	KBRO	NWS	Brownsville, TX	25.91	97.42	74	KTYR	FAA	Tyler, TX	32.36	95.40
37	KBMQ	FAA	Burnet, TX	30.74	98.23	75	KVCT	NWS	Victoria, TX	28.86	96.93
38	KCLL	FAA	College Station, TX	30.58	96.36	76	KACT	NWS	Waco, TX	31.62	97.23

Table C-3.4 Automated Surface Observing System (ASOS) sites (continued)

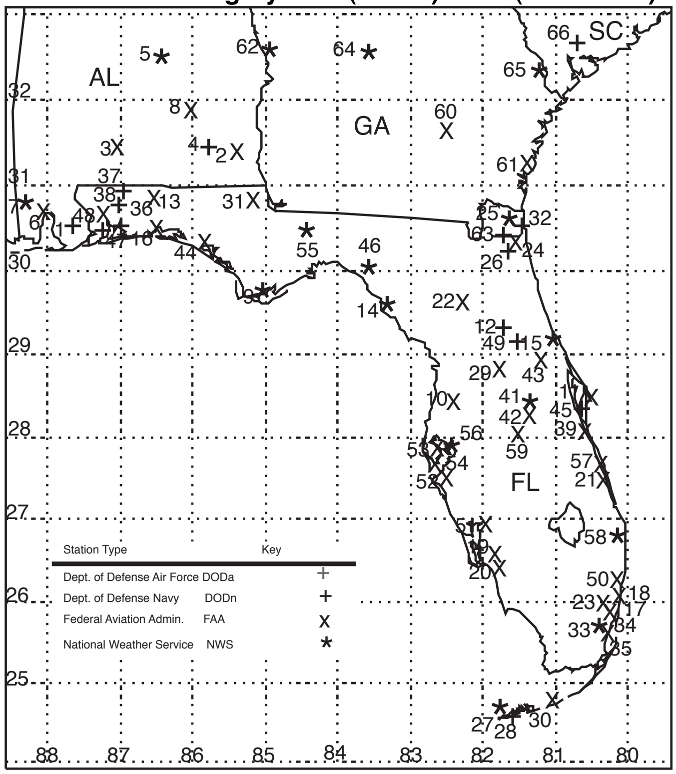

#	ID	Agency	Site Name	Lat. (N)	Lon (W)	#	ID	Agency	Site Name	Lat. (N)	Lon (W)
1	KNBJ	DODn	Barin, AL	30.39	87.63	34	KOPF	FAA	Miami, FL	25.91	80.23
2	KDHN	FAA	Dothan, AL	31.31	85.44	35	KTMB	FAA	Miami, FL	25.64	80.43
3	KGZH	FAA	Evergreen, AL	31.42	87.05	36	KNDZ	DODn	Milton, FL	30.70	87.02
4	KLOR	DODn	Fort Rucker, AL	31.36	85.75	37	KNFJ	DODn	Milton, FL	30.51	86.95
5	KMGM	NWS	Montgomery, AL	32.30	86.41	38	KNSE	DODn	Milton, FL	30.73	87.02
6	KBFM	FAA	Mobile, AL	30.61	88.06	39	KMLB	FAA	Melbourne, FL	28.10	80.64
7	KMOB	NWS	Mobile, AL	30.69	88.25	41	KMCO	NWS	Orlando, FL	28.42	81.33
8	KTOI	FAA	Troy, AL	31.86	86.01	42	KORL	FAA	Orlando, FL	28.55	81.34
9	KAQQ	NWS	Apalachicola, FL	29.73	85.02	43	KSFB	FAA	Orlando, FL	28.78	81.25
10	KBKV	FAA	Brooksville, FL	28.47	82.45	44	KPFN	FAA	Panama City, FL	30.21	85.89
11	CCAS1	FAA	Cape Canaveral, FL	28.48	80.58	45	PAFB1	DODa	Patrick AFB, FL	28.23	80.60
12	KNZC	DODn	Cecil, FL	30.21	81.87	46	K40J	NWS	Perry Foley, FL	30.07	83.57
13	KCEW	FAA	Crestview, FL	30.77	86.52	47	KNPA	DODn	Pensacola, FL	30.36	87.32
14	KCTY	NWS	Cross City, FL	29.55	83.11	48	KPNS	FAA	Pensacola, FL	30.48	87.19
15	KDAB	NWS	Daytona Beach, FL	29.17	81.06	49	KNAE	DODn	Pinecastle, FL	29.14	81.63
16	KDTS	FAA	Destin, FL	30.39	86.47	50	KPMP	FAA	Pompano Beach, FL	26.25	80.11
17	KFLL	FAA	Fort Lauderdale, FL	26.07	80.15	51	KPGD	FAA	Punta Gorda, FL	26.92	81.99
18	KFXE	FAA	Fort Lauderdale, FL	26.20	80.13	52	KSRQ	FAA	Sar./Braden., FL	27.41	82.56
19	KFMY	FAA	Fort Myers, FL	26.58	81.86	53	KPIE	FAA	St. Peter./Clear., F	27.91	82.69
20	KRSW	FAA	Fort Myers, FL	26.53	81.77	54	KSPG	FAA	St Petersburg FL	27.77	82.63
21	KFPR	FAA	Fort Pierce, FL	27.50	80.38	55	KTLH	NWS	Tallahassee, FL	30.39	84.35
22	KGNV	FAA	Gainesville, FL	29.69	82.28	56	KTPA	NWS	Tampa, FL	27.96	82.54
23	KHWO	FAA	Hollywood, FL	26.00	80.24	57	KVRB	FAA	Vero Beach, FL	27.66	80.41
24	KCRG	FAA	Jacksonville, FL	30.34	81.51	58	KPBI	NWS	West Palm Beach, FL	26.68	80.10
25	KJAX	NWS	Jacksonville, FL	30.49	81.69	59	KGIF	FAA	Winter Haven, FL	28.06	81.76
26	KNIP	DODn	Jacksonville, FL	30.23	81.67	60	KAMG	FAA	Alma, GA	31.54	82.51
27	KEYW	NWS	Key West, FL	24.55	81.75	61	KSSI	FAA	Brunswick, GA	31.15	81.39
28	KNQX	DODn	Key West, FL	24.57	81.68	62	KCSG	NWS	Columbus, GA	32.52	84.94
29	KLEE	FAA	Leesburg, FL	28.82	81.81	63	KNBQ	DODn	Kings Bay, GA	30.79	81.56
30	KMTH	FAA	Marathon, FL	24.73	81.05	64	KMCN	NWS	Macon, GA	32.69	83.65
31	KMAI	FAA	Marianna, FL	30.84	85.18	65	KSAV	NWS	Savannah, GA	32.12	81.20
32	KNRB	DODn	Mayport, FL	30.40	81.42	66	KNBC	DODn	Beaufort, SC	32.49	80.70
33	KMIA	NWS	Miami, FL	25.79	80.32						

Table C-3.4 Automated Surface Observing System (ASOS) sites (continued)

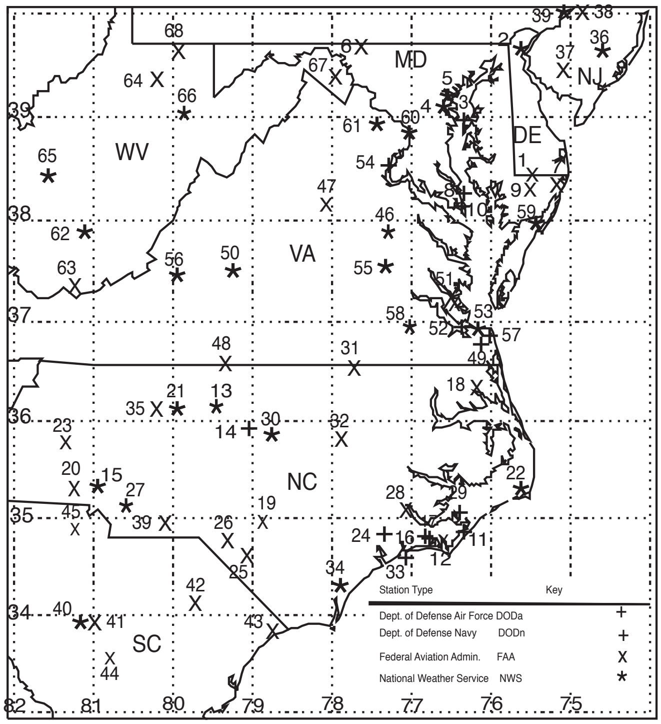

#	ID	Agency	Site Name	Lat. (N)	Lon (W)	#	ID	Agency	Site Name	Lat. (N)	Lon (W)
1	KGED	FAA	Georgetown, DE	38.69	75.36	35	KINT	FAA	Winston Salem, NC	36.13	80.22
3	KNAK	DODn	Annapolis, MD	38.99	76.43	36	KACY	NWS	Atlantic City, NJ	39.46	74.59
4	KBWI	NWS	Baltimore, MD	39.17	76.68	37	KMIV	FAA	Millville, NJ	39.37	75.08
5	KDMH	NWS	Baltimore, MD	39.28	76.61	38	KVAY	FAA	Mount Holly, NJ	39.94	74.84
6	KHGR	FAA	Hagerstown, MD	39.71	77.73	39	KPNE	NWS	Philadelphia, PA	40.08	75.01
7	KN80	FAA	Ocean City, MD	38.31	75.12	40	KCAE	NWS	Columbia, SC	33.94	81.11
8	KNHK	DODn	Patuxent River, MD	38.28	76.41	41	KCUB	FAA	Columbia, SC	33.97	80.99
9	KSBY	FAA	Salisbury, MD	38.34	75.50	42	KFLO	FAA	Florence, SC	34.18	79.73
10	KNUI	DODn	St Inigoes, MD	38.15	76.42	43	KCRE	FAA	Myrtle Beach, SC	33.82	78.72
11	KNLT	DODn	Atlantic City, NC	34.89	76.34	44	KOGB	FAA	Orangeburg, SC	33.46	80.85
12	KMRH	FAA	Beaufort, NC	34.73	76.66	45	K29J	FAA	Rock Hill, SC	34.98	81.06
13	KBUY	NWS	Burlington, NC	36.05	79.47	46	KOFP	NWS	Ashland, VA	37.71	77.43
14	KIGX	DODn	Chapel Hill, NC	35.93	79.06	47	KCHO	FAA	Charlottesville, VA	38.14	78.46
15	KCLT	NWS	Charlotte, NC	35.21	80.95	48	KDAN	FAA	Danville, VA	36.57	79.35
16	KNKT	DODn	Cherry Point, NC	34.90	76.88	49	KNFE	DODn	Fentress, VA	36.70	76.13
17	KNIS	DODn	Cherry Point, NC	34.89	76.86	50	KLYH	NWS	Lynchburg, VA	37.32	79.21
18	KECG	FAA	Elizabeth City, NC	36.26	76.18	51	KPHF	FAA	Newport News, VA	37.13	76.49
19	KFAY	FAA	Fayetteville, NC	34.99	78.88	52	KNGU	DODn	Norfolk, VA	36.93	76.30
20	KAKH	NWS	Gastonia, NC	35.20	81.16	53	KORF	NWS	Norfolk, VA	36.90	76.19
21	KGSO	NWS	Greensboro, NC	36.10	79.94	54	KNYG	DODn	Quantico, VA	38.51	77.29
22	KILG	NWS	Wilmington, DE	39.67	75.60	55	KRIC	NWS	Richmond, VA	37.51	77.32
22	KHSE	NWS	Hatteras, NC	35.23	75.62	56	KROA	NWS	Roanoke, VA	37.32	79.97
23	KHKY	FAA	Hickory, NC	35.74	81.38	57	KNTU	DODn	Virginia Beach, VA	36.82	76.03
24	KNCA	DODn	Jacksonville, NC	34.71	77.44	58	KAKQ	NWS	Wakefield, VA	36.98	77.00
25	KLBT	FAA	Lumberton, NC	34.61	79.06	59	KWAL	NWS	Wallops Island, VA	37.94	75.46
26	KMEB	FAA	Maxton, NC	34.79	79.37	60	KDCA	NWS	Washington, DC	38.84	77.03
27	KEQY	NWS	Monroe, NC	35.02	80.60	61	KIAD	NWS	Washington, DC	38.93	77.45
28	KEWN	FAA	New Bern, NC	35.07	77.05	62	KBKW	NWS	Beckley, WV	37.80	81.12
29	KNBT	DODn	Piney Island, NC	35.02	76.46	63	KBLF	FAA	Bluefield,	0.00	37.30
30	KRDU	NWS	Raleigh/Durham, NC	35.87	78.79	64	KCKB	FAA	Clarksburg, WV	39.30	80.22
31	KRZZ	FAA	Roanoke Rapids, NC	36.44	77.71	65	KCRW	NWS	Charleston, WV	38.38	81.59
32	KRWI	FAA	Rocky Mount Wil., NC	35.85	77.90	66	KEKN	NWS	Elkins, WV	38.89	79.85
33	KNJM	DODn	Swansboro, NC	34.69	77.03	67	KMRB	FAA	Martinsburg, WV	39.40	77.98
34	KILM	NWS	Wilmington, NC	34.27	77.91	68	KMGW	FAA	Morgantown, WV	39.65	79.92

Table C-3.4 Automated Surface Observing System (ASOS) sites (continued)

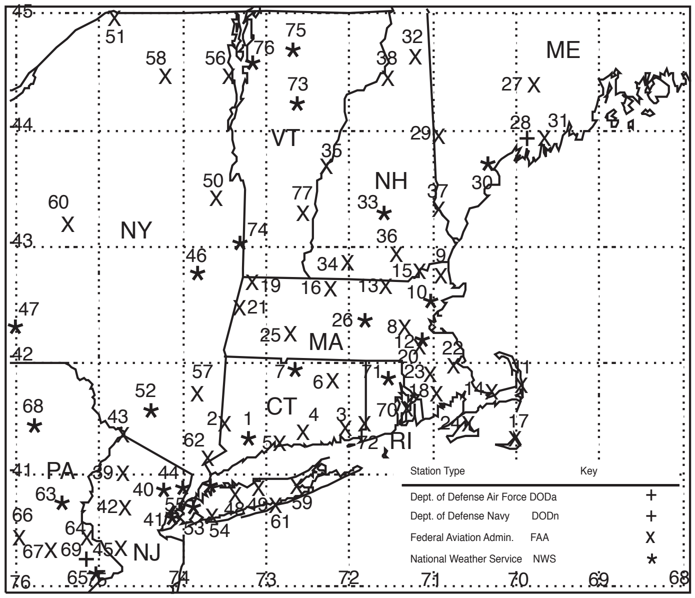

#	ID	Agency	Site Name	Lat. (N)	Lon (W)	#	ID	Agency	Site Name	Lat. (N)	Lon (W)
1	KBDR	NWS	Bridgeport, CT	41.16	73.13	39	K12N	NWS	Andover, NJ	41.01	74.74
2	KDXR	FAA	Danbury, CT	41.37	73.48	40	KCDW	FAA	Caldwell, NJ	40.88	74.28
3	KGON	FAA	Groton/N. Lon, CT	41.33	72.05	41	KEWR	NWS	Newark, NJ	40.68	74.17
4	KHFD	FAA	Hartford, CT	41.33	72.65	42	KN52	FAA	Somerville, NJ	40.62	74.67
5	KHVN	FAA	New Haven, CT	41.26	72.89	43	KFWN	FAA	Sussex, NJ	41.20	74.63
6	KIJD	FAA	Willimantic, CT	41.74	72.18	44	KTEB	NWS	Teterboro, NJ	40.85	74.06
7	KBDL	NWS	Windsor Locks, CT	41.94	72.68	45	KTTN	FAA	Trenton, NJ	40.28	74.82
8	KBED	FAA	Bedford, MA	42.47	71.29	46	KALB	NWS	Albany, NY	42.75	73.80
9	KBVY	FAA	Beverly, MA	42.58	70.92	47	KBGM	NWS	Binghamton, NY	42.21	75.98
10	KBOS	NWS	Boston, MA	42.36	71.01	48	KFRG	FAA	Farmingdale, NY	40.73	73.42
11	KCQX	FAA	Chatham, MA	41.69	69.99	49	KISP	FAA	Islip, NY	40.79	73.10
12	KMQE	NWS	East Milton, MA	42.21	71.11	50	KGFL	FAA	Glens Falls, NY	43.34	73.61
13	KFIT	FAA	Fitchburg, MA	42.55	71.56	51	KMSS	FAA	Massena, NY	44.93	74.85
14	KHYA	FAA	Hyannis, MA	41.67	70.27	52	KMGJ	NWS	Montgomery, NY	41.51	74.27
15	KLWM	FAA	Lawrence, MA	42.71	71.13	53	KNYC	NWS	New York City, NY	40.78	73.97
16	KORE	FAA	Orange, MA	42.57	72.28	54	KJFK	NWS	New York City, NY	40.64	73.76
17	KACK	FAA	Nantucket, MA	41.25	70.06	55	KLGA	NWS	New York City, NY	40.78	73.88
18	KEWB	FAA	New Bedford, MA	41.68	70.97	56	KPLB	FAA	Plattsburgh, NY	44.68	73.53
19	KAQW	FAA	North Adams, MA	42.70	73.17	57	KPOU	FAA	Poughkeepsie, NY	41.63	73.88
20	KOWD	FAA	Norwood, MA	42.19	71.17	58	KSLK	FAA	Saranac Lake, NY	44.39	74.20
21	KPSF	FAA	Pittsfield, MA	42.43	73.29	59	KHWV	FAA	Shirley, NY	40.82	72.87
22	KPYM	FAA	Plymouth, MA	41.91	70.73	60	KUCA	FAA	Utica, NY	43.14	75.38
23	KTAN	FAA	Taunton, MA	41.88	71.02	61	KFOK	FAA	West Hampton Bch, NY	40.85	72.62
24	KMVY	FAA	Vineyard Haven, MA	41.39	70.62	62	KHPN	FAA	White Plains, NY	41.06	73.70
25	KBAF	FAA	Westfield, MA	42.16	72.71	63	KABE	NWS	Allentown, PA	40.65	75.45
26	KORH	NWS	Worcestor, MA	42.27	71.87	64	KN88	FAA	Doylestown, PA	40.33	75.12
27	KAUG	FAA	Augusta, ME	44.32	69.80	65	KPNE	NWS	Philadelphia, PA	40.08	75.01
28	KNHZ	DODn	Brunswick, ME	43.90	69.94	66	KRDG	FAA	Reading, PA	40.37	75.96
29	KIZG	FAA	Fryeburg, ME	43.99	70.95	67	KPTW	FAA	Pottstown, PA	40.24	75.56
30	KPWM	NWS	Portland, ME	43.64	70.30	68	KAVP	NWS	Wilkes B./Scran., PA	41.34	75.73
31	KIWI	FAA	Wiscasset, ME	43.96	69.71	69	KNXX	DODn	Willow Grove, PA	40.19	75.14
32	KBML	FAA	Berlin, NH	44.58	71.18	70	KUUU	FAA	Newport, RI	41.53	71.23
33	KCON	NWS	Concord, NH	43.20	71.50	71	KPVD	NWS	Providence, RI	41.72	71.43
34	KAFN	FAA	Jaffrey, NH	42.81	72.00	72	KWST	FAA	Westerly, RI	41.35	71.80
35	KLEB	FAA	Lebanon, NH	43.63	72.31	73	KMPV	NWS	Barre/Montpelier, VT	44.20	72.57
36	KMHT	FAA	Manchester, NH	42.93	71.44	74	KDDH	NWS	Bennington, VT	42.89	73.25
37	K6B1	FAA	Rochester, NH	43.28	70.92	75	KMPV	NWS	Burlington, VT	44.47	73.15
38	KHIE	FAA	Whitefield, NH	44.37	71.55	76	KMVL	NWS	Morrisville, VT	44.20	72.57
						77	KVSF	NWS	Springfield, VT	43.34	72.52

Table C-3.4 Automated Surface Observing System (ASOS) sites (continued)

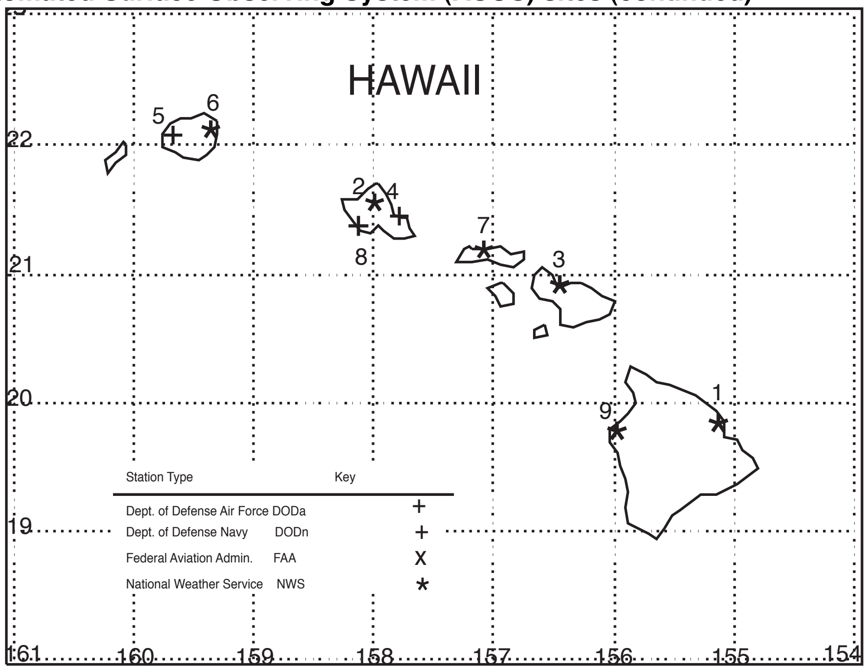

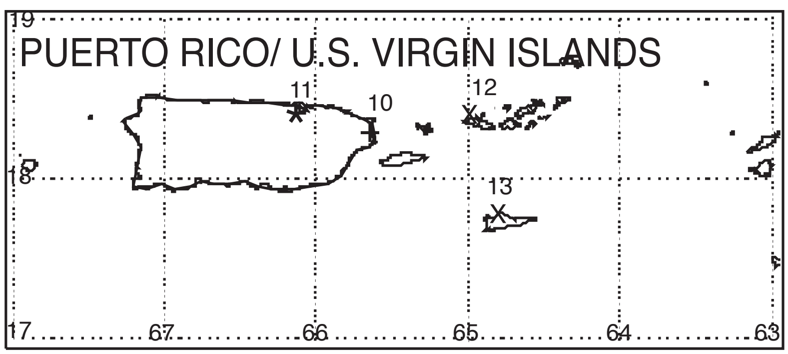

#	ID	Agency	Site Name	Lat. (N)	Lon (W)
1	PHTO	NWS	Hilo, HI	19.72	155.05
2	PHNL	NWS	Honolulu, HI	21.32	157.94
3	PHOG	NWS	Kahului, HI	20.89	156.43
4	PHNG	DODn	Kaneohoe, HI	21.45	157.77
5	PHBK	DODn	Kekaha, HI	22.04	159.79
6	PHLI	NWS	Lihue, HI	21.98	159.34
7	PHMK	NWS	Molokai, HI	21.16	157.10
8	PHNA	DODn	Oahu, HI	21.31	158.07
9	PHKO	NWS	Kailua/Kona, HI	19.74	156.05
10	TJNR	DODn	Roosevelt Roads, PR	18.26	65.64
11	TJSJ	NWS	San Juan, PR	18.43	66.01
12	KSTT	FAA	Charlotte Amali, VI	18.34	64.98
13	KSTX	FAA	Christiansted, VI	17.70	64.81

C.4 NWS and DOD Locations/Contacts-2001

Table C-4.1 DOD RAWIN/RAOB locations/contacts

Station Identifier	Address/Location	Sqdrn. Co/Fac. Cmdr.	Telephone Numbers
COF (74795)	45th Wea. Squadron/CC 1201 Edward H. White St. Patrick AFB, FL 32925-3238	Col. Neil Wyse Squadron Commander Lt. Col. Dewey Harms Chief of Systems	321-494-7012 321-494-7426 DSN[1]: 854-7426 CSR[2]: 853-8211 FAX: 321-853-4315 FAX: 321-853-8295
VPS (72221)	46th WS 601 W. Choctawhatchee Suite 60 Eglin AFB, FL 32542-5719	Lt. Col. Michael G. Bedard Squadron Commander Joe Kerwin Chief, Range Support	850-882-5449 850-882-4800 850-882-5224 850-882-5960 850-882-5323 DSN[1]: 872-5323 FAX: 850-882-3341
TXKF[2] (78016)	P.O. Box 123 St. Georges Bermuda GEBX	Mr. Roger Williams	441-293-5339 441-293-5078 FAX: 441-293-6658

[1] DSN: Defense Switched Network.

[2] The facility at Bermuda is not military. Mr. Roger Williams is the manager of the meteorology office.

Note 1: MCI can be used to call Bermuda from HRD/AOML; however, you must have an MCI FTS 2001 credit card (see Gladys Medina if you need an MCI FTS 2001 credit card for official business).

To place a call using an MCI FTS 2001 card:

(a) Follow instructions on the back of your MCI FTS 2001 credit card.
(b) Division secretaries or Gladys Medina can assist placing calls.

Note 2: In recent years, CSR operated the meteorological station at Antigua under a contract with the USAF. Meteorological operations at Antigua were terminated May 1, 1993. During the 1999 field program, if additional rawinsonde/radiosonde data from the eastern Caribbean area are required, the MGOC representative should contact the Meteorological Office, Saint Martin (Saint Maarten), Netherlands Antilles [TNCM (78866)]. Petier Trappenberg is the Director of the facility. He can be contacted as follows:

For further information or assistance, contact Albert Mongeon (NWS) at 301-713-0882, ext. 140.

Note 3: Additional rawinsondes/radiosondes from DOD rawinsonde sites, including Patrick AFB, Eglin AFB, and NAS Guantanamo (Cuba), can be requested through the CARCAH at TPC/NHC (see Appendix F, section F.3, 3g)].

Note 4: When requesting additional RAWINs/RAOBs from any DOD or other facility, the MGOC representative should:

(a) State the beginning and ending date(s) and time(s) [UTC].
(b) Specify the desired frequency of rawinsondes/radiosondes (3-, 6-, or 12-hourly intervals).
(c) State that rawinsondes/radiosondes should be "flown" (at least) to the 100-hPa level.
(d) Request that all data (*i.e.,* raw data **and** worked-up soundings) be sent to Howard A. Friedman, AOML/HRD, 4301 Rickenbacker Causeway, Miami, Florida, 33149.

Table C-4.2 NWS/Eastern Region RAWIN/RAOB locations/contacts[1]

Station Identifier	Address/Location	MIC/OIC	Telephone Numbers
CHS (72208)	NWS/WSO, NOAA 5777 S. Aviation Avenue Charleston, SC 29406	Steve Rich MIC Stephen.Rich@noaa.gov	843-744-0303 843-744-0211 843-727-4395 FAX: 843-747-5405
GSO (72317)	NWS/WSO, NOAA Centennial Campus NCSU 1005 Capability Dr. Research Building III, Suite 300 Raleigh, NC 27606	Steve Harned MIC Steve.Harned@noaa.gov	919 515-8209 FAX: 919-515-5405
MHX (72305)	NWS/WSO, NOAA 533 Roberts Road Newport, NC 28570	Thomas Kriehn MIC Thmoas.Kriehn@noaa.gov	252-223-5122 252-223-5631 252-223-2328 FAX: 252-223-3673 1-800-697-7374
OKX (72501)	NWS/WSFO, NOAA 175 Brookhaven Avenue Bld. # NWS 1 Upton, NY 11973	Michael E. Wyllie MIC Micheal.Wyllie@noaa.gov	631-924-0517 631-924-0037 FAX: 631-924-0519
WAL (72402)	NWS/WSCMO[2,3] Building N162 Wallops Island, VA 23337	Bryan Cunnigham Chief, UA Section	757-824-1586 757-824-1160 FAX: 757-854-0843
	Weather Office[3,4] Building E106 Wallops Island, VA 23337	Ted Wilz[5] MIC	757-824-1325 757-824-1638 FAX: 757-824-2410

[1] Additional rawinsondes or radiosondes may be requested from the NWS/ER or NWS/SR stations listed in Tables C-4.2 and C-4.3: (a) via AFOS [contact NHC's Communications Unit personnel for assistance]; (b) through the duty Hurricane Specialist (NHC); or (c) directly by phone. Messages sent via AFOS should contain a statement asking that the appropriate NWS station(s) acknowledge and confirm each request. Remember to identify the program as "**HRD/Hurricane Field Program**" and follow instructions in Note 4, at the bottom of Table C-4.1.

[2] Normal hours of operation: 0600-2230 EDT (or EST, when appropriate).

[3] If you can't reach your party on any of the numbers shown, contact the NASA switchboard operator (757-824-1000) and ask to have your party paged.

[4] Normal hours of operation: 0530-1600 EDT (or EST, when appropriate).

[5] Home phone number is 410-860-2108.

Table C-4.3 NWS/Southern Region RAWIN/RAOB locations/contacts[1]

Station Identifier	Address/Location	MIC/OIC	Telephone Numbers
BMX (72230)	NWS/WSO, NOAA 465 Weathervane Road Calera, AL 35040-5079	Gary S. Petti MIC Gary.Petti@noaa.gov	205-621-5645 205-621-5646 205-621-5647 205-664-3010 FAX: 205-664-7821
BRO (72250)	NWS/WSO, NOAA 20 South Vermillion Road Brownsville, TX 78521-5798	Richard R. Hagan MIC Richard.Hagan@noaa.gov	956-504-3084 956-504-3354 956-504-1432 956-504-3184 956-504-1631 FAX: 956-982-1766
CRP (72251)	NWS/WSO, NOAA International Airport 300 Pinson Drive Corpus Christi, TX 78406-1803	Kenneth Graham MIC Kenneth.Graham@noaa.gov	361-299-1353 361-299-1354 361-289-0959 FAX: 361-289-7823
EYW (72201)	NWS/WSO, NOAA International Airport 3535 S. Roosevelt Blvd. Ste.105 Key West, FL 33040-5234	Bobby McDaniel MIC Bobby.McDaniel@ noaa.gov	305-295-1324 305-295-1316 FAX: 305-293-9987 *(call ahead)*
FFC (72215)	NWS/WSMO, NOAA 4 Falcon Drive Peachtree City, GA 30269	Lans Rothfusz MIC Lans.Rothfusz@noaa.gov	770-486-1133 770-486-1333 770-486-0026 770-486-0027 FAX: 770-486-9333
FWD (72249)	NWS/WSFO, NOAA 3401 Northern Cross Blvd. Forth Worth, TX 76137-3610	Gifford "Skip" Ely MIC Skip.Ely@noaa.gov	817-831-1581 817-831-1157 817-831-1574 817-831-1595 FAX: 817-831-3025
JAN (72235)	NWS/WSFO, NOAA 234 Weather Service Drive Jackson, MS 39208	Jim Spefkovich MIC Jim.Spefkovich@noaa.gov	601-965-4639 601-965-4638 601-939-2786 601-936-2189 FAX: 601-965-4028
JAX (72206)	NWS/WSO, NOAA 13701 Fang Drive Jacksonville, FL 32218	Stephen M. Letro MIC Steve.Letro@noaa.gov	904-741-4370 904-741-4411 904-741-5186 FAX: 904-741-0078

Table C-4.3 NWS/Southern Region RAWIN/RAOB locations/contacts[1] (continued)

Station Identifier	Address/Location	MIC/OIC	Telephone Numbers
LCH (72240)	NWS/WSO, NOAA 500 Airport Blvd., #115 Lake Charles, LA 70607-0668	Steve Rinard MIC Steve.Rinard@noaa.gov	337-477-3422 337-477-2495 337-477-0354 FAX: 337-474-8705
LZK (72340)	NWS/WSO, NOAA N. Little Rock Airport 8400 Remount Road N. Little Rock, AR 72118	Renee Fair MIC Renee.Fair@noaa.gov	501-834-9102 501-834-3955 501-834-0308 FAX: 501-834-0715
MFL (72203)	NWS/WSMO, NOAA 11691 S.W. 17th Street Miami, FL 33165-2149	Russell "Rusty" Pfost MIC Rusty.Pfost@noaa.gov	305-229-4500 305-229-4501 305-229-4523 305-229-4528 FAX: 305-229-4553 FAX: 305-559-4503
SHV (72248)	NWS/WSO, NOAA 5655 Hollywood Avenue Shreveport, LA 71109-7750	Lee Harrison MIC Lee.Harrison@noaa.gov	318-635-9398 318-636-7345 318-636-4594 318-635-8734 FAX: 318-636-9620
SIL (72233)	NWS/WSFO, NOAA 62300 Airport Road Slidell, LA 70460-5243	Paul S. Trotter MIC Paul.Trotter@noaa.gov	985-649-0429 504-589-2808 985-649-0357 985-645-0565 FAX: 985-649-2907
TBW (72210)	NWS/WSO, NOAA 2525 14th Avenue, S.E. Ruskin, FL 33570 [Tampa Bay Area]	Ira Brenner MIC Ira.Brenner@noaa.gov	813-641-2512 813-645-4111 813-641-1720 813-641-1807 FAX: 813-641-2441 FAX: 813-641-2619
SJU (78526)	NWS/WSFO, NOAA 4000 Carretera 190 Carolina, PR 00979	Israel Matos[4] MIC Israel.Matos@noaa.gov Rafael Mojica WCM	787-253-4501 787-253-4504 UA:[3] 787-253-4587 FAX: 787-253-7802
TLH (72214)	NWS/WSO, NOAA Regional Airport 3300 Capital Circle, S.W. Box 33 Tallahassee, FL 32310-8723	Paul Duval MIC Paul.Duval@noaa.gov	850-942-8398 850-942-9394 FAX: 850-942-9396

[1] See footnote 1 in Table C-4.2.
[2] Hours: 0400-2000 CDT (or CST, when appropriate).
[3] UA: Upper air station.
[4] Pager: 1-800-652-0608

Table C-4.4 NWS/Eastern Region coastal radar locations/contacts

Station Identifier/ Type Radar/ Lat./Lon.	Address/Location	MIC/OIC	Telephone Numbers
KAKQ (93773) WSR-88D 36.9839°N 77.0072°W	NWS/WSO, NOAA 10009 General Mahone Hwy. Wakefield, VA 23888	Anthony Siebers MIC Anthony.Siebers@ noaa.gov	757-899-5734 757-899-5735 757-899-4200 FAX: 757-899-3605
KCLX (53845) WSR-88D 32.6555°N 81.0422°W	NWS/WSO, NOAA 5777 S. Aviation Avenue Charleston, SC 29406	Stephen T. Rich MIC Stephen.Rich@noaa.gov	843-744-0303 843-744-0211 843-554-4851 FAX: 843-747-5405
KLTX (93774) WSR-88D 33.9894°N 78.4289°W	NWS/WSO, NOAA 2015 Gardner Drive Wilmington, NC 28405	Richard W. Anthony MIC Richard.Anthony@ noaa.gov	910-763-8331 910-762-4289 910-762-9476 FAX: 910-762-1288
KLWX (93767) WSR-88D 38.9753°N 77.4778°W	NWS/WFO, NOAA 44087 Weather Service Rd Sterling, VA	Jim Travers MIC James.Travers@noaa.gov	703-260-0107 X222 Fax: (703) 260-0809
KMHX (93768) WSR-88D 34.7761°N 76.8761°W	NWS/WSO, NOAA 533 Roberts Road Newport, NC 28570	Thomas Kriehn MIC Thomas.Kriehn@noaa.gov	252-223-5122 252-223-2328 FAX: 252-223-3673
KOKX (94703) WSR-88D 40.8656°N 72.8639°W	NWS/WSO, NOAA 175 Brookhaven Avenue Bldg #NWS 1. Upton, NY 11973	Michael E. Wyllie MIC Michael.Wyllie@noaa.gov	631-924-0517 631-924-0037 FAX: 613-924-0519
KRAX (93772) WSR-88D 35.6656°N 78.4897°W	NWS/WSO, NOAA Centennial Campus NCSU 1005 Capability Dr. Research Building III, Suite 300 Raleigh, NC 27606	Steve Harned MIC Steve.Harned@noaa.gov	919-515-8209 FAX: 919-515-8213

Note 1: NWS/ER point of contact for WSR-88D information is the Eastern Region Hurricane Watch Office (516-244-0172).

Table C-4.5 NWS/Southern Region coastal radar locations/contacts

Station Identifier/ Type Radar/ Lat./Lon.	Address/Location	MIC/OIC	Telephone Numbers
KBRO (12919) WSR-88D 25.9161°N 97.4189°W	NWS/WSO, NOAA 20 South Vermillion Road Brownsville, TX 78521-6851	Richard R. Hagan MIC Richard.Hagan@noaa.gov	956-504-3084 956-504-3354 956-504-3184 956-504-1631 FAX: 956-982-1766
KCRP (12924) WSR-88D 27.7842°N 97.5111°W	NWS/WSO, NOAA International Airport 300 Pinson Drive Corpus Christi, TX 78406	Kenneth Graham MIC Kenneth.Graham@noaa.gov	361-289-1353 361-289-1354 FAX: 361-289-7823
KBYX(92804) WSR-88D 24.5975°N 81.7031°W	NWS/WSO, NOAA Key West International Airport 3535 S. Roosevelt Blvd. #.105 Key West, FL 33040-5234	Bobby McDaniel MIC Bobby.McDaniel@ noaa.gov	305-295-1324 305-295-1316 FAX: 305-293-9987 *(call ahead)*
KHGX (03980) WSR-88D 29.4719°N 95.0792°W	NWS/WSO, NOAA 1620 Gill Road Dickinson, TX 77539	William "Bill" Read MIC Bill.Read@noaa.gov	281-337-5192 281-337-5285 281-534-2157 281-534-5625 FAX: 281-337-3798
KJAX (13889) WSR-88D 30.4847°N 81.7019°W	NWS/WSO, NOAA 13701 Fang Drive Jacksonville, FL 32218	Stephen M. Letro MIC Steve.Letro@noaa.gov	904-741-4411 904-741-5186 904-741-4370 FAX: 904-741-0078
KLCH (03937) WSR-88D 30.1253°N 93.2158°W	NWS/WSO, NOAA 500 Airport Boulevard, #115 Lake Charles, LA 70605	Steve Rinard MIC Steve.Rinard@noaa.gov	337-477-3422 337-477-2495 337-477-0354 FAX: 337-474-8705
KLIX (53813) WFSR-88D 30.3367°N 89.8256°W	NWS/WSFO, NOAA 62300 Airport Road Slidell, LA 70460	Paul S. Trotter MIC Paul.Trotter@noaa.gov	985-649-0984 985-649-0429 504-589-2808 985-649-0899 985-645-0565 FAX: 985-649-2907

Table C-4.5 NWS/Southern Region coastal radar locations/contacts (continued)

Station Identifier/ Type Radar/ Lat./Lon.	Address/Location	MIC/OIC	Telephone Numbers
KAMX (12899) WSR-88D 25.6111°N 80.4128°W	NWS/WSFO/NOAA 11691 S.W. 17th Street Miami, FL 33165-2149	Russell "Rusty" Pfost MIC Rusty.Pfost@noaa.gov	305-229-4500 305-229-4501 305-229-4520 305-229-4528 FAX: 305-229-4553 305-559-4503
KMLB (12838) WSR-88D 28.1133°N 80.6542°W	NWS/WSO, NOAA 421 Croton Road Melbourne, FL 32935	Bart Hagemeyer MIC Bart.Hagemeyer@noaa.gov	321-254-6083 321-254-6923 321-259-7589 321-259-7618 FAX: 321-255-0791
KMOB (13894) WSR-88D 30.6794°N 88.2397°W	NWS/WSO, NOAA 8400 Airport Boulevard, Bldg # 11 Mobile, AL 36608	Randall McKee MIC Randall.McKee@noaa.gov	334-633-0921 334-633-7342 334-633-6443 334-633-2471 FAX: 334-607-9773
KTBW (92801) WSR-88D 27.7056°N 82.4022°W	NWS/WSO, NOAA 2525 14th Avenue, S.E. Ruskin, FL 33570 [Tampa Bay Area]	Ira Brenner MIC Ira.Brenner@noaa.gov	813-645-4111 813-641-2512 813-641-1720 FAX: 813-641-2619 813-641-2441
TJUA(11655) WSR-88D 18.1156°N 66.0781°W	NWS/WSFO, NOAA 4000 Carretera 190 Carolina, PR 00979	Israel Matos MIC Israel.Matos@noaa.gov Rafael Mojica WCM	787-253-4501 787-253-4502 FAX: 787-253-7802
KTLH (93805) WSR-88D 30.3975°N 84.3289°W	NWS/WSO, NOAA Regional Airport 3300 Capital Circle, S.W. Box 33 Tallahassee, FL 32310-8723	Paul Duval MIC Paul.Duval@noaa.gov	850-942-8398 850-942-9394 850-942-9395 FAX: 850-942-9396

Note 1: NWS/SR official contact for WSR-88D information is Victor Murphy (W/SR/SRH), WSR-88D Meteorologist (817-978-2367 ext. 130).

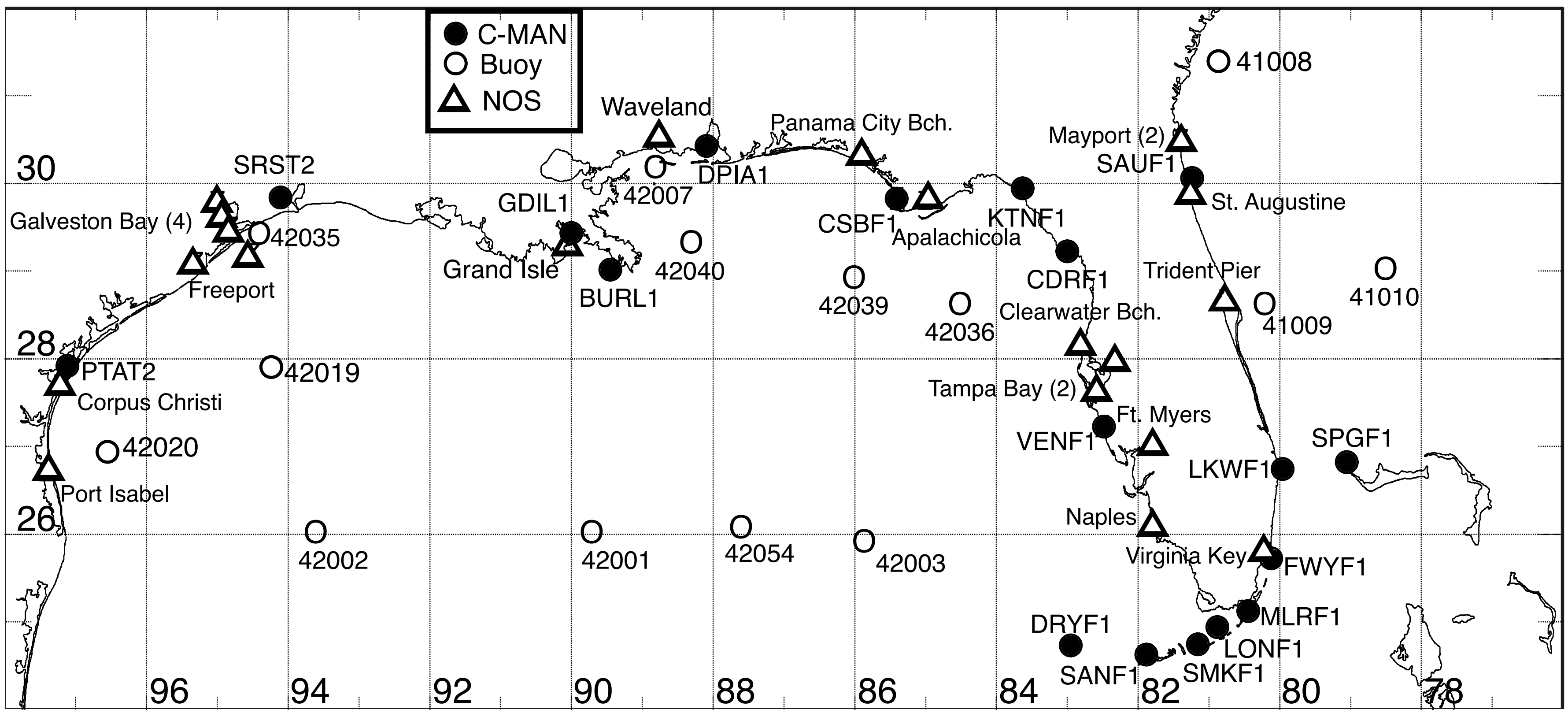

Fig. C-2. Marine buoy, C-MAN, and NOS (lower case) locations in the Gulf of Mexico, Florida, and southern Georgia. See Tables C-3.1 -- C3.3

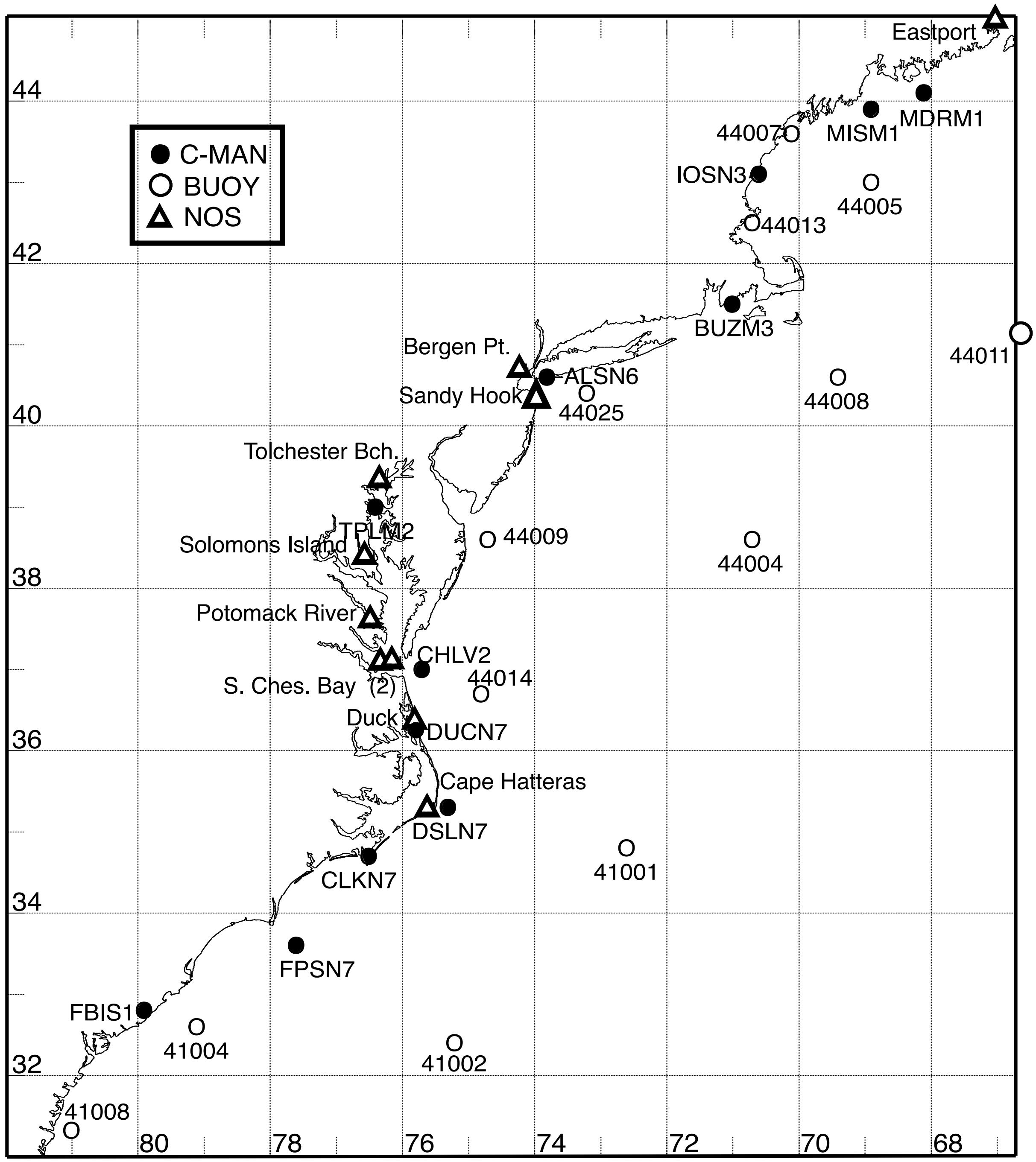

Fig. C-3. Marine buoy, C-MAN, and NOS (lower case) locations for the U.S. east coast. See Tables C-3.1 -- C-3.4.

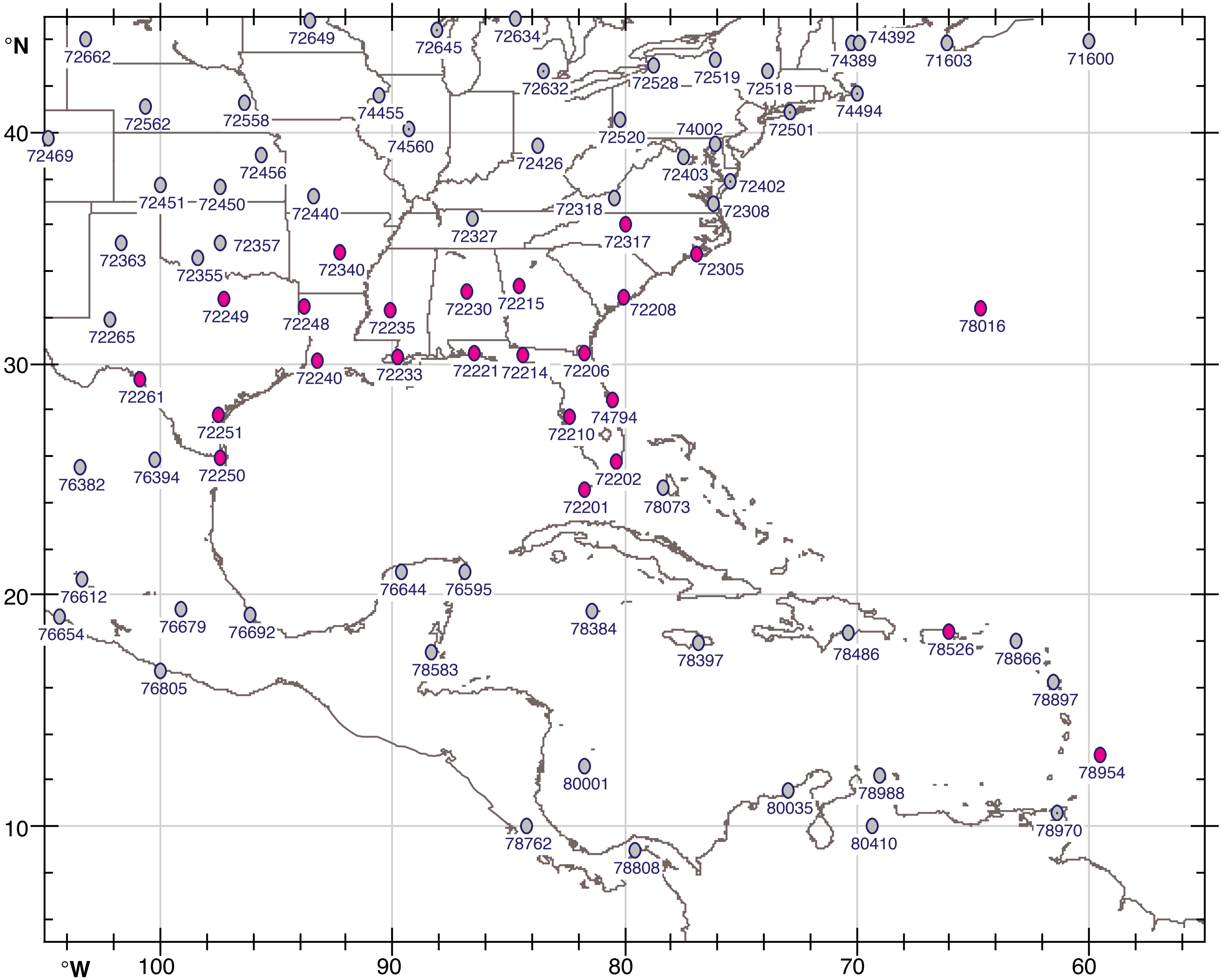

Fig. C-4. Locations of RAWIN/RAOB stations. See Tables C-4.1-C-4.5 for information about stations shown as dark circles.

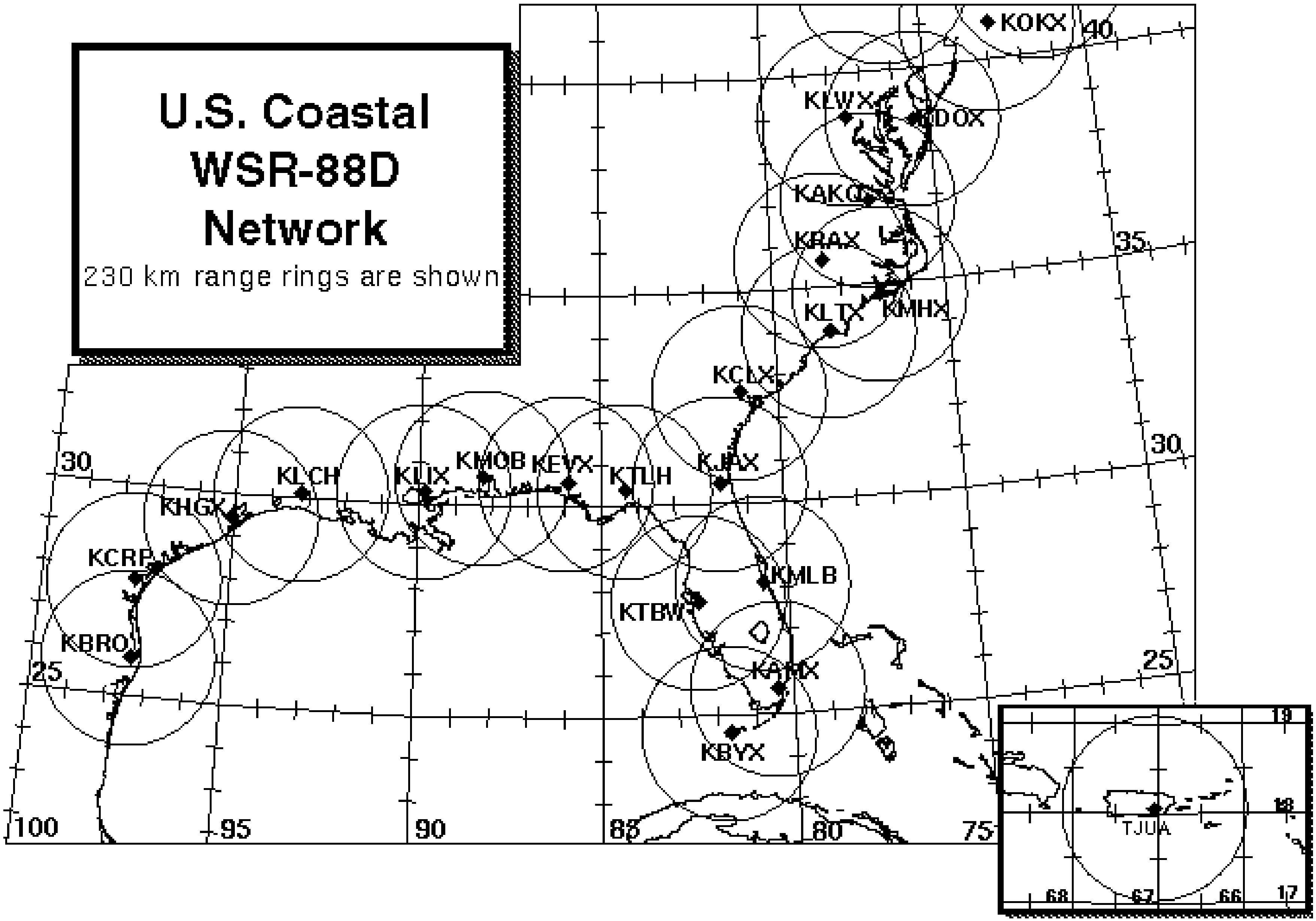

Fig. C-5. Locations of coastal WSR-88D stations. See tables C-4.1 -- C-4.5 for complete information.

APPENDIX D

PRINCIPAL DUTIES OF THE NOAA SCIENTIFIC PERSONNEL

PRINCIPAL DUTIES OF THE NOAA SCIENTIFIC PERSONNEL

CAUTION

Flight operations are routinely conducted in turbulent conditions. Shock-mounted electronic and experimental racks surround most seat positions. Therefore, for safety onboard the aircraft all personnel should wear long pants and closed toed shoes. For comfort, personnel should bring a jacket or sweater as the cabin gets cold during flight.

Smoking is prohibited within 50 ft of the aircraft while they are on the ground. No smoking is permitted on the aircraft at any time.

GENERAL INFORMATION FOR ALL SCIENTIFIC MISSION PARTICIPANTS

Mission participants are advised to carry the proper personal identification [i.e., travel orders, "shot" records (when appropriate), and passports (when required)]. Passports will be checked by AOC personnel prior to deployment to countries requiring it. All participants must provide their own meals for in-flight consumption. AOC provides a refrigerator, microwave, coffee, utensils, condiments, ice, water, and soft drinks for a mandatory **$2.00** per flight "mess" fee.

D.1 Field Program Director;

(1) Responsible to the HRD director for the implementation of the Hurricane Field Program Plan.

(2) Only official communication link to AOC. Communicates flight requirements and changes in mission to AOC.

(3) Only formal communication link between AOML and CARCAH during operations. Coordinates scheduling of each day's operations with AOC only after all (POD) reconnaissance requirements are completed between CARCAH and AOC.

(4) Convenes the Hurricane Field Program Operations Advisory Panel. This panel selects missions to be flown in comparison with others as specified in sections 9-15 of this plan.

(5) Provides for pre-mission briefing of flight crews, scientists, and others (as required).

(6) Assigns duties of field project scientific personnel.

(7) Coordinates press statements with NOAA/Public Affairs.

D.2 Assistant Field Program Director

(1) Assumes the duties of the field program director in his absence.

D.3 Miami Ground Operations Center: Senior Team Leader

(1) During operations, the MGOC senior team leader is responsible for liaison between HRD base and field personnel and other organizations as requested by the field program director, the director of HRD, or their designated representatives.

D.4 Named Experiment Lead Project Scientist

(1) Has overall responsibility for the experiment.

(2) Coordinates the project and sub-project requirements.

(3) Determines the primary modes of operation for appropriate instrumentation.

(4) Assists in the selection of the mission.

(5) Provides a written summary of the mission to the field program director (or his designee) at the experiment's debriefing.

D.5 Lead Project Scientist

(1) Has overall scientific responsibility for his/her aircraft.

(2) Makes in-flight decisions concerning alterations of: (a) specified flight patterns; (b) instrumentation operation; and (c) assignment of duties to on-board scientific project personnel.

(3) Acts as project supervisor on the aircraft and is the focal point for all interactions of project personnel with operational or visiting personnel.

(4) Conducts preflight and post flight briefings of the entire crew. Completes formal checklists of instrument operations, noting malfunctions, problems, etc.

(5) Provides a written report of each mission day's operations to the field program director at the mission debriefing.

D.6 Cloud Physics Scientist

(1) Has overall responsibility for the cloud physics project on the aircraft.

(2) Briefs the on-board lead project scientist on equipment status before takeoff.

(3) Determines the operational mode of the cloud physics sensors (i.e., where, when, and at what rate to sample).

(4) Operates and monitors the cloud physics sensors and data systems.

(5) Provides a written preflight and post flight status report and flight summary of each mission day's operations to the on-board lead project scientist at the post flight debriefing.

D.7 Boundary-Layer Scientist

(1) Insures that the required number of AXCPs, AXBTs, and AXCTDs are on the aircraft for each mission.

(2) Operates the AXCP, AXBT, and AXCTD equipment (as required) on the aircraft.

(3) Briefs the on-board lead project scientist on equipment status before takeoff.

(4) Determines where and when to release the AXCPs, AXBTs, and AXCTDs (as appropriate) subject to clearance by flight crew.

(5) Performs preflight, inflight, and post flight checks and calibrations.

(6) Provides a written preflight and post flight status report and a flight summary of each mission day's operations to the on-board lead project scientist at the post flight debriefing.

D.8 Radar Scientist

(1) Determines optimum meteorological target displays. Continuously monitors displays for performance and optimum mode of operations. Thoroughly documents modes and characteristics of the operations.

(2) Provides a summary of the radar display characteristics to the on-board lead project scientist at the post flight debriefing.

(3) Maintains tape logs and changes magnetic tape (as needed).

(4) During the ferry to the storm, the radar scientist should record a tape of the sea return on either side of the aircraft at elevation angles varying from -20° through +20°. This tape will allow correction of any antenna mounting biases or elevation angle corrections.

D.9 Dropsonde Scientist

(1) Examines dropsonde observations for accuracy.

(2) Determines the most likely values of temperature, dew-point depression, and horizontal wind at mandatory and significant (pressure) levels.

(3) Provides final code to the data system technician for ASDL, transmission or insures correct code in case of automatic data transmission.

D.10 Workstation Scientist

(1) Operates HRD's workstation.

(2) Runs programs that determine wind center and radar center as a function of time, composite flight-level and radar reflectivity relative to storm center and then process and code dropwindsonde observations.

(3) Checks data for accuracy and sends appropriate data to ASDL computer.

(4) Maintains records of the performance of the workstation and possible software improvements.

APPENDIX E

NOAA RESEARCH OPERATIONAL PROCEDURES AND CHECK LISTS

NOAA RESEARCH OPERATIONAL PROCEDURES AND CHECK LISTS

E.1 Procedures and Mission Directives: "Conditions-of-Flight" Commands

Mission participants should be aware of the designated "conditions-of-flight." There are five designated basic conditions of readiness encountered during flight. The pilot will set a specific condition and announce it to all personnel over the aircraft's PA (public address) and ICS (interphone communications systems). All personnel are expected to act in accordance with the instructions for the specific condition announced by the pilot. These conditions and appropriate actions are shown below.

CONDITION 1: TURBULENCE/PENETRATION. All personnel will stow loose equipment and fasten safety belts.

CONDITION 2: HIGH ALTITUDE TRANSIT/FERRY. There are no cabin station manning requirements.

CONDITION 3: NORMAL MISSION OPERATIONS. All scientific and flight crew stations are to be manned with equipment checked and operating as dictated by mission requirements. Personnel are free to leave their ditching stations.

CONDITION 4: AIRCRAFT INSPECTION. After take-off, crew members will perform wings, engines, electronic bays, lower compartments, and aircraft systems check. All other personnel will remain seated with safety belts fastened and headsets on.

CONDITION 5: TAKE-OFF/LANDING. All personnel will stow or secure loose equipment, don headsets, and fasten safety belts/shoulder harnesses.

E.2 Lead Project Scientist

E.2.1 Preflight

_____ 1. Participate in general mission briefing.

_____ 2. Determine specific mission and flight requirements for assigned aircraft.

_____ 3. Determine from CARCAH or field program director whether aircraft has operational fix responsibility and discuss with AOC flight director/meteorologist and CARCAH unless briefed otherwise by field program director.

_____ 4. Contact HRD members of crew to:
   a. Assure availability for mission.
   b. Arrange ground transportation schedule when deployed.
   c. Determine equipment status.

_____ 5. Meet with AOC flight crew at least 90 minutes before takeoff, provide copies of flight requirements, and provide a formal briefing for the flight director, navigator, and pilots.

_____ 6. Report status of aircraft, systems, necessary on-board supplies and crews to appropriate HRD operations center (MGOC in Miami).

E.2.2 In-Flight

_____ 1. Confirm from AOC flight director that satellite data link is operative (information).

_____ 2. Confirm camera mode of operation.

_____ 3. Confirm data recording rate.

_____ 4. Complete Form E-2.

E.2.3 Post flight

_____ 1. Debrief scientific crew.

_____ 2. Report landing time, aircraft, crew, and mission status along with supplies (tapes, *etc.*) remaining aboard the aircraft to MGOC.

_____ 3. Gather completed forms for mission and turn in at the appropriate operations center. [**Note**: all data removed from the aircraft by HRD personnel should be cleared with the AOC flight director.]

_____ 4. Obtain a copy of the 10-s flight listing from the AOC flight director. Turn in with completed forms.

_____ 5. Determine next mission status, if any, and brief crews as necessary.

_____ 6. Notify MGOC as to where you can be contacted and arrange for any further coordination required.

_____ 7. Prepare written mission summary using form E-2 p.3 (due to Field Program Director1 week after the flight).

Lead Project Scientist Check List

Date _______________ **Aircraft** ______________ **Flight ID** ____________________

A. —Participants:

HRD		AOC	
Function	**Participant**	**Function**	**Participant**
Lead Project Scientist		Flight Director	
Cloud Physics		Pilots	
Radar		Navigator	
Workstation		Systems Engineer	
Photographer/Observer		Data Technician	
Dropwindsonde		Electronics Technician	
AXBT/AXCP/Guest		Other	

Take-Off: ________ Location: _______________ Landing: ________ Location: _________________

Number of Eye Penetrations: ______

B. —Past and Forecast Storm Locations:

Date/Time	Latitude	Longitude	MSLP	Maximum Wind

C. —Mission Briefing:

D. —Equipment Status (Up ↑, Down ↓, Not Available **—**, Not Used **O**)

Equipment	**Pre-Flight**	**In-Flight**	**Post-Flight**	**# of DATs or Expendables**
Aircraft				
Radar/LF				
Radar/TA (Doppler)				
Cloud Physics				
Data System				
GPS sondes				
AXBT/AXCP				
Workstation				
Videography				

REMARKS:

Mission Summary
Storm name
YYMMDDA# Aircraft 4_RF

Scientific Crew (4 RF)
Lead Project Scientist ___________________________
Radar Scientist__________________________________
Cloud Physics Scientist___________________________
Dropwindsonde Scientist_________________________
Boundary-Layer Scientist_________________________
Workstation Scientist____________________________
Observers______________________________________

Mission Briefing: (include sketch of proposed flight track or page #)

Mission Synopsis: (include plot of actual flight track)

Evaluation: (did the experiment meet the proposed objectives?)

Problems:(list all problems)

Page __of __

Observer's Flight Track Worksheet

Date __________________ Flight __________________ Observer ___________________

Latitude (°)

Longitude (°)

Lead Project Scientist Event Log

Date ________________ **Flight** ________________ **LPS** ______________________

Time	Event	Position	Comments

E.3 Cloud Physics Scientist

The on-board cloud physics scientist (CPS) is responsible for cloud physics data collection on his/her assigned aircraft. Detailed operational procedures are contained in the cloud physics kit supplied for each aircraft. General procedures follow. (Check off and initial.)

E.3.1 Preflight

_____ 1. Determine status of cloud physics instrumentation systems and report to the on-board lead project scientist (LPS).

_____ 2. Confirm mission and pattern selection from the on-board LPS.

_____ 3. Select mode of instrument operation.

_____ 4. Complete appropriate instrumentation preflight check lists as supplied in the cloud physics operator's kit.

E.3.2 In-Flight

_____ 1. Operate instruments as specified in the cloud physics operator's kit and as directed by the on-board LPS.

E.3.3 Post flight

_____ 1. Complete summary checklist forms and all other appropriate forms.

_____ 2. Brief the on-board LPS on equipment status and turn in completed check sheets to the LPS.

_____ 3. Take cloud physics data tapes and other data forms and turn these data sets in as follows:

a. Outside of Miami-to the LPS.
b. In Miami-to AOML/HRD. [**Note**: all data removed from the aircraft by HRD personnel should be cleared with the AOC flight director.]

_____ 4. Debrief as necessary at MGOC or the hotel during a deployment.

_____ 5. Determine the status of future missions and notify MGOC as to where you can be contacted.

Cloud Physics Scientist Check List

Date ____________________ **Aircraft** ____________ **Flight ID** ___________________

A. —Instrument Status and Performance:

System	Pre-Flight	In-Flight	Downtime	# of Tapes
Johnson-Williams				
PMS Probes:				
—2D-P				
—2D-C				
—FSSP				
—Data System				
—Recorder				
FORMVAR				
DRI Charge Probe				
DRI Field Mills				
King Probe				

B. —Remarks:

Form E-3

2-D Knollenberg Data Tape Log

Date ________________ **Flight** _________________ **Operator** ___________________

Tape #	EOF #	Time On	Time Off	Comments

FORMVAR Log

Date ______________ **Flight** _________________ **Operator** _____________________

Roll #	Time On	Time Off	Frame Count at Start	Comments

E.4 Boundary-Layer Scientist

The on-board boundary-layer scientist (BLS) is responsible for data collection from AXBTs, AXCPs, AXCTDs, BUOYs, and SST radiometers (if these systems are used on the mission). Detailed calibration and instrument operation procedures are contained in the air-sea interaction (ASI) manual supplied to each operator. General supplementary procedures follow. (Check off and initial.)

E.4.1 Preflight

_____ 1. Determine the status of equipment and report results to the on-board lead project scientist (LPS).

_____ 2. Confirm mission and pattern selection from the on-board LPS.

_____ 3. Select the mode of operation for instruments after consultation with the HRD/BLS and the on-board LPS.

_____ 4. Complete appropriate preflight check lists as specified in the ASI manual and as directed from the on-board LPS.

E.4.2 In-Flight

_____ 1. Operate the instruments as specified in the ASI manual and as directed by the on-board LPS.

E.4.3 Post flight

_____ 1. Complete summary checklist forms and all other appropriate check list forms.

_____ 2. Brief the on-board LPS on equipment status and turn in completed checklists to the LPS.

_____ 3. Debrief as necessary at MGOC or the hotel during a deployment.

_____ 4. Determine the status of future missions and notify MGOC as to where you can be contacted.

AXBT/AXCP Check Sheet Summary

Flight __________________ **Aircraft** ______________ **Operator** __________________

Number

(1) Probes dropped ________

(2) Failures ________

(3) Failures with no signal ________

(4) Failures with sea surface temperature, but terminated above thermocline ________

(5) Probes that terminated above 250 m, but below thermocline ________

(6) Probes used by channel number CH12 ________

CH14 ________

CH16 ________

CH__ ________

NOTES:

Form E-4
Page 2 of 3

AXBT and AXCP Check Sheet

Flight Number ______________________ AXBT/AXCP Contract Number ________________

Take-Off Time ______________________ Landing Time ______________________________

Storm __________________________ Storm Direction/Speed _______________________

AXCP/ AXBT #/Type	Channel Number	Lot Number	Drop Time (HHMMSS)	Lat. Deg. Min.		Long. Deg. Min.		Surface Temp. AXBT IRT		MLD (m)	Comments

Form E-4

AXCP Log

Flight Number ______________________ AXBT/AXCP Contract Number ________________

Take-Off Time ______________________ Landing Time ______________________________

Storm ____________________________ Storm Direction/Speed ______________________

Leg Number	Out/In	RA (m)	PMIN (hPa)	VMAX (m/s)	RMAX (km)	Time PMIN	Time VMAX	Time End Pass

Leg/ Drop #	Tube #	Channel #	Probe Type		Ground Speed	Drop Time (HHMMSS)	Latitude (deg min)	Longitude (deg min)	Status		Comments
			Slow	Reg					Good	Bad	

E.5 Radar Scientist

The on-board radar scientist is responsible for data collection from all radar systems on his/her assigned aircraft. Detailed operational procedures and checklists are contained in the operator's manual supplied to each operator. General supplementary procedures follow. (Check off and initial.)

E.5.1 Preflight

_____ 1. Determine the status of equipment and report results to the on-board lead project scientist (LPS).

_____ 2. Confirm mission and pattern selection from the on-board LPS.

_____ 3. Select the operational mode for radar system(s) after consultation with the on-board LPS.

_____ 4. Complete the appropriate preflight calibrations and check lists as specified in the radar operator's manual.

E.5.2 In-Flight

_____ 1. Operate the system(s) as specified in the operator's manual and as directed by the on-board LPS or as required for aircraft safety as determined by the AOC flight director or aircraft commander.

_____ 2. Maintain a written commentary in the radar logbook of tape and event times, such as the start and end times of F/AST legs. Also document any equipment problems or changes in R/T, INE, or signal status.

E.5.3 Post flight

_____ 1. Complete the summary checklists and all other appropriate check lists and forms.

_____ 2. Brief the on-board LPS on equipment status and turn in completed forms to the LPS.

_____ 3. Hand-carry all radar tapes and arrange delivery as follows:

a. Outside of Miami-to the LPS.
b. In Miami-to MGOC or to AOML/HRD. [**Note**: all data removed from the aircraft by HRD personnel should be cleared with the AOC flight director.]

_____ 4. Debrief at MGOC or the hotel during a deployment.

_____ 5. Determine the status of future missions and notify MGOC as to where you can be contacted.

HRD Radar Scientist Check List

Flight ID: ______________________________

Aircraft Number: ______________________________

Radar Operators: ______________________________

Radar Technician: ______________________________

Number of digital magnetic tapes on board: __________

Component Systems Status:

MARS ______________________ Computer ______________________

DAT1______________________ DAT2 ______________________

LF ______________________ R/T Serial # ______________________

TA ______________________ R/T Serial # ______________________

Time correction between radar time and digital time: ____

Radar Post flight Summary

Number of digital tapes used: DAT1 ____________________

DAT2 ____________________

Significant down time:

DAT1 ____________________ Radar LF ____________________

DAT2 ____________________ Radar TA ____________________

Other Problems:

HRD Radar Tape Log

Flight _______________ **Aircraft** ________ **Operator** ________________ Sheet ____ of ____

LF RPM ________________ TA RPM _______________

(Include start and end times of DATs, as well as times of F/AST legs and any changes of radar equipment status)

Tape #	F/AST On?	Event Time (HHMMSS)	Event

Form E-5
Page 3 of 3

HRD Radar Down-Time Log

Flight _______________ **Aircraft** ________ **Operator** _______________ Sheet ____ of ____

Item	Time Down (HHMMSS)	Time Up (HHMMSS)	Problem

Item List: DAT1, DAT2, COMP, MARS, LF, and TA.

Include serial numbers of any new R/Ts.

E.6 Dropsonde Scientist

The on-board lead project scientist (LPS) on each aircraft is responsible for determining the distribution patterns for dropwindsonde releases. Predetermined desired data collection patterns are illustrated on the flight patterns. However, these patterns often are required to be altered because of clearance problems, etc. Operational procedures are contained in the operator's manual. The following list contains more general supplementary procedures to be followed. (Check off and initial.)

E.6.1 Preflight

_____ 1. Determine the status of equipment and report results to the on-board LPS.

_____ 2. Confirm the mission and pattern selection from the LPS and assure that the proper number and distribution (frequency) of dropsondes are on board the aircraft.

_____ 3. Complete the appropriate preflight calibrations and checklists.

E.6.2 In-Flight

_____ 1. Operate the system as specified in the operator's manual.

_____ 2. Obtain drop release approval (for each drop) from the AOC flight director or navigator for each specific time and location of drop.

_____ 3. Report to the LPS as soon as it is determined that the dropsonde is (or is not) transmitting a good signal.

_____ 4. Report completion of each drop and readiness for the next drop.

_____ 5. Complete Form E-6.

E.6.3 Post flight

_____ 1. Complete the summary form for GPS sondes.

_____ 2. Brief the on-board LPS on equipment status and turn in reports and completed forms to the LPS.

_____ 3. Hand-carry all dropwindsonde data tapes and printouts and inform the AOC flight director that you are arranging delivery as follows:

a. Outside of Miami-to the LPS.
b. In Miami-to AOML/HRD (temporarily), either directly or via MGOC, for conversion to 9-track magnetic tapes.

_____ 4. Debrief at the MGOC or the hotel during a deployment.

_____ 5. Determine the status of future missions and notify MGOC as to where you can be contacted.

HRD GPS Dropwindsonde Scientist Log (Revised 6/1999)

Storm ____________ Flight Director ____________ Page ___ of ___

Flight ID ____________ Dropwindsonde Scientists ____________ Takeof ____________ UTC

Mission ID ____________ AVAPS Operators ____________ Landing ____________ UTC

Drop #	Sonde ID #	Time(UTC)	Lat (°N)	Lon (°W)	Surface Pressure (mb)	10m wind (knt)	MBL wind (knt)	XBT SST (°C)	Location Comment	Comments	Ob #

APPENDIX F

GROUND OPERATION

GROUND OPERATION

In support of each field operation, a ground coordination team will serve on the staff of the HRD director. The ground coordination team will consist of the Miami Ground Operations Center (MGOC).

(1) Staff:

H. Friedman (senior team leader)
R. Jones (team leader)
J. Berkeley (meteorological technical support)

(2) Operational Scheduling:

During research missions the MGOC staff will form three teams as follows: one team leader and, when necessary and available, one meteorological technician support person. Each team will work an (approximately) 8-h shift; shifts will continue for the duration of operations or until MGOC personnel are released by the field program director or his designee.

(3) General Duties:

During operations, the MGOC acts as the liaison between HRD and other organizations as required by the field program director, the HRD director, or their designated representatives. Duties of the MGOC include the following:

a. Collect, plot, and file data from NHC.

b. Update messages on the auto-phone tape at MGOC (NHC).

c. Coordinate the acquisition of satellite photos for operational and research purposes.

d. Make motel/hotel reservations at alternate recovery sites as requested by field operations personnel.

e. Handle press affairs in Miami as follows:

- Refer press inquiries to J. Goldman, OAR/PA.
- Refer forecast inquiries to NHC.

f. Communicate with AOC ground coordinator, as required.

g. Make requests for special radar and/or rawinsonde (upper air) observations, subject to approval by the HRD director.

h. Maintain a crew status report of HRD participants for current and proposed missions. When missions are being conducted away from Miami, crew status information will be reported to MGOC by the field program director or his designee.

(4) Phone numbers:

NHC Public Affairs/F. Lepore	(305)-229-4404
AOC	(813)-828-3310
AOC (FAX, J. McFadden)	(813)-828-6881
AOC (auto line)	(813)-828-3310
	—— (ext. 3128)
HRD (auto line at MGOC/TPC/NHC)	(305)-221-3679
HRD (voice line at MGOC/TPC/NHC)	(305)-221-4381
HRD FAX number	(305)-361-4402
AOC's long distance auto announce phone number	(800)-729-6622
	—— (ext. 3128)
OAR/PA (J. Goldman)	(301)-713-2483
TPC/NHC (WFO)	(305)-229-4528
Miami Ground Operations Center (MGOC) at NHC	(305)-229-4407
Miami Ground Operations Center (MGOC) at HRD/AOML	(305)-361-4400
Zephyr/WIS Center at HRD/AOML	(305)-361-4368
TRDIS Operations at NHC	(305)-229-4429
Storm Surge Group at NHC	(305)-229-4456
WWV (for time check)	(303)-499-7111
Telepager (beeper) numbers for MGOC team leaders, H. Willoughby and F. Marks (HRD), and J. McFadden (AOC)	—— TBA

Aircraft support contact numbers for:

Barbados
Sam Lord's Castle
(246) 423 7350
(246) 423 5918 (fax)

International Aircraft Management
(246) 428 1704
(246) 428 1686
Contact: Paul Worrell

St. Croix
Tamarind Reef Hotel
(340) 773 4455
(340) 773 3989 (fax)

Bohlke International Airways Inc:
(340) 778-9177
(340) 772-5932 (fax)

Bermuda
Princess Hotel (Hamilton)
(441) 295 3000
(441) 295 1914 (fax)

Aircraft Services
(441) 293 1333
(441) 293 8529 (fax)

Biloxi
53rd WRD/DOO
(228) 377 1940 (fax)

(5) Supplies:

a. Up-to-date phone list

b. Current copies of the following:

- HRD Hurricane Field Program Plan
- AOC Hurricane Operations Plan (if available)
- MGOC Manual (black, loose-leaf book)

(6) Information Pool:

Interface with NHC and others as required, and at appropriate times, obtain:

a. Satellite fixes at forecast times and 3-hourly intermediate fixes.

b. NHC official releases:

- Storm position and current strength and movement (including maximum wind and minimum—pressure).
- Forecast storm position and strength (wind and pressure) for 12, 24, 48, and 72 h.
- 0400, 1000, 1600, 2200 UTC and all intermediate advisories (based on synoptic 0000, 0600, 1200, and 1800 UTC).
- Public advisories.

c. NHC supplied additional data:

- 3-hourly storm positions.
- Aircraft reconnaissance reports (request extra copy from NHC Communications Unit).
- HURCAS computer product (request extra copy from NHC/Tropical Satellite and Analysis Center: 2130, 0330, 0930, 1530 EDT availability).

APPENDIX G

NOAA EXPENDABLES AND SUPPLIES

NOAA EXPENDABLES AND SUPPLIES

Table G-1. DAT Tape, GPS-sonde, AXBT/AXCP/AXCTD Requirements Per Experiment[1]

Experiment	DAT Tapes Cloud Physics	Slow/Fast/Radar	DW[2]	OP[2]
Coordinated Observations of Vortex Evolution and Structure (COVES) (Single-option, dual-aircraft mission)				
High-level aircraft.	03	01/ 00 / 04	44	18
Low-level aircraft.	03	01 / 00 / 04	15	48
Extended Cyclone Dynamics Experiment (single-option, Single-aircraft mission)	01	01 / 00 / 04	30	18
Tropical Cyclone Wind fields at Landfall (dual-option, single-aircraft mission)	01	01 / 02 / 04	25	18
Hurricane Synoptic-Flow Experiment (Single-option, single-aircraft mission)	02	01 / 00 / 04	65	18
Extratropical Transition Experiment (dual-option, single-aircraft mission)	01	01 / 02 / 04	25	18
Tropical Cyclogenesis Experiment (single-option, dual-aircraft mission)				
High-level aircraft.	03	01 / 00 / 04	30	18
Low-level aircraft.	03	01 / 02 / 04	10	18
Clouds and Climate Study (Single-option dual-aircraft mission)	03	01 / 02 / 05	15	00

[1] A mission is defined as one launch and recovery for research purposes. Entries shown for dual-aircraft (nonsequential mode) missions are for the total number of DAT tapes, GPS-sondes, AXBTs, AXCPs, and AXCTDs required for each experimental day's operation. Entries shown for two-aircraft, sequential mode operation missions are the requirements for each aircraft participating on each experimental day's operation.

[2] DW: GPS-sondes; OP: AXBT, AXCP, and AXCTD probes.

APPENDIX H

SYSTEMS OF MEASURE AND UNIT CONVERSION FACTORS

SYSTEMS OF MEASURE AND UNIT CONVERSION FACTORS

Table H-1 Systems of measure: Units, symbols, and definitions

Quantity	SI Unit	Early Metric	Maritime	English
length	meter (m)	centimeter (cm)	foot (ft)	foot (ft)
distance	meter (m)	kilometer (km)	nautical mile (nmi)	mile (mi)
depth	meter (m)	meter (m)	fathom (fa)	foot (ft)
mass	kilogram (kg)	gram (g)		
time	second (s)	second (s)	second (s)	second (s)
speed	meter per second (mps)	centimeter per second (cm s^{-1})	knot (kt) (nmi h^{-1})	miles per hour (mph)
		kilometers per hour (km h^{-1})		
temperature -sensible	degree Celsius (°C)	degree Celsius (°C)	---	degree Fahrenheit (°F)
-potential	Kelvin (K)	Kelvin (K)	---	Kelvin (K)
force	Newton (N) (kg m s^{-2})	dyne (dy) (g cm s^{-2})	poundal (pl)	poundal (pl)
pressure	Pascal (Pa) (N m^{-2})	millibar (mb) (10^3 dy cm^{-2})	inches (in) mercury (Hg)	inches (in) mercury (Hg)

Table H-2. Unit conversion factors

Parameter	Unit	Conversions
length	1 in	2.540 cm
	1 ft	30.480 cm
	1 m	3.281 ft
distance	1 nmi (nautical mile)	1.151 mi
		1.852 km
		6080 ft
	1 mi (statute mile)	1.609 km
		5280 ft
	1° latitude	59.996 nmi
		69.055 mi
		111.136 km
depth	1 fa	6 ft
		1.829 m
mass	1 kg	2.2 lb
force	1 N	10^5 dy
pressure	1 mb	102 Pa
		0.0295 in Hg
	1 lb ft^{-2}	4.88 kg m^{-2}
speed	1 m s^{-1}	1.9
	at. 6 h^{-1}	10 kt

ACRONYMS AND ABBREVIATIONS

θ_e	equivalent potential temperature
ABL	atmospheric boundary-layer
A/C	aircraft
ACLAIM	Airborne Coherent Lidar for Advanced In-flight Measurements
AES	Atmospheric Environment Service (Canada)
AFRES	U. S. Air Force Reserve
AMPR	Advanced Microwave Precipitation Radiometer
AOC	Aircraft Operations Center
AOML	Atlantic Oceanographic and Meteorological Laboratory
ASDL	aircraft-satellite data link
ATOLL	Atlantic Tropical Oceanic Lower Layer
AXBT	airborne expendable bathythermograph
AXCP	airborne expendable current probe
AXCTD	airborne expendable conductivity, temperature, and depth probe
BLS	boundary layer scientist
CARCAH	Chief, Aerial Reconnaissance Coordinator, All Hurricanes
CAMEX-4	Fourth Convection and Moisture Experiment
CDO	central dense overcast
CIRA	Cooperative Institute for Research in the Atmosphere
C-MAN	Coastal-Marine Automated Network
COVES	Coordinated Observations of Vortex Evolution and Structure Experiment
CP	coordination point
CRT	cathode-ray tube
C-STAR	Conically-Scanning Two-look Airborne Radiometer
CVA	cyclonic vorticity advection
CW	cross wind
DLM	deep-layer mean
DOD	Department of Defense
DOW	Doppler on Wheels
DRI	Desert Research Institute (at Reno)
E	vector electric field
EDOP	ER-2 Doppler Radar
EHAD	ER-2 High Altitude Dropsonde
EPAC	Eastern Pacific
ETL	Environmental Technology Laboratory
EVTD	extended velocity track display
FAA	Federal Aviation Administration
F/AST	fore and aft scanning technique
FEMA	Federal Emergency Management Agency
FL	flight level
FP	final point
FSSP	forward scattering spectrometer probe
GFDL	Geophysical Fluid Dynamics Laboratory
G-IV	Gulfstream IV-SP aircraft
GOMWE	Gulf of Mexico Warm Eddy
GPS	global positioning system
HAMSR	High Altitude MMIC Sounding Radiometer

HL	Hurricanes at Landfall
HRD	Hurricane Research Division
ICATS	NASA DC-8 Information Collection and Transmission System
INE	inertial navigation equipment
IP	initial point (or initial position)
IWRS	Improved Weather Reconnaissance System
JW	Johnson-Williams
Ku-SCAT	Ku-band scatterometer
LASE	Lidar Atmospheric Sensing Experiment
LF	lower fuselage (radar)
LIP	Lightning Instrument Package
LPS	Lead Project Scientist
MAS	MODIS Airborne Simulator
MCS	mesoscale convective systems
MGOC	Miami Ground Operations Center
MLD	Mixed Layer Depth
MMS	Meteorological Measuring System
MODIS	Moderate Resolution Imaging Spectroradiometer
MPO	Meteorology and Physical Oceanography
MTP	Microwave Temperature Profiler
NASA	National Aeronautics and Space Administration
NCAR	National Center for Atmospheric Research
NCEP	National Centers for Environmental Prediction
NDBC	NOAA Data Buoy Center
NESDIS	National Environmental Satellite, Data and Information Service
NHC	National Hurricane Center
NOAA	National Oceanic and Atmospheric Administration
NWS	National Weather Service
ODW	Omega-based generation of dropwindsonde
OML	oceanic mixed-layer
PDD	pseudo-dual Doppler
PMS	Particle Measuring Systems
POD	Plan of the Day
PPI	plan position indicator
PR-2	dual-Frequency Airborne Precipitation Radar
PV	potential vorticity
RA	radar altitude
RAOB	radiosonde (upper-air observation)
RAWIN	rawinsonde (upper-air observation)
RECCO	reconnaissance observation
RHI	range height indicator
RSMAS	Rosenstiel School of Marine and Atmospheric Science
SFMR	Stepped-Frequency Microwave Radiometer
SLOSH	sea, lake, and overland surge from hurricanes (operational storm surge model)
SRA	Scanning Radar Altimeter
SST	sea-surface temperature
TA	tail (radar)

TAS	true airspeed
TC	tropical cyclone
TOPEX	The Ocean Topography Experiment
TPC	Tropical Prediction Center (at NHC)
UMASS	University of Massachusetts (at Amherst)
USACE	United States Army Corps of Engineers
USAF	United States Air Force
USWRP	U. S. Weather Research Program
UTC	universal coordinated time (U.S. usage; same as “GMT” and "Zulu" time)
VICBAR	name for a barotropic hurricane track prediction model (not an acronym)
VTD	velocity-track display
XCDX	Extended Cyclone Dynamics Experiment

HURRICANE FIELD PROGRAM PLAN DISTRIBUTION—2001

Department of Commerce/National Oceanic and Atmospheric Administration

Aircraft Operations Center

J. McFadden, AOCx4
R. Maxson, AOC
Staff, AOC (20 copies)

Atlantic Oceanographic and Meteorological Laboratory (R/AOML)

K. Katsaros, OD
H. Friedman, HRD
S. Garzoli, PHOD
J. Gray, OD.
P. Ortner, OCD
J. Proni, OCD
C. Stewart, OD
H. Willoughby, HRD
Library, AOML
Staff, HRD/AOML (20 copies)

Geophysical Fluid Dynamics Laboratory (R/GFDL)

M. Bender
R. Tuleya

National Center for Environmental Prediction

S. Lord, W/NP2
N. Surgi, W/NP2
L. Uccellini, W/NP

National Data Buoy Center

M. Burdette, W/DB2
E. Meindl, W/DB4

National Environmental Satellite, Data, and Information Service

D. Clark, E/SP3
N. Everson, E/RA22
A. Gruber, E/RA2
J. Wilkerson, E/RA3

National Ocean Service

S. Gill, N/OS4

National Severe Storm Laboratory

J. Kimpel, R/E/NS

National Weather Service

R. Dumont, FC
P. Hirschberg, W/OMx2
J. Kelly, W
D. Wernly, W/OM11

NWS/Eastern Region

D. Gulezian, W/ER (2 copies)
J. Guiney, W/ER1

NWS/Pacific Region

R. Hagemeyer, W/PR

NWS/Southern Region

X.W. Proenza, W/SR
R. Pfost, W/WSFO-Miami
B. Hagemeyer, W/SR49

NWS Training Center

Director, W/OS61

Office of Marine and Aviation Operations

E. Fields, OMAO

Office of Global Programs

M. Hall, R/OGP

Office of Oceanic and Atmospheric Research

D. Evans, R (2 copies)
D. Rogers, R/E
J. Gaynor, USWRP IPO
K. Groninger, R/OM12
L. Koch, R
M. Langlais, R/OM

Office of Systems Operations

R. Racer, W/OSO1x3
W. Telesetsky, W/OPS
T. Trunk, W/OSO14

Public Affairs

Barbara Semedo, PA
J. Goldman, PA (OAR) (2 copies)

Techniques Development Laboratory

W. Shaffer, W/OSD22

Tropical Prediction Center/National Hurricane Center (W/NP8)

L. Avila
R. Burpee (ret.)
C. Burr
J. Franklin
J. Gross
F. Horsfall
B. Jarvinen
M. Lawrence
F. Lepore
M. Mayfield (2 copies)
C. McAdie
R. Pasch
E. Rappaport
S. Stewart

WSR-88D Operational Support Facility

E. Berkowitz, W/OPS42
D. Burgess, W/OPS45
T. Crum, W/OPS41
M. Fresch, W/OPS41
R. Reed, W/OPS43
A. White, W/OPS44

Department of Defense

U.S. Air Force

D. Harmes, Patrick AFB
J. Kerwin, Eglin AFB
R. Lafbare, Eglin AFB
J. Pavone, CARCAH
D. Urbanski, Patrick AFB
USAFETAC/DOL, Scott AFB
53rd WRS, Keesler AFB (12 copies)

U.S. Army

OJCS/J3/ESD

U.S. Army Corps of Engineers

R. Jensen, WES

U.S. Navy

Chairman, Dept. of Meteorology, NPS
Commander in Chief, U.S. Atlantic Command, Code J37
Commander, Atlantic Missile Range
R. Abbey, ONR
C. Bishop, FNMOC, Monterey
T. Bosse, NAVLANTMETOCFAC JAC/NAS, Jacksonville
R. Elsberry, NPS (2 copies)
L. Ritchie, Code 63ES
K. St. Germain, Code 7223

Department of Transportation/Federal Aviation Administration
Federal Aviation Administration, ATR-150

National Aeronautics and Space Administration
D. Atlas, Code 610
R. Hood, ES-43
R. Kakar, Code SEP
J. Rothermel, ES-43
J. Simpson, Code 612
O. Vaughan, ES-43
J. Wang, Code 675

National Center for Atmospheric Research
R. Carbone
D. Carlson
A. Heymsfield
W.-C. Lee
M. LeMone
L. Radke

National Research Council
F. White

National Science Foundation
S. Nelson
P. Stephens

NTTC/NTIS Projects
National Technology Transfer Center

Private Sector
G. Holland, Aerosonde Robotic Aircraft
C. Neumann, SAIC
I. Popstefanija, Quadrant Engineering
C. Samsury, TWC
R. Williams, St. Georges, Bermuda
S. Yueh, JPL

University Corporation for Atmospheric Research
R. Anthes

University Scientists
B. Albrecht, U. of Miami/RSMAS
G. Barnes, U. of Hawaii
H. Bluestein, U. of Oklahoma

L. Bosart, SUNY/Albany
S. Chen, U. of Miami/RSMAS
K. Emanuel, MIT
S. Esbensen, Oregon State U.
W. Frank, PSU
M. Fritsch, PSU
S. Gedzelman, CCNY
W. Gray, CSU
J. Hallett, DRI/U. of Nevada
R. Houze, Jr., U. of Washington
R. Johnson, CSU
K. Knupp, U. of Alabama/Huntsville
T. Krishnamurti, FSU
J. Lawrence, U. of Houston
S. Leatherman, IHC
E.W. McCaul, U. of Alabama/Huntsville
J. Molinari, SUNY/Albany
M. Montgomery, CSU
R. Pfeffer, FSU
J. Prospero, U. of Miami, CIMAS
P. Ray, FSU
D. Raymond, NM Institute for Mines and Technology
C. Rooth, U. of Miami/RSMAS
F. Roux, Laboratorie D'Aerologie
S. Rutledge, CSU
F. Sanders, MIT (ret.)
W. Schubert, CSU
L. Shapiro, U. of Munich
L. Shay, U. of Miami/RSMAS
R. Smith, U. of Munich
R. Smith, Yale U.
W. Smith, NASA/Langley Research Center
S. Stage, FSU
J. Straka, U. of Oklahoma
C. Swift, U. of Massachusetts/Amherst (3 copies)
G. Tripoli, U. of Wisconsin
C. Velden, U. of Wisconsin
T. Wilheit, Texas A&M U.
J. Wurman, U. of Oklahoma
E. Zipser, U. of Utah

U.S. Coast Guard

Commandant, G-OIO

U.S. Nuclear Regulatory Commission

R. Kornasiewicz, NL-007

World Meteorological Organization, Geneva, Switzerland

K. Abe
G.O.P. Obasi
WMO Library

Acknowledgment

The preparation of HRD's **2001 Hurricane Field Program Plan** was a team effort. The authors would like to express their appreciation to: the HRD scientists that contributed information on specific experiments; Shirley Murillo, Sean White, and Joyce Berkeley, for their efforts on updating the information in Appendix C.